IN THE UNITED STATES PATENT AND TRADEMARK OFFICE

In re application of: Date: August 2, 2004

PETERS et al. Art Unit: 1764

Serial No.: 10/022,102 Examiner: W. D. Griffin

Filed: Docket No.: W9003-04

For: REDUCED NOx COMBUSTION PROMOTER FOR USE IN FCC PROCESSES

DECLARATION UNDER 37 CFR 1.132

I, George Yaluris, hereby declare as follows

1. I received my Ph.D. in chemical engineering from the University of Wisconsin-Madison in 1995.

2. From 1995 to present I have been employed by and continue to work for W. R. Grace & Co.-Conn.

3. During my employment at W. R. Grace & Co.-Conn., I have held the position of Research Engineer, Senior Research Engineer, Principal Engineer, and currently Senior Marketing Specialist.

4. I am a named author in at least 14 peer reviewed publications, including two peer reviewed publications on the origin and control of NOx in a Fluid Catalytic Cracking (FCC) unit regenerator, as well as on the development of new methods for testing in the laboratory NOx reducing catalytic compositions.

5. I am a named author in at least 11 other publications in trade journals and other publications, including two publications on NOx chemistry and control in the FCC unit regenerator.

6. I am a named inventor in one U.S. patent issued, and in several U.S. patent applications currently pending before the PTO.

7. I worked closely with Dr. Peters, one of the inventors of the present invention while he was alive, and I am familiar with the contents of the above referenced patent application.

8. An oxygen storage component requires an element (typically a metal) which under the conditions it is used in catalytic applications can have more than one valence states. The requirement for an oxygen storage element to have multiple valence states is the result of the necessity that the element can form oxides with different oxygen stoichiometries, so that oxygen can be stored or released as the element switches from

one valence state to the other, i.e., from an oxide with one oxygen stoichiometry to one with another. Discussing the subject of oxygen storage in their paper included in the book "Catalysis by Ceria and Related Materials", A. Trovarelli Ed., Catalytic Science Series, Series Ed. G. J. Hutchings, vol. 2, Imperial College Press, 2002, ISBN 1-86094-299-7, Shelef *et al.* on page 345 write the following:

> *"The existence of oxides with varying oxygen stoichiometries is well known. In particular, among the rare-earth oxides, those of Ce, Pr and Tb contain, under a wide range of conditions, metal ions of different valence and are able to incorporate more or less oxygen into their crystal structure depending on various parameters such as the gaseous atmosphere with which they are in contact, temperature, and pressure."*

When having an element capable of forming oxides with different stoichiometries, the amount of oxygen which can be stored and released in an oxygen storage component may depend on a number of factors. In addition, to the factors named by Shelef *et al.* (gaseous atmosphere, temperature and pressure), Di Monte and Kaspar on page 52 pf their peer-reviewed paper (Topics in Catalysis, 28 (2004) 47-57) consider as such additional factors influencing oxygen storage capacity, sintering (oxide structure stability), sample pre-treatment, phase purity, surface and bulk properties, and the nature of the gaseous reducing component. However, as it becomes apparent from this publication, while the amount of oxygen which can be stored and released may depend on a number of factors, the ability to reduce the metal to a lower valence state is a necessary requirement for having oxygen storage capability.

9. Group IIIB metals (by newer Periodic Table designations 3A or IIIA) are Sc, Y, and La. According to the authoritative book "Advanced Inorganic Chemistry" F. A. Cotton, G. Wilkinson, C. A. Murillo, and M. Bochmann, 6th Edition, John Wiley and Sons, 1999, ISBN 0-471-19957-5, p 1108, actinium should also be included, but in general it is commonly associated with the elements which follow it (the actinides). Group IIIB does not include ceria. According to Cotton *at al.* the group which follows La, Ce through Lu (atomic numbers 58 through 71) is formally known as the lanthanides. While the lanthanides in combination with La and at times Y, are commonly referred to as the rare earths, according to Cotton *at al.* (p. 1108), Group IIIB does not include the lanthanides.

10. As it is clearly indicated by the Periodic Table of the Elements published by CRC Handbook of Chemistry and Physics, 76th Edition, CRC Press, 1995, ISBN 0-8493-0476-8, as well as the description of the elements in the same book (pages 4-1 to 4-34), all the elements in this group, including La, have only one valence +3. Since IIIB elements lack the ability to form oxides with multiple stoichiometries, none of these elements can be an oxygen storage component. According to the CRC Handbook of Chemistry and Physics, the main valence state of the lanthanides is +3. However, Ce and Tb can also have a valence of +4, and Sm, Eu and Yb can have a valence of +2. Cotton *et al.* on page 1109 also write that some of the lanthanide elements can have

multiple valences (Ce, Tb and Pr may form +3 and +4 states, Sm, Eu and Yb may form +3 and +2 states).

11. Several references in the open literature support the conclusion that La_2O_3 can not be reduced to a lower valence state and cannot be used as an oxygen storage component. For example, Fu *et al.* (Q. Fu, S. Fiore, H. Saltsburg, X. Qi, and M. Flytzani-Stephanopoulos, Fuel Chemistry Division Preprints 2002, 47(2), 605-606, presented at the 224th National Meeting of The American Chemical Society, Boston, MA August 18-22 2002), consider La and Zr as dopants added to ceria in order to suppress its crystal growth at high temperatures (sintering), and increase its reducibility. Kaspar *et al.* (J. Kaspar, P. Fornasiero, and N. Hickey, Catalysis Today, 77 (2003) 419-449) on page 424 of their peer-reviewed paper in describing the key components of three way catalysts, list lanthana as a stabilizer of the surface area of the alumina support. Kim *et al.* (D. H. Kim, S. I. Woo, J. M. Lee, O-B. Yang, Catalysis Letters, 70 (2000) 35-41) on page 35 of their peer-reviewed paper, also state that in three way catalysts "...La_2O_3 is known to act as a good promoter to increase the dispersion and thermal stability of Pd. In addition, CeO_2 plays an important role as an oxygen storage capacitor (OSC) which

12. I further declare that all statements made herein of my own knowledge are true and that all statements made on information and belief are believed to be true; and further that these statements were made with the knowledge that willful false statements and the like so made are punishable by fine or imprisonment, or both, under section 1001 of title 18 of the United States Code, and that such willful false statements may jeopardize the validity of the application or any patent issuing thereon.

08/09/04
Date

George Yaluris
George Yaluris, PhD

Catalytic Science Series — Vol. 2

Series Editor: Graham J. Hutchings

Catalysis by Ceria and Related Materials

edited by

Alessandro Trovarelli
Università di Udine, Italy

ICP

Imperial College Press

CHAPTER 10

CERIA AND OTHER OXYGEN STORAGE COMPONENTS IN AUTOMOTIVE CATALYSTS

MORDECAI SHELEF, GEORGE W. GRAHAM, and ROBERT W. McCABE
Ford Research Laboratories, Dearborn, Michigan 48121, USA

10.1. Origin and Evolution of "Oxygen Storage" in Automotive Catalysts

The introduction of catalytic treatment of automotive exhaust in the United States in the first part of the 1970s began with the removal of the products of incomplete combustion, carbon monoxide and residual hydrocarbons. This task can be accomplished by using a simple oxidation catalyst, where, in the presence of excess air, noble metal catalysts promote the additional oxidation of the products of incomplete oxidation from the IC engine. The regulations necessitating the catalytic removal of nitrogen oxides, formed in the combustion chamber, kicked-in in 1980. It initially seemed that the simplest way to accomplish this would be to use a "dual" system where the upstream catalyst bed is fed by exhaust resulting from combustion of a slightly rich mixture of fuel and air. Under these conditions the reduction of NO_x is fast and nearly complete. Secondary air is then injected ahead of a downstream oxidation catalyst to remove the CO and hydrocarbons. This seemingly straightforward approach was found to contain a hidden flaw: the reduction of the NO_x in the upstream catalyst resulted in a majority of the product being ammonia, due to the presence of hydrogen in the exhaust. When re-oxidized on the downstream catalyst the ammonia reverted back to NO_x, vitiating the whole approach [1].

Another solution to the problem was called for. It was proposed by Gross et al [2] that if one could catalytically equilibrate an exhaust resulting from the combustion of an exactly stoichiometric combustion mixture it is thermodynamically possible to remove all three pollutants, leaving only water, CO_2 and nitrogen. This is a single three-way catalyst (TWC). In the same time frame the other systems needed for tight combustion control have matured technologically, such as affordable computerized electronic engine controls and exhaust composition sensors (electrochemical solid-state oxygen sensors). (See Fig. 10.1)

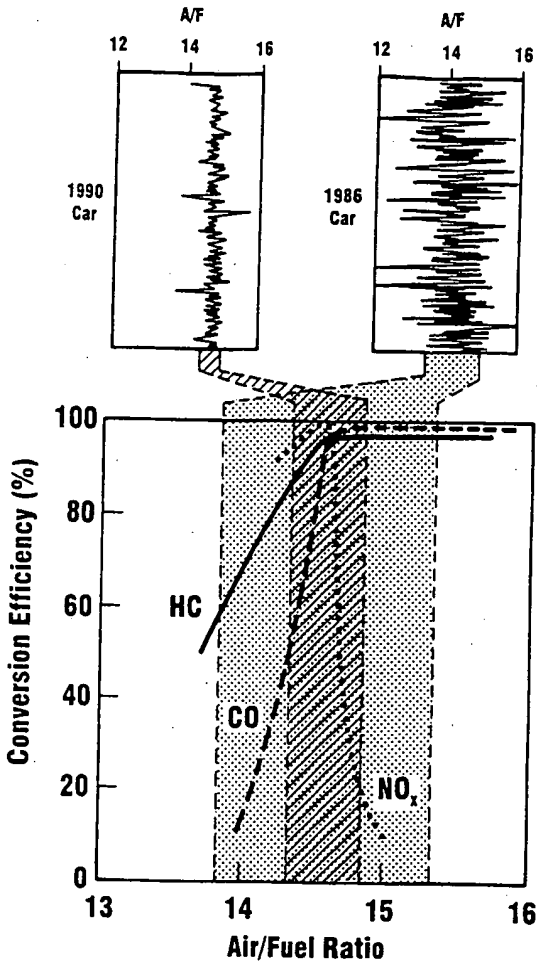

Figure 10.1. Typical TWC conversion efficiency plot for hydrocarbons (HC), CO, and NO_x as a function of air-fuel ratio. Also shown are representative air-fuel ratio vs. time traces for 1986 and 1990 vehicles with control bandwidth mapped onto the catalyst efficiency plot. [3]

Nevertheless, the required tight stoichiometry constraints in a randomly oscillating dynamic combustion were not easily attainable. There was a need for a composition smoothing device/material akin to a surge tank in a hydraulic system or

a capacitor in an electrical circuit. This is where the incorporation of such a material into the catalyst came into consideration.

The existence of oxides with varying oxygen stoichiometries is well known. In particular, among the rare-earth oxides, those of Ce, Pr and Tb contain, under a wide range of conditions, metal ions of different valence and are able to incorporate more or less oxygen into their crystal structure depending on various parameters such as the gaseous atmosphere with which they are in contact, temperature, and pressure. The release of the oxygen can be accomplished in some cases without the use of a reducing agent, by switching to a lower oxygen pressure or higher temperature or both. In practice, however, the release of the oxygen is enhanced by a reductant such as CO, H_2 or a hydrocarbon, which itself undergoes oxidation in the process.

The rate of the uptake of the oxygen is accelerated by the presence of catalysts capable of dissociatively adsorbing dioxygen, which is a necessary step in the incorporation of oxygen ions from diatomic gaseous oxygen into a solid. The same catalysts also strongly promote the reduction of the solid by the reductant gaseous molecules. Since the scission of the oxygen bond at the surface is energetically demanding, the reduction half of the overall cycle tends to be rate limiting.

The first description in the open literature of the use of "oxygen storage" to buffer the lean-rich swings of the exhaust gas composition was in 1976 [4]. Initially, the main role of the "oxygen-storage component" was to extend the three-way "window" on the lean side of stoichiometry by acting as a sink for gas-phase oxygen during rich-to-lean transients. This uptake of oxygen allowed NO_x conversion to continue for an interval of time proportional to the oxygen storage capacity (OSC), as shown in Fig. 10.2 (top). On the other hand, the oxygen storage component could also promote oxidation of reductants, like CO, during lean-to-rich transients, as shown in Fig. 10.2 (bottom). Early on, ceria was recognized as a promising storage material because of its combination of facile redox cycling between the trivalent and tetravalent oxidation states of the Ce ions, good thermal stability, ease of impregnation onto alumina, compatibility with noble metals and, most importantly, availability and affordability. In addition, while other, distinct, components were at first identified for their water-gas shift (WGS) and steam-reforming activities, further extending the "window" on the rich side under steady-state conditions, ceria was found to perform these functions, as well. For many years, ceria has been the chief oxygen storage component for three-way catalysts, and the mechanisms by which it works have been the subject of many studies and excellent review papers, including a recent detailed survey by Trovarelli [5].

Topics in Catalysis Vol. 28, Nos. 1–4, April 2004 (© 2004)

On the role of oxygen storage in three-way catalysis

Roberta Di Monte and Jan Kašpar*

Dipartimento di Scienze Chimiche, Università di Trieste, Via Giorgieri 1, Trieste, 34127, Italy

The role of the so-called oxygen storage and release capacity (OSC) in promoting the activity of noble metals in the three-way catalysts (TWCs) is critically discussed. It is shown that the promoting effects of CeO_2 in the TWCs cannot be attributed to a simple redox type of effect according to the reaction $CeO_2 \leftrightarrow CeO_{2-x} + x/2O_2$, since multiple and sometimes intriguing effects of CeO_2 promoter have been observed, particularly in the latest generation of TWCs containing modified CeO_2–ZrO_2 mixed oxides.

KEY WORDS: three-way catalysts; CeO_2–ZrO_2 mixed oxides; oxygen storage promoters

1. Introduction

In this paper the aspects related to the role of the oxygen storage in the three-way catalysts (TWCs) are addressed. The paper is organised as follows: first the correlation between the oxygen storage and release capacity (OSC) and activity is commented upon, then the nature of OSC and its correlation to catalytic activity are addressed. The mechanism of the redox processes in CeO_2–ZrO_2 mixed oxides is addressed in detail and is critically discussed to show how properties of present and future materials can be developed. As far as the issue of thermal stability and use of composite CeO_2–ZrO_2–Al_2O_3 OSC promoters is concerned, even if relevant to the OSC, they are not included in the present review as they have been addressed in a recent review [1].

2. The role of the oxygen storage in the TWC efficiency

The advent, in the early 1980s, of the TWC has represented a major breakthrough in the development of the automotive pollution control devices. As is well known, TWCs are capable of simultaneously and efficiently converting CO, hydrocarbon (HC) and NO_x into harmless CO_2, H_2O and N_2, provided that the air-to-fuel ratio (A/F) is constantly kept in the exhaust at the stoichiometric point, i.e., under conditions where the amount of oxidants is equal to that of reducing agents. A/F is defined as

$$\mathrm{A/F} = \frac{\text{mass of air consumed by the engine}}{\text{mass of fuel consumed by the engine}};$$

for stoichiometric combustion of isooctane (ideal fuel) A/F = 14.65 which represents the stoichiometric point. The engine-out exhaust gas composition is also commonly classified in terms of λ:

$$\lambda = \frac{\text{actual engine A/F}}{\text{stoichiometric engine A/F}}.$$

* To whom correspondence should be addressed.
E-mail: kaspar@univ.trieste.it

The fundamental relationship between the TWC efficiency and the oscillations in the air-to-fuel ratio is represented in figure 1.

A perusal of figure 1 reveals some important aspects of the three-way catalysis that are: (i) due to the opposite nature of the reactions responsible for the removal of the pollutants, i.e. oxidation of HC and CO and simultaneous reduction of NO_x, the conversions required by the legislation (<95%) are attained only in a narrow window of A/F, close to the stoichiometric point; (ii) strong deviations/oscillations of A/F from the stoichiometric point lead to widening of the operating A/F window resulting in an average poor performance of the TWCs.

It is worth recalling that uncontrolled emissions of 40–60 g of CO/km were common to most of the passenger vehicles by the end of the 60s; this amount decreased to 2.3 g CO/km in 2000 and will be phased down to 1 g of CO/km in 2005 by European legislation (Euro phases 3 and 4). These limits therefore represent reduction of respectively 94–96% and 97–98% compared to uncontrolled emissions. US Tier 2 legislation, issued by EPA, challenged even more the catalyst/vehicle producers: besides the quite restrictive limits on the emissions, durability as high as 120,000 miles (about 200,000 km) will be phased-in by 2004 [2]. Clearly, an extreme efficiency and durability is nowadays required to the TWCs [3,4]. As illustrated in figure 1, such high efficiency is achieved over TWCs in a very narrow A/F window, which requires a highly efficient control of the exhaust composition, in particular in terms of residual oxygen concentration.

Generally speaking, an integrated strategy is employed to control A/F under operating conditions (figure 2), which is based on (i) an "engineering control" of the A/F using an integrated electronic system that controls fuel and air injection using a feedback signal by continuously monitoring the oxygen concentration in the exhaust with a λ (oxygen) sensor, (ii) a "chemical control" of A/F, which is achieved by adding a CeO_2-containing promoter of the so-called OSC. The latter

1022-5528/04/0400-0047/0

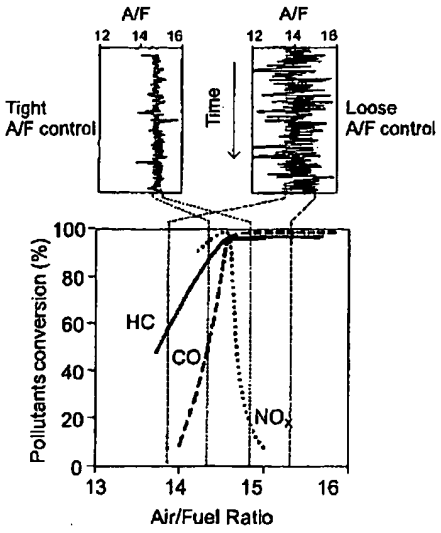

Figure 1. Relationship between the oscillations in the A/F in the exhaust and TWC efficiency (adapted from [127]).

component is added because of its ability to adsorb and release oxygen under, respectively, fuel-lean and fuel-rich conditions, according to the reaction:

$$CeO_2 \underset{H_2O/CO_2}{\overset{H_2/CO}{\rightleftharpoons}} CeO_{2-x} + x/2O_2 \qquad (1)$$

Reduction/oxidation of the noble metal, Pd in particular [5], can also contribute to the oxygen storage/release but is not considered in the present paper which is focused on the role of the CeO_2–ZrO_2 promoters.

Strictly speaking the definition of the OSC, i.e. capability to store and release oxygen, ignores a fundamental aspect of the OSC that is the nature of the oxidising and reducing agents that may interact with the CeO_2 moiety. Equation [1] therefore presents a very simplified picture of the redox behaviour of the CeO_2-containing promoters under the exhaust conditions, due to the presence of continuously changing reaction conditions and presence of a variety of oxidants/reductants, e.g., H_2O, CO_2, CO, HC, H_2, that easily interfere with the pure redox process [6–8].

It is important to recognise that the beneficial effects of cycled (between reducing and oxidising conditions) feed stream upon NO_x, CO and HC conversion as compared to feeds with stationary-stoichiometric composition have been identified in the early studies reported shortly after the introduction of CeO_2 into TWC formulations [9–16]. This is an important consideration and the apparent contradiction with the effect of A/F fluctuation on the conversion can be rationalised in terms of critical importance of amplitude and frequency of the A/F oscillations in the feed, which may lead to a different state of the noble metal at the surface resulting in different activity [17,18]. For example, CO oxidation over Pt metal is self-inhibited by excess of CO which covers the metal surface and blocks O_2 dissociation sites: oscillating conditions in the exhaust that periodically free the metal surface may favour O_2 dissociation and hence the overall reaction rate. However, if inappropriate frequency and amplitude of the A/F oscillations is used, this effect will no longer be seen. Consistent with this, a review paper [19] concluded that such enhancement due to cycled feed stream, may be observed only in a limited range of temperature, the usual oscillation frequency (1 Hz) being not optimal. It must be observed that, following these initial papers published in the 1980s, the effects of cycled feed stream have seldom been addressed [20]. Keeping in mind the massive progress of the TWC technology in the past 25 years and the great enhancements in the properties of the OSC promoters, this fact is somehow surprising as insights, particularly on the role of spillover phenomena and rate of redox processes (in bulk and at the surface) in these advanced materials, would be very useful.

An important corollary of these observations is that the extent of A/F oscillations plays a fundamental role in the efficiency and hence detection of efficiency of the TWCs. As shown in figure 2, monitoring of A/F is continuously performed by the λ sensors at the inlet and outlet of the catalytic converter. In the absence of the OSC function, comparable fluctuation of A/F is expected at both λ sensors, whereas the presence of an efficient OSC promoter results in a dampening of the fluctuation at the outlet, as a result of the buffering capacity (equation (1)). Wide fluctuation in the O_2 concentration detected by the second λ sensor signal is indicative of deactivation of the OSC promoter and is correlated to the catalyst efficiency. Figure 3 shows an example of a correlation between the OSC and the TWC efficiency [21]. Even though a simple correlation is not found, the precise nature of these correlations is in fact related to the particular engine–engine control–TWC system used, and monitoring OSC efficiency using the λ sensor is employed as a measure of the TWC performance. This is indeed the principle, which most of the current on-board diagnostics (OBD) technologies employ to detect deactivation/failure of the TWCs [22].

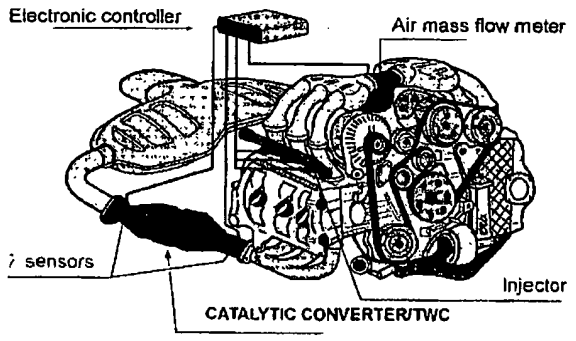

Figure 2. Modern TWC/engine/oxygen sensor (λ) control loop for engine exhaust control.

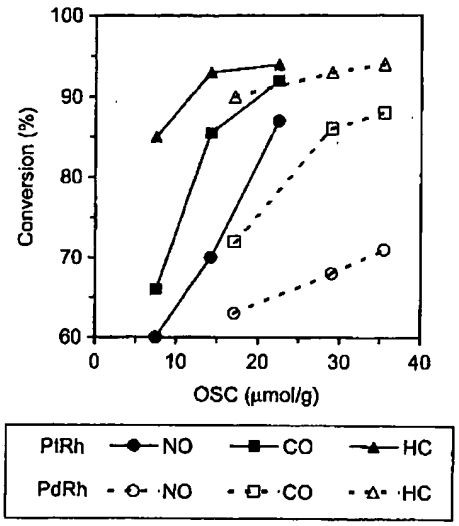

Figure 3. Correlation between the catalytic efficiency of PtRh and PdRh catalysts engine-bench aged for 25, 50 and 200 h (T_{max} 950 °C) and the OSC measured by alternating CO/O_2 pulses: conversion of the different pollutants (NO, CO and HC) are given over PtRh and PdRh as a function of CO-OSC (adapted from [21]).

In summary, the efficiency of the TWCs is unambiguously related to the efficiency of the OSC function: loss of OSC signals deactivation of the TWC.

3. Oxygen storage: measurement, mechanism and its role in the TWC

3.1. Measurement of OSC

According to equation (1), the oxygen storage is formally considered as the amount of oxygen released (left-to-right) or stored (right-to-left) under the rich (net reducing)/lean (net oxidising) excursions of A/F.

From the thermodynamic point of view, the standard potential for reduction of Ce^{4+} to Ce^{3+} is 1.74 V in solution [23] which indicates that Ce(IV) in solution is a strong oxidant. In the solid state, the situation is different. CeO_2 crystallises in the fluorite structure in which each cerium ion is co-ordinated by eight oxygen neighbours. This co-ordination stabilises the Ce^{4+} state and makes the reduction of CeO_2 unfavourable. In fact, the fluorite structure of ceria is a direct result of the ionic nature of ceria and of the charge and size of the ions. Model calculation has shown that it is formed when a sufficiently high number of CeO_2 units (about 50) are clustered together [24]. The ability of CeO_2 to undergo a relatively easy reduction (*vide infra*) compared to other oxides, can in principle also be related to the general property of fluorite structure/mixed valence oxides to strongly deviate from stoichiometry [25]. It is worth recalling that of the two processes (reduction/oxidation), oxidation is fast [26], and occurs deep into the bulk even at room temperature (RT), whereas reduction typically occurs above 473 K [27–29].

Two types of measurements of OSC were distinguished by Yao and Yu Yao [30]: the so-called complete or ultimate oxygen storage capacity (total OSC), i.e. an oxygen storage measured under thermodynamic control (*vide infra*); and the kinetic oxygen storage, (dynamic OSC), i.e. measured under kinetic control. The total OSC represents the widest "limiting" amount of oxygen transferable from the catalyst at a given temperature and generally is limited in the case of CeO_2 by formation of some non-stoichiometric CeO_{2-x} compound [27,28,31]. Consistently, isothermal reduction of CeO_2 at 973 and 773 K led respectively to $CeO_{1.8}$ and $CeO_{1.89}$ [32]. Total OSC is typically measured using the temperature programmed reduction (TPR) technique or by an oxidation following a reduction at a fixed temperature [33].

The dynamic OSC is typically measured by alternatively injecting pulses of an oxidising, usually O_2 in inert gas, and reducing, usually CO or H_2 in inert gas or even inert gas itself at a high temperature [34], mixtures into a flow of inert carrier passing through the catalysts bed at a fixed temperature. It is considered to be more related to the real exhaust conditions, since O_2 release/accumulation is measured under dynamic conditions; on the other hand, standard conditions for these measurement are lacking so that comparing data from different sources is difficult. Also the fact that the redox cycles are often much slower compared to the rate of A/F (1 Hz) oscillations due to physical constraints, are factors that make this technique much less used compared to the traditional and readily available TPR technique. It is important to underline the point that correlations between the dynamic OSC and total OSC have been found [35,36]. Also worth to be noticed that, as shown below, the nature of the reducing agent plays a key role in the OSC. Accordingly, in the following text the H_2- and CO-OSC will be distinguished to indicate whether hydrogen or carbon monoxide has been used as reducing agent. In fact, HC have only sparingly been employed as reducing agent, more complex reaction do in fact occur on the surface in this case, rather then a pure redox process [35].

3.2. Role and mechanism of the OSC

3.2.1. NM–CeO_2 interactions and CeO_2 and NM/CeO_2 reduction behaviour

As shown in Section 2, the OSC is a crucial property of the TWCs directly linked to its efficiency. However, it is important to recognise that the impact of OSC on the catalytic performance of the TWC cannot be limited to a pure oxygen buffering effect as indicated by the redox process reported in equation (1). In fact, it is an ambitious task to define the role of the CeO_2 in the three-way catalysis since evidence for multiple effects of this promoter have been found. Ceria has been suggested to:

- promote the noble metal dispersion;
- increase the thermal stability of the Al_2O_3 support;

- promote the water gas shift (WGS) and steam reforming reactions;
- favour catalytic activity at the interfacial metal-support sites;
- promote CO removal through oxidation employing a lattice oxygen;
- store and release oxygen under respectively lean and rich conditions.

A detailed discussion of all these effects is outside the scope of this paper, we refer the reader to exhaustive reviews on the role of CeO_2-based promoters (see for example [35,37,38]) and companion papers in this issue. A perusal of the above listed effects suggests, however, that there is a common point in most of the chemical effects, which are related to the role of NM/CeO_2 (NM = noble metal) system in the TWCs. This is to promote under the reaction conditions, the rate of migration/exchange of oxygen species between the different reactants. Under such a broad perspective, most of the above quoted promoting phenomena can be somehow related to equation (1). The promotion of the WGS by CeO_2 can be cited in this respect as an example [39]. Two reaction pathways were proposed for this reaction [40–42]: an "associative" mechanism in which a hydroxyl group produced by dissociation of water can combine with an adsorbed carbon monoxide to further react to give CO_2 and H_2 via a formate intermediate and a "regenerative" mechanism, where water oxidises the surface producing hydrogen and an oxidised surface capable of interacting with CO to give CO_2. The discrepancy between the two proposals can be accounted for when a bifunctional mechanism is considered for the NM/CeO_2 systems where, in addition to the reaction catalysed at the NM sites, a reaction path is considered that involves a reaction between CO adsorbed on the NM and oxygen from CeO_2 at the NM/CeO_2 interface [39,43].

The reaction mechanism is generally investigated under stationary feed stream where the occurrence of a "regenerative", i.e. redox type of reaction mechanism is less likely, whereas occurrence of such a mechanism is highly probable under a feed stream cycled between oxidising and reducing conditions, where reduction/oxidation of CeO_2 sites can effectively occur. Consistently, TWC activity of a model $Pt/CeO_2/Al_2O_3$ catalyst was much more effectively promoted when water was added to the simulated exhaust mixture under cycled feed stream compared to stationary streams, either reducing or oxidising [44]. Under cycled conditions, most of the reduced ceria moiety is oxidised by water in the exhaust, generating H_2 [18,44]. Production of H_2 under reaction condition is an important aspect as NO_x reduction is very fast when H_2 is used as reducing agent even under oxidising conditions (lean $DeNO_x$) [45–47] and, in addition, it promotes removal of adsorbed SO_x [48].

These considerations indicate that OSC may be considered as a complex phenomenon in that the pure redox process (equation (1)) can hardly be considered apart from the whole reaction network that occurs under the exhaust conditions, as many of the chemical reactions are intimately linked together. On the other hand, it has been unequivocally shown that catalytic properties, in particular those of CeO_2 and NM/CeO_2, are directly linked to the reducibility of CeO_2 at low temperature (≤770 K) [49].

As shown in figure 4, upon redox ageing at 1000 °C, both CeO_2 and Rh/CeO_2 strongly sinter with surface area dropping below 10 $m^2\ g^{-1}$. Fresh samples feature the typical two reduction peak TPR profile where the low temperature (LT, <800 K) peak is associated with reduction of the surface whereas the peak at high temperature (HT, ≈1100 K) is associated with reduction in the bulk of CeO_2 [30,50]. In the presence of the NM,

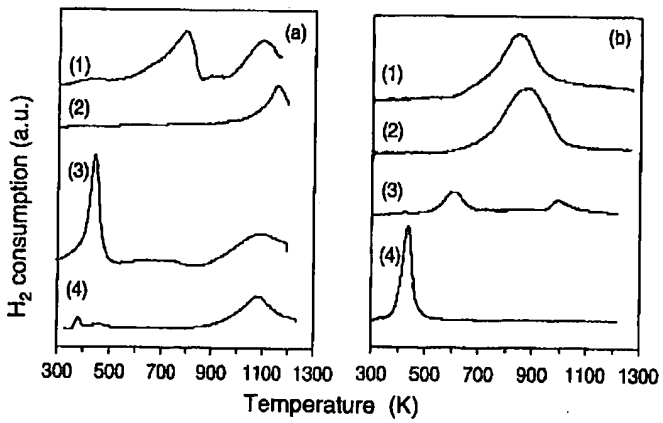

Figure 4. Effect of redox ageing on the H_2-TPR profiles of (a) CeO_2 [1,2] and Rh/CeO_2 [3,4]. Surface areas: fresh: 190 $m^2\ g^{-1}$ [1,3] and redox-aged: < 10 $m^2\ g^{-1}$ [2,4]; (b) $Ce_{0.5}Zr_{0.5}O_2$ [1,2] and $Rh/Ce_{0.5}Zr_{0.5}O_2$ [3–5]; Surface areas: fresh: 65 $m^2\ g^{-1}$ [1,3], redox-aged: <10 $m^2\ g^{-1}$ [2,4] and calcined 1873 K <10 $m^2\ g^{-1}$ [5] (adapted from [35,64,95,128]). The peak at 1000 K in fresh $Rh/Ce_{0.5}Zr_{0.5}O_2$ is attributed to reduction of some CeO_2 not incorporated into the solid solution.

the LT peak shifts down to 450 K, which is associated with the ability of Rh to activate and spill hydrogen over the support thus facilitating surface reduction.

In reality, more complex processes occur during the TPR experiment. Due to poor thermal stability of CeO_2 under a reducing atmosphere [51], sintering of the high surface area material occurs concurrently to the reduction process. Consistent with this, the TPR profile of such high surface nano-crystalline materials could be modelled by considering a two component system: nanocrystalline and bulk CeO_2 where the latter reduce and simultaneously sinter to form bulk CeO_2 in the TPR experiment [52,53]. As a consequence of the loss of surface area (sintering), the low temperature reduction peaks disappear in the TPR profile of the aged sample. Notice that also the NM–CeO_2 interaction, detected by the shift of the LT peak to lower temperature, is no longer detected in the aged samples indicating permanent loss of LT reduction capability, i.e. total OSC.

The critical importance of the extent of the surface area of CeO_2 for the low temperature redox processes suggested that at the usual converter working temperatures, and under the periodic A/F operations, redox processes in a NM/CeO_2 system are essentially limited to the surface. These observations immediately point out the major issue of the late 1980s and early 1990s TWCs, which was the thermal stability of the surface area of the CeO_2 promoter: a drop in the CeO_2 surface area is directly related to catalyst deactivation.

3.3. *Effect of ZrO_2 on the redox behaviour of CeO_2*

Modification of CeO_2 by addition of ZrO_2 has represented a major breakthrough in the development of the OSC promoters, and hence TWC technology [3,49,54,55]. It is interesting to note that use of ZrO_2 as a TWC ingredient can be traced back nearly 20 years [56–58], but a major reason in these early attempts was to place the Rh component onto ZrO_2, thus preventing the undesirable interaction of Rh and Al_2O_3 leading to hardly reducible species Rh^{3+} species. Formation of isolated Rh^{3+} species is not favoured over ZrO_2 [59]. Only later, the beneficial effects of ZrO_2 on the efficiency and thermal stability of the OSC promoter have been recognised [60–63] and it is now well accepted that formation of a CeO_2–ZrO_2 solid solution represents a key factor to improve both thermal stability and OSC of CeO_2.

The effect of insertion of ZrO_2 into the CeO_2 lattice on the total OSC is striking as denoted by the persistence of the LT peak in the TPR profiles of ZrO_2-containing aged samples (figure 4), in contrast to CeO_2 and Rh/CeO_2. Since comparable sintering was experienced by both types of catalyst, ZrO_2 clearly and significantly modifies the chemical behaviour so that even reduction in the bulk occurs at a low temperature.

The major point is that the HT peak, that in CeO_2 is associated with reduction in the bulk, moves to temperatures comparable to those of the LT peak in CeO_2, associated with surface (nano-crystalline) reduction. The fact that bulk properties may play a significant role in the reduction of CeO_2–ZrO_2 was pointed out by early investigations [63,64] of NM/CeO_2–ZrO_2 prepared by a solid state synthesis, i.e. by firing at 1873 K. The observation that an efficient low temperature redox process occurred over such systems, nearly fully sintered, provided that an appropriate amount of ZrO_2 is inserted into the host CeO_2 lattice, could in principle lead to intrinsically thermally stable promoters since the bulk rather than the surface alone may act as an oxygen reservoir.

For practical applications, however, high surface area (HSA) is needed to allow efficient NM dispersion. This adds complexity to the system, due to the meta-stable nature of the CeO_2–ZrO_2 solid solutions that makes the preparation difficult and detection of a single phase CeO_2–ZrO_2 HSA product. For a detailed discussion of these aspects we refer the reader to a recent review [1], whereas here we will focus on aspects related to the redox property and in particular the reduction mechanism with the aim to provide a guide for developing novel materials.

3.3.1. *OSC of CeO_2–ZrO_2 and NM/CeO_2–ZrO_2 systems using H_2 as reducing agent (H_2–OSC)*

Reduction behaviour of CeO_2–ZrO_2 and NM/CeO_2–ZrO_2-containing materials has been intensively investigated in the last years [49]. However, due to the difficulty in obtaining single phase HSA products by synthesis [1,49], a rationale for the H_2-OSC of these systems is difficult to derive. An attempt to provide some better insight into this topic is made here.

A reduction scheme for the reduction process in CeO_2 is depicted in Scheme 1 [27,65–68]. It consists of five steps, four of which are essentially related to the surface, whereas the last one involves bulk. These are:

(1) dissociative chemisorption of H_2 at the surface to form hydroxyls,
(2) reversible reduction of Ce^{4+},
(3) water formation at the surface with creation of oxygen vacancies,
(4) desorption of water,
(5) diffusion of the surface anionic vacancies into the bulk.

In their kinetic investigation of reduction of CeO_2 and Rh/CeO_2, El Fallah *et al.* [65] observed that between 573 and 673 K the reduction starts at the surface through successive H_2 dissociation and anionic vacancy formation, followed by a much slower bulk diffusion step. H_2 dissociation was suggested as the limiting step of the surface process on pure ceria. On Rh/CeO_2 samples the surface reduction becomes very fast, due to the efficient hydrogen dissociation on metallic rhodium.

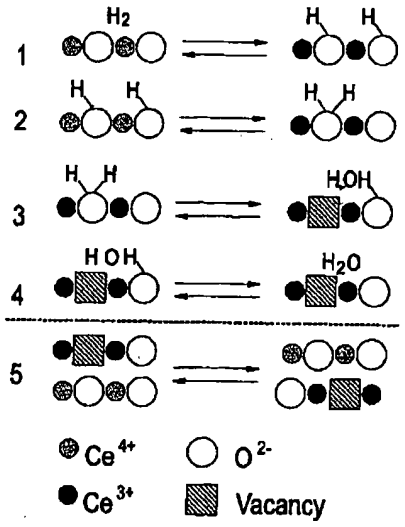

Scheme 1. Proposed reduction mechanism for CeO_2 using H_2 as reducing agent [27,65–68]. Step 2 takes into account the reversible H_2 chemisorption/reduction of CeO_2 as detected by Bernal *et al.* [67–69].

It appears reasonable to extend this model also to the reduction of the CeO_2–ZrO_2 systems: accordingly, the shift of HT peak in aged Rh/CeO_2 to low temperature in the highly sintered $Rh/Ce_{0.5}Zr_{0.5}O_2$ (figure 4) was attributed to promotion of the rate of migration of oxygen in the bulk of the mixed oxide [64]. Consistent with this interpretation, the temperature of the LT reduction peak depends on the CeO_2–ZrO_2 composition: samples with the highest ZrO_2 content compatible with a pseudo-cubic symmetry (around 50 mol% of ZrO_2) were shown to be reduced at the lowest temperatures [64]. This early observation therefore suggested an important role of the CeO_2–ZrO_2 structure – phase nature – upon the H_2-OSC. From a structural point of view, there is a quite significant misfit between the ionic radii of Ce(IV) and Zr(IV) (0.097 versus 0.084 nm [70]), which is responsible for modifications of the CeO_2 lattice upon insertion of ZrO_2. As the amount of ZrO_2 increases, the fluorite lattice of CeO_2 (Fm3m space group) starts to be tetragonally ($P4_2/nmc$ space group) distorted: first a simple oxygen displacement occurs (*t''*-phase) then also the *c/a* lattice parameter increases above 1 (*t'*- and *t*-phase) [71,72]. There are no well-defined boundaries between these phases as the distortion continuously changes with sample composition and is sensitive also to the particle size of the mixed oxide [49,73].

Furthermore, the presence of ZrO_2 in the CeO_2 lattice makes the lattice defective, the highest amount of defects being present at the *t''*–*t'* phase transition [64]. The presence of the defective/distorted structure has been noted as a key factor in promoting the mobility of oxygen in the bulk of the CeO_2–ZrO_2 mixed oxides and hence responsible for the shift of the HT (in CeO_2) reduction peak to LT [64,74]. The exact nature of such defects is still a matter of investigation: Mamontov *et al.* [75,76] recently detected both oxygen vacancy and Frenkel interstitial defects in a CeO_2–ZrO_2 mixed oxide that did not disappear upon annealing at high temperature, in contrast to CeO_2.

This model agrees nicely with the presence of strong distortions in the oxygen sublattice of CeO_2–ZrO_2 that have been detected by EXAFS [74,77]: the low Zr–O coordination number (CN < 8) compared to CN = 8 expected for a fluorite lattice, detected by EXAFS, is perfectly consistent with displacement of oxygen towards octahedral sites as suggested by Mamontov *et al.* [75,76]. Correlation between these defects and LT OSC was inferred on the basis of the observation that both LT OSC and concentration of Frenkel defects declined upon thermal treatment of CeO_2 [76].

The presence of ZrO_2 is crucial to ensure thermal stability of these defects: the smaller Zr(IV) compared to Ce(IV) decreases the lattice parameter of the solid solution, which generates stress that forces migration of oxygen from the small tetrahedral sites to the large octahedral ones. It is consistently found that although the fine structural properties are dependent of the degree of sintering of the sample, oxygen sublattice disorder is always detected [78]. Some subtle details still need to be defined. For example, in contrast to Mamontov *et al.*'s observations, no appreciable amount of Ce^{3+} was detected by magnetic measurement in HSA CeO_2–ZrO_2 [36,79]. Nevertheless, the overall picture well explains the high mobility of the bulk oxygen species in CeO_2–ZrO_2 mixed oxides compared to CeO_2, particularly in nanocrystalline materials [80,81].

So far, the importance of the structural factors in generating efficient low temperature H_2-OSC in CeO_2–ZrO_2 has been underlined. Both composition, and even the mutual cation distribution, e.g. presence of pyrochlore-related ordered structures [82–86], have been invoked as favourable factors leading to enhanced OSC.

However, in addition to these issues, the TPR profiles of CeO_2–ZrO_2 mixed oxides are sensitive to a variety of factors such as degree of sintering [63,73,87,88], sample pre-treatment [36,83,86–92] and phase purity [49,73,93,94]. As exemplified in figure 5, a redox sequence with pre-treatments including sequences of the type: severe oxidation (SO)/severe reduction (TPR)/mild oxidation (MO), produces CeO_2–ZrO_2 oxides that are reduced at remarkably low temperature, despite the fact that no appreciable modification of the bulk structural properties could be detected in the sample [95]. Noticeably, the improvement of the LT reduction is reversibly destroyed by a SO leading to a kind of variable redox behaviour where the reduction temperature depends on the pre-treatment.

The independence of this kind of behaviour on structural properties was confirmed by investigating the TPR behaviour of two single phase – to the detection limits of the criteria discussed in [1,96,97], i.e. after calcination at 1273 K for 5 h – $Ce_{0.2}Zr_{0.8}O_2$ samples. In

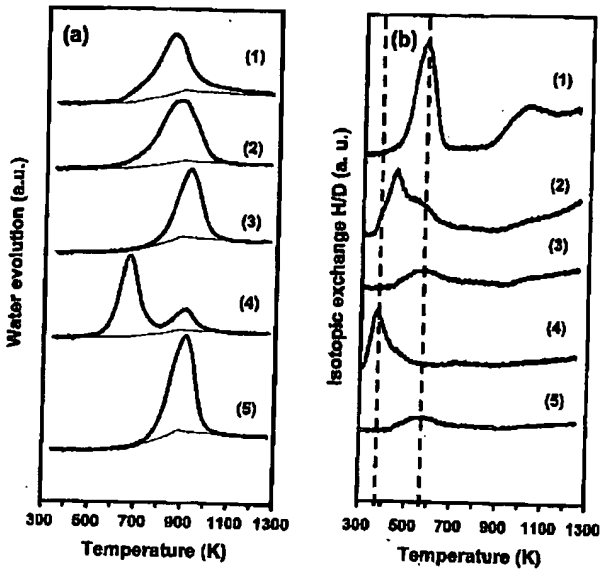

Figure 5. Effects of pre-treatments on *in situ* (a) D_2-TPR profiles and (b) H_2/D_2 scrambling obtained for single phase $Ce_{0.5}Zr_{0.5}O_2$. Pre-treatments: (1) fresh, (2) MO, (3) SO, (4) MO, (5) SO. MO (mild oxidation) = oxidation at 700 K, SO (severe oxidation) = oxidation at 1273 K. Instrumental baseline is added under each trace in (a).

this case, TPR behaviour and dynamic H_2- and CO-OSC were compared for a sinterable and a thermally stable $Ce_{0.2}Zr_{0.8}O_2$, analysing the effects of redox pre-treatments [98]. A remarkably different redox behaviour was observed: the sinterable $Ce_{0.2}Zr_{0.8}O_2$ (BET area 4 $m^2\ g^{-1}$ after calcination at 1273 K) featured a modifiable TPR behaviour of the type depicted in figure 5, whereas pre-treatment insensitive behaviour was detected for the texturally stable $Ce_{0.2}Zr_{0.8}O_2$ (BET area 22 $m^2\ g^{-1}$ after calcination at 1273 K). This highlighted the importance of textural/surface properties in the reduction behaviour of the CeO_2–ZrO_2 mixed oxides in that a strong sintering (including a HT step under oxidising condition) appears as a necessary pre-requisite to obtain low temperature reduction profiles [95].

It must be underlined at this stage that achieving LT reduction in these oxides in the absence of the supported metal is considered an important property since it should lead to thermally stable OSC promoters where the redox property does not depend on the intimate contact between the supported metal and the mixed oxide. This contact, which leads to enhanced reduction at low temperatures (figure 4), can in fact be lost upon sintering of the NM leading to deactivation of the catalyst. On the other hand, the necessity of inclusion of a sintering step at some stage of the preparation of the active species [86,91,95], makes these systems of little interest in real applications as dynamic-OSC property is related also to the extent of surface area of the material (see below).

The H_2/D_2 scrambling profiles reported in figure 5 show significant modification of the capability of the surface to activate hydrogen as a function of the pre-treatment. Noticeably, in all cases scrambling occurs at temperatures well below the temperature of the reduction of the samples as documented by comparison with water evolution profiles (figure 5). This indicates that step 1 in Scheme 1 is not a rate limiting step for reduction under these experimental conditions. A detailed kinetics study of the TPR profiles using H_2 and D_2 as reducing agents [95,99] revealed the presence of an isotopic effect for the HT peak and its absence for the LT peak, indicating that oxygen migration in the bulk could be rate limiting only for the reduction processes occurring at low temperatures. This is an important consideration since it highlights that by appropriately modifying the surface properties of the CeO_2–ZrO_2 mixed oxides, active sites could be generated at the surface that promote LT reduction. Consistently, the sintered species that feature in the LT peak in figure 5 had a modified surface composition compared to the starting oxide even though distinction between the nature of the surface modification induced by SO or MO could not be detected [95].

We have elaborated on these findings to some extent, investigating the effects of modifications at the surface of a single phase — texturally stable — $Ce_{0.2}Zr_{0.8}O_2$ product [100]. As shown in figure 6, a conventional single phase product features a single reduction peak that is centred around 800 K, which is consistent with previous observations [49]. However, when this high surface area sample (52 $m^2\ g^{-1}$) was modified using an advanced surface process operating at an intimate particle nano-morphology, remarkably low reduction could be achieved without any loss of BET area or structural modifications (figure 6, [100]). Although our investigation in progress is aimed at an understanding of the mechanism of this remarkable modification of the reduction behaviour of these mixed oxides, which to our knowledge has been obtained for the first time on HSA samples, we believe that the important message of this finding is that surface properties play a key role in

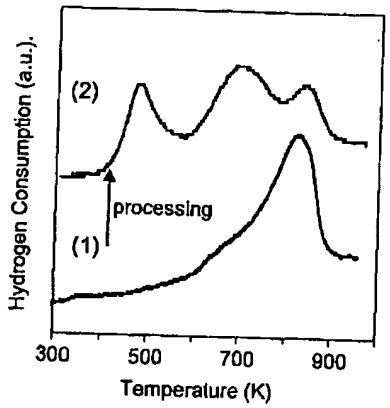

Figure 6. H_2-TPR of (1) conventional and (2) advanced – surface processed single phase $Ce_{0.2}Zr_{0.8}O_2$ products [100].

allowing activation of hydrogen at low temperatures. Consistently, D_2-TPR experiments performed on these advanced products showed the occurrence of hydrogen scrambling at fairly low temperatures.

As shown in figure 4, the presence of NMs fundamentally modifies the reduction (using H_2) behaviour of the CeO_2–ZrO_2 mixed oxides. As stressed above, efficient H_2 activation (step 1 in Scheme 1) plays a key role in producing LT reduction profiles. Over NMs, H_2 activation is an easy reaction. Accordingly, other phenomena, i.e. other steps of the reduction process, become important for the OSC function and may dominate the kinetics of the reduction.

It has long been recognised that H_2 can be effectively adsorbed at the CeO_2, with the NMs, and particularly Rh, playing a key role in this phenomenon, leading to the so-called reversible reduction of CeO_2 [67,68,101]. The term reversible arises from the observation that simple RT evacuation, that desorbs H_2 previously adsorbed on the system, leads to re-oxidation of the reduced Ce^{3+} sites (step 2 in Scheme 1), without creation of oxygen vacancies. Accordingly, Bernal *et al.* [67,68,101] distinguished this "reversible" process from the so-called irreversible reduction, i.e. reduction of CeO_2 leading to creation of oxygen vacancies either surface (step 4 in Scheme 1) or in the bulk (step 5 in Scheme 1). Oxygen or oxygen-containing moieties are necessary to annihilate the oxygen vacancies generated in the irreversible reduction [7,68,102–104].

The relative contribution of these two reduction pathways strongly depends on the temperature of the interaction of the NM/CeO_2-containing system with H_2, as observed in TPD studies that showed different ratios of H_2/H_2O desorption following H_2 adsorption at various temperatures [105]. Significant H_2-OSC was detected as H_2O production generated by alternatively pulsing H_2 and O_2 at RT, over Pt/CeO_2 and Pt/$Ce_{0.68}Zr_{0.32}O_2$ catalysts [106]. Almost no activity was detected over similarly loaded Pt/Al_2O_3, ruling out H_2/O_2 titration at the metal surface as being responsible for the observed H_2-OSC. At RT creation of oxygen vacancies is unlikely, allowing attribution of this OSC to spillover phenomena. A subsequent detailed investigation, in fact, revealed linear correlations between the amount of H_2 spilt over the support, the RT H_2-OSC and the extent of BET surface area of the CeO_2-contaning catalysts [107]. A corollary of these experiments is that measurements of the amount of H_2 spilt over the support can be used to estimate the CeO_2 surface in the TWCs [108,109]. Keeping in mind that under real exhaust conditions the OSC is monitored by measuring the oxygen concentration, it is clear that such spillover phenomena may contribute to the OSC properties at low temperatures. In this context, it is important to underline that the linear relationships between RT H_2-OSC and extent of surface area showed higher spillover efficiency, i.e. higher slope, for Pt/$Ce_{0.68}Zr_{0.32}O_2$ compared to Pt/CeO_2 suggesting a key role of ZrO_2 in promoting the spillover capabilities of CeO_2, in addition to increased oxygen mobility and hence reducibility in the bulk. As the temperatures of the H_2-OSC was increased from RT to 473 K, a shift from a spillover-type of phenomenon to a bulk type of irreversible reduction was observed as denoted by the fact that a SO/TPR/MO (compare above) pre-treated/promoted sintered Pt/$Ce_{0.68}Zr_{0.32}O_2$ featured higher H_2-OSC at 473 K, compared to the initial HSA sample [110].

3.3.2. *OSC of CeO_2–ZrO_2 and NM/CeO_2–ZrO_2 systems using CO as reducing agent (CO-OSC)*

OSC using CO as a reducing agent has received relatively little attention despite the fact that CO represents the most abundant reducing agent contained in the automotive exhaust. Two reasons may account for this: (i) compared to H_2 as reducing agent, there is no such spectacular promotion of the CeO_2 reduction behaviour induced by the supported noble metal [111]; (ii) the need for a more complex experimental set-up to carry out the CO-OSC experiments [33]. The reduction profile is generally measured by detecting the formed CO_2 and/or consumed CO/O_2. CO_2/CO, however, can be formed/consumed both by CO oxidation, which leads to creation of oxygen vacancies and by WGSR of adsorbed CO with surface OH groups leading to dehydroxylation of the support. In fact, the latter reaction was found to significantly contribute to the overall reduction process for Al_2O_3 supported CeO_2 [112]. Finally, the occurrence of disproportionation of CO to give surface carbon and CO_2 cannot be discounted under the CO-TPR/dynamic CO-OSC conditions. The occurrence of the latter reaction can be discriminated by detecting simultaneously both the rates of CO consumption and CO_2 production. However, only a simultaneous quantitative detection of evolved water, together with CO and CO_2, allows an unambiguous assignment of the reduction process in the CO-TPR since both the WGSR and CO oxidation consume/form respectively CO and CO_2 at equivalent rates. Unfortunately, the detection of evolved water is not easy due to its extensive adsorption on the surface of CeO_2.

On the other hand, CO-TPR presents interesting features due to the fact that CO does not diffuse into the bulk of CeO_2 particles. Accordingly, the reduction may be envisaged as a measure of the oxygen diffusion towards the surface where it is removed by interaction with CO in this experiment [38]. Generally speaking, surface processes appear rate limiting in the reduction process when CO is used as reducing agent [113–115]. The effect of ZrO_2 addition to CeO_2 is of little or no benefit under stationary conditions [76,115,116], whereas under a cycled-feed stream (dynamic-CO) improvement of performance is detected [113–116], particularly on aged samples [115].

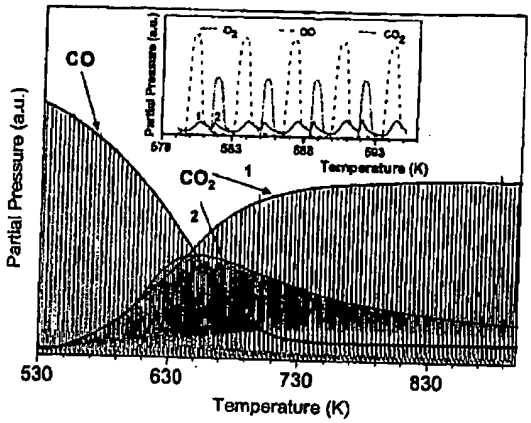

Figure 7. CO oxidation under oscillating (pulses of O_2 and CO) feed stream over $Ce_{0.5}Zr_{0.5}O_2$. Dotted line $m/e = 28$, solid line $m/e = 44$, $m/e = 32$ omitted for clarity, while peak maxima are evidenced by a solid line. The different contributions to CO_2 signal are detailed in the inset (Courtesy of Prof. A. Trovarelli, University of Udine [117]).

It was observed that at low temperatures (573–773 K) diffusion of oxygen in the bulk of the mixed oxides is much faster (two orders of magnitude) higher then in pure CeO_2, suggesting that participation of oxygen from the bulk may contribute to the promotional effect of ZrO_2 addition [115]. As discussed above, the extent of surface area plays a key role in the CO-OSC due to the fact that complex phenomena with surface reduction, CO storage and CO desorption are detected [110]. This is exemplified in figure 7 where two distinct contributions to CO_2 production are identified. The first one, which reaches a steady state at 750 K and appears to coincide with the CO pulse is associated with the direct reaction of CO with oxygen from the support, whereas the second one, which depends on the extent of the surface area, is attributed to desorption of CO_2 induced by the O_2 pulse and/or reaction of adsorbed CO or C_{ads} derived from the disproportionation reaction [26,110,112,117]. It is important to realise that, even if different reaction networks are considered, both contributions can participate in the OSC in that they both regulate the O_2 partial pressure. The presence of the different processes clearly underline the importance of the surface area in the CO-OSC as different reaction pathways are possible depending also on the redox state of the surface [110]. The comparison with the H_2-OSC data clearly point out the necessity of a systematic investigation of the interaction of CO with the surface of these materials to develop the basic knowledge that allows the design of novel materials with tuneable catalytic (redox) properties.

4. Conclusions and perspectives

The picture of the OSC here reported clearly reveals the complexity of this apparently simple redox phenomenon, with clear links between the different phenomena, WGSR, steam reforming, spillover etc., and OSC being established. In fact we believe that a definition of OSC such as that given in equation (1) represents a quite restrictive view of this functionality of the TWCs; consistently the efficiency of the TWCs in the real exhaust is monitored by/related to the oxygen concentration, which in turn is regulated by a complex network of reactions/interactions. The capability of CeO_2-based materials to provide/abstract oxygen at the catalytic sites is perhaps a better description of this OSC functionality where spillover properties, creation/annihilation of oxygen vacancies and various metal support interactions combine to promote the activity of the supported metal. The CeO_2–ZrO_2 based mixed oxides, which are the key OSC promoters, show an almost incredible variability of chemical behaviour despite the apparent simplicity of the system. Both surface and bulk properties play a role. The understanding of the reduction mechanism of these oxides [95] indicated a viable route to produce novel materials where tuneable redox properties, with respect to H_2 as reducing agent, can be achieved on a "real" HSA material. The possibility of producing novel redox materials with tuneable capability to activate simple reactants, where spillover capabilities can be adequately designed, appears as a novel frontier in designing catalysts/catalyst promoters for specific catalytic reactions. For example, the targets obtained in the development of materials for TWCs constitute an important scientific background for the design of new catalytic systems for on-board hydrogen production. In fact, the on-board fuel reformer unit employs a number of catalytic steps involving reactions that routinely occur under the exhaust conditions; most of them appear to be promoted by the NM/CeO_2 interactions [49], and are indirectly linked to OSC as discussed above. Consistently, M/CeO_2–ZrO_2 materials were reported to feature good activities for fuel reforming, water gas shift reaction and preferential oxidation [39,118–126].

Acknowledgments

The authors gratefully thank Prof. M. Graziani, Drs. G. Balducci, P. Fornasiero, N. Hickey, University of Trieste, and Drs. H. Bradshaw, P. Moles, C. Norman from MEL Chemicals for their valuable contribution to the development of the chemistry of CeO_2–ZrO_2 mixed oxides and helpful discussions. MEL Chemicals, University of Trieste, Fondo Trieste 1999, MURST – PRIN 2002 "Stabilisation under reaction conditions of catalysts based on nano-dispersed metals for use in selective oxidation reactions", and Regione Friuli Venezia Giulia, are gratefully acknowledged for financial support.

References

[1] J. Kaspar and P. Fornasiero, J. Solid State Chem. 171 (2003) 19.
[2] Environmental Protection Agency, Federal Register, 65 (2000) 6697.
[3] M. Shelef and R.W. McCabe, Catal. Today 62 (2000) 35.
[4] R.M. Heck and R.J. Farrauto, *Catalytic Air Pollution Control. Commercial Technology*, Van Nostrand Reinhold, New York, 1995, p. 1.
[5] R.J. Farrauto, J.K. Lampert, M.C. Hobson and E.M. Waterman, Appl. Catal. B: Environ. 6 (1995) 263.
[6] C. Padeste, N.W. Cant and D.L. Trimm, Catal. Lett. 18 (1993) 305.
[7] K. Otsuka, M. Hatano and A. Morikawa, J. Catal. 79 (1983) 493.
[8] E.C. Su and W.G. Rothschild, J. Catal. 99 (1986) 506.
[9] H.S. Gandhi, A.G. Piken, M. Shelef and R.G. Delosh, SAE, Paper 760201 (1976), p. 55.
[10] R.K. Herz, Ind. Eng. Chem. Prod. Res. Dev. 20 (1981) 451.
[11] G. Kim, Ind. Eng. Chem. Prod. Res. Dev. 21 (1982) 267.
[12] R.K. Herz, Ind. Eng. Chem. Prod. Res. Dev. 22 (1983) 387.
[13] K.C. Taylor and R.M. Sinkewitch, Ind. Eng. Chem. Prod. Res. Dev. 22 (1983) 45.
[14] R.K. Hertz and E.J. Shinouskis, Ind. Eng. Chem. Prod. Res. Dev. 24 (1985) 385.
[15] H. Muraki, H. Shinjoh, H. Sobukawa, K. Yokota and Y. Fujitani, Ind. Eng. Chem. Prod. Res. Dev. 24 (1985) 43.
[16] B.K. Cho and L.A. West, Ind. Eng. Chem. Fundam. 25 (1986) 158.
[17] J.T. Kummer, J. Phys. Chem. 90 (1986) 4747.
[18] J.C. Schlatter and P.J. Mitchell, Ind. Eng. Chem. Prod. Res. Dev. 19 (1980) 288.
[19] P.L. Silveston, Catal. Today 25 (1995) 175.
[20] S.J. Cornelius, N. Collings and K. Glover, Top. Catal. 16 (2001) 57.
[21] R. Taha, D. Duprez, N. Mouaddib-Moral and C. Gauthier, Oxygen storage capacity of three-way catalysts : a global test for catalyst deactivation in: *Catalysis and Automotive Pollution Control* IV, eds. N. Kruse, A. Frennet and J.M. Bastin (Elsevier Science B.V., Amsterdam, 1998) pp. 549–558.
[22] M. Sideris, Methods for Monitoring and Diagnosing the Efficiency of Catalytic Converters. A Patent Oriented Survey. Vol. 115 (Elsevier Science B.V., Amsterdam, 1997)
[23] T. Moeller, The Lanthanides in: *Comprehensive Inorganic Chemistry*, eds. J.C. Bailar, H.J. Emeleus, R. Nyholm and A.F. Trotman-Dickenson, Ch. 44, (Pergamon Press, Oxford, UK, 1982) p. 1.
[24] H. Cordatos, D. Ford and R.J. Gorte, J. Phys. Chem. 100 (1996) 18128.
[25] J.A. Killner and B.C.H. Steele, *Mass Transport in Anion-Deficient Fluorite Oxides*, in: *Non-Stoichiometric Oxides*, O.T. Sorensen, Ch. 5, (Academic Press, New York, 1981) pp. 233–267.
[26] A. Holmgren and B. Andersson, J. Catal. 178 (1998) 14.
[27] A. Laachir, V. Perrichon, A. Badri, J. Lamotte, E. Catherine, J.C. Lavalley, J. El Fallah, L. Hilaire, F. Le Normand, E. Quemere, N.S. Sauvion and O. Touret, J. Chem. Soc., Faraday Trans. 87 (1991) 1601.
[28] V. Perrichon, A. Laachir, G. Bergeret, R. Frety, L. Tournayan and O. Touret, J. Chem. Soc., Faraday Trans. 90 (1994) 773.
[29] A. Badri, J. Lamotte, J.C. Lavalley, A. Laachir, V. Perrichon, O. Touret, N.S. Sauvion and E. Quemere, Eur. J. Solid State Inorg. Chem. 28 (1991) 445.
[30] H.C. Yao and Y.F. Yu Yao, J. Catal. 86 (1984) 254.
[31] M. Ricken, J. Nolting and I. Riess, J. Solid State Chem. 54 (1984) 89.
[32] J.L.G. Fierro, J. Soria, J. Sanz and J.M. Rojo, J. Solid State Chem. 66 (1987) 154.
[33] M. Boaro, M. Vicario, C. de Leitenburg, G. Dolcetti and A. Trovarelli, Catal. Today 77 (2003) 407.
[34] S. Bernal, G. Blanco, M.A. Cauqui, P. Corchado, J.M. Pintado and J.M. Rodriguez-Izquierdo, Chem. Commun. (1997) 1545.
[35] J. Kaspar, M. Graziani and P. Fornasiero, *Ceria-Containing Three Way Catalysts in: Handbook on the Physics and Chemistry of Rare Earths: The Role of Rare Earths in Catalysis*, eds. K.A. Gschneidner Jr. and L. Eyring, Ch. 184, (Elsevier Science B.V., Amsterdam, 2000) pp. 159–267.
[36] H. Vidal, J. Kaspar, M. Pijolat, G. Colon, S. Bernal, A.M. Cordon, V. Perrichon and F. Fally, Appl. Catal. B: Environ. 27 (2000) 49.
[37] K.C. Taylor, Automobile catalytic converters in: *Catalysis-Science and Technology*, eds. J.R. Anderson and M. Boudart, Ch. 2, (Springer-Verlag, Berlin, 1984) pp. 119–170.
[38] A. Trovarelli, Catal. Rev.-Sci. Eng. 38 (1996) 439.
[39] T. Bunluesin, R.J. Gorte and G.W. Graham, Appl. Catal. B: Environ. 15 (1998) 107.
[40] J. Barbier and D. Duprez, Appl. Catal. B: Environ. 4 (1994) 105.
[41] M. Weibel, F. Garin, P. Bernhardt, G. Maire and M. Prigent, Influence of water in the activity of catalytic converters in: *Catalysis and Automotive Pollution Control II*, ed. A. Crucg (Elsevier, Amsterdam, 1991) pp. 195–205.
[42] T. Shido and Y. Iwasawa, J. Catal. 141 (1993) 71.
[43] R.H. Nibbelke, M.A.J. Campman, J.H.B.J. Hoebink and G.B. Marin, J. Catal. 171 (1997) 358.
[44] J.R. Gonzalez-Velasco, J.A. Botas, J.A. Gonzalez-Marcos and M.A. Gutierrez-Ortiz, Appl. Catal. B: Environ. 12 (1997) 61.
[45] S. Satokawa, Chem. Lett. (2000) 294.
[46] W.C. Hecker and A.T. Bell, J. Catal. 88 (1984) 289.
[47] R. Burch and M.D. Coleman, Appl. Catal. B: Environ. 23 (1999) 115.
[48] H. Hirata, I. Hachisuka, Y. Ikeda, S. Tsuji and S. Matsumoto, Top. Catal. 16 (2001) 145.
[49] J. Kaspar, P. Fornasiero and M. Graziani, Catal. Today 50 (1999) 285.
[50] M.F.L. Johnson and J. Mooi, J. Catal. 103 (1987) 502.
[51] V. Perrichon, A. Laachir, S. Abouarnadasse, O. Touret and G. Blanchard, Appl. Catal. A. Gen. 129 (1995) 69.
[52] F. Giordano, A. Trovarelli, C. de Leitenburg, G. Dolcetti and M. Giona, Ind. Eng. Chem. Res. 40 (2001) 4828.
[53] F. Giordano, A. Trovarelli, C. de Leitenburg and M. Giona, J. Catal. 193 (2000) 273.
[54] R.M. Heck and R.J. Farrauto, Appl. Catal. A: Gen. 221 (2001) 443.
[55] H.S. Gandhi, G.W. Graham and R.W. McCabe, J. Catal. 216 (2003) 433.
[56] H.K. Stepien, W.B. Williamson and H.S. Gandhi, *SAE Technical Paper Series*, 800843 (1980) 6.
[57] Y. Fujitani, H. Muraki, S. Kondoh, M. Tomita, K. Yokota, H. Sobukawa and T. Nakamura, Kabushiki Kaisha Toyota Chuo Kenkyusho (Aichi,J., assignee. 4,316,822 (Issued: 1982), Priority: 214,279 (Appl. Date: 1980 Dec. 8).
[58] H.C. Yao, H.K. Stepien and H.S. Gandhi, J. Catal. 61 (1980) 547.
[59] R. Burch and P.K. Loader, Appl. Catal. A: Gen. 143 (1996) 317.
[60] T. Murota, T. Hasegawa, S. Aozasa, H. Matsui and M. Motoyama, J. Alloys Comp. 193 (1993) 298.
[61] S. Matsumoto, N. Miyoshi, T. Kanazawa, M. Kimura and M. Ozawa, *The effect of complex oxides in Ce–La and Ce–Zr systems on thermal resistant three way catalyst*, in: *Catalytic Science and Technology*, ed. S. Yoshida (VCH-Kodansha, Weinheim-Tokyo, 1991) pp. 335–338.
[62] M. Ozawa, M. Kimura and A. Isogai, J. Alloys Comp. 193 (1993) 73.
[63] G. Ranga Rao, J. Kaspar, R. Di Monte, S. Meriani and M. Graziani, Catal. Lett. 24 (1994) 107.
[64] P. Fornasiero, R. Di Monte, G. Ranga Rao, J. Kaspar, S. Meriani, A. Trovarelli and M. Graziani, J. Catal. 151 (1995) 168.

[65] J. El Fallah, S. Boujana, H. Dexpert, A. Kiennemann, J. Majerus, O. Touret, F. Villain and F. Le Normand, J. Phys. Chem. 98 (1994) 5522.
[66] F. Le Normand, L. Hilaire, K. Kili, G. Krill and G. Maire, J. Phys. Chem. 92 (1988) 2561.
[67] S. Bernal, J.J. Calvino, G.A. Cifredo, J.M. Rodriguez-Izquierdo, V. Perrichon and A. Laachir, J. Catal. 137 (1992) 1.
[68] S. Bernal, J.J. Calvino, G.A. Cifredo and J.M. Rodriguez-Izquierdo, J. Phys. Chem. 99 (1995) 11794.
[69] S. Bernal, J.J. Calvino, G.A. Cifredo, J.M. Gatica, J.A. Perez-Omil and J.M. Pintado, J. Chem. Soc., Faraday Trans. 89 (1993) 3499.
[70] R.D. Shannon, Acta Crystallogr. A32 (1976) 751.
[71] M. Yashima, H. Arashi, M. Kakihana and M. Yoshimura, J. Am. Ceram. Soc. 77 (1994) 1067.
[72] M. Yashima, M. Kakihana and M. Yoshimura, Solid State Ion. 86–88 (1996) 1131.
[73] P. Fornasiero, G. Balducci, R. Di Monte, J. Kaspar, V. Sergo, G. Gubitosa, A. Ferrero and M. Graziani, J. Catal. 164 (1996) 173.
[74] G. Vlaic, R. Di Monte, P. Fornasiero, E. Fonda, J. Kaspar and M. Graziani, J. Catal. 182 (1999) 378.
[75] E. Mamontov and T. Egami, J. Phys. Chem. Solids 61 (2000) 1345.
[76] E. Mamontov, T. Egami, R. Brezny, M. Koranne and S. Tyagi, J. Phys. Chem. B 104 (2000) 11110.
[77] G. Vlaic, P. Fornasiero, S. Geremia, J. Kaspar and M. Graziani, J. Catal. 168 (1997) 386.
[78] P. Fornasiero, E. Fonda, R. Di Monte, G. Vlaic, J. Kaspar and M. Graziani, J. Catal. 187 (1999) 177.
[79] M. Daturi, E. Finocchio, C. Binet, J.C. Lavalley, F. Fally, V. Perrichon, H. Vidal, N. Hickey and J. Kaspar, J. Phys. Chem. B 104 (2000) 9186.
[80] M. Boaro, A. Trovarelli, J.H. Hwang and T.O. Mason, Solid State Ion. 147 (2002) 85.
[81] G. Chiodelli, G. Flor and M. Scagliotti, Solid State Ion. 91 (1996) 109.
[82] A. Suda, Y. Ukyo, H. Sobukawa and M. Sugiura, J. Ceram. Soc. Jpn. 110 (2002) 126.
[83] N. Izu, T. Omata and S. Otsuka-Yao-Matsuo, J. Alloys Comp. 270 (1998) 107.
[84] H. Kishimoto, T. Omata, S. Otsuka-Yao-Matsuo, K. Ueda, H. Hosono and H. Kawazoe, J. Alloys Comp. 312 (2000) 94.
[85] T. Omata, H. Kishimoto, S. Otsuka-Yao-Matsuo, N. Ohtori and N. Umesaki, J. Solid. State. Chem. 147 (1999) 573.
[86] S. Otsuka-Yao-Matsuo, T. Omata, N. Izu and H. Kishimoto, J. Solid. State. Chem. 138 (1998) 47.
[87] G. Balducci, P. Fornasiero, R. Di Monte, J. Kaspar, S. Meriani and M. Graziani, Catal. Lett. 33 (1995) 193.
[88] H. Vidal, J. Kaspar, M. Pijolat, G. Colon, S. Bernal, A. Cordon, V. Perrichon and F. Fally, Appl. Catal. B: Environ. 30 (2001) 75.
[89] R.T. Baker, S. Bernal, G. Blanco, A.M. Cordon, J.M. Pintado, J.M. Rodriguez-Izquierdo, F. Fally and V. Perrichon, Chem. Commun. (1999) 149.
[90] K. Nakano, T. Masui and G. Adachi, J. Alloys Comp. 344 (2002) 342.
[91] T. Masui, K. Nakano, T. Ozaki, G. Adachi, Z.C. Kang and L. Eyring, Chem. Mater. 13 (2001) 1834.
[92] T. Ozaki, T. Masui, K. Machida, G. Adachi, T. Sakata and H. Mori, Chem. Mater. 12 (2000) 643.
[93] Y. Nagai, T. Yamamoto, T. Tanaka, S. Yoshida, T. Nonaka, T. Okamoto, A. Suda and M. Sugiura, Catal. Today 74 (2002) 225.
[94] Y. Nagai, T. Yamamoto, T. Tanaka, S. Yoshida, T. Nonaka, T. Okamoto, A. Suda and M. Sugiura, J. Synchrotron. Radiat. 8 (2001) 616.
[95] P. Fornasiero, T. Montini, M. Graziani, J. Kaspar, A.B. Hungria, A. MartinezArias and J.C. Conesa, PCCP 4 (2002) 149.
[96] J. Kaspar and P. Fornasiero, *Structural properties and thermal stability of ceria-zirconia and related materials* in: *Catalysis by Ceria and Related Materials*, ed. A. Trovarelli, (Imperial College Press, London, 2002) Ch.6, pp. 217–241.
[97] P. Fornasiero, R. Di Monte, J. Kaspar, T. Montini and M. Graziani, Stud. Surf. Sci. Catal. 130 (2000) 1355.
[98] J. Kaspar, R. Di Monte, P. Fornasiero, M. Graziani, H. Bradshaw and C. Norman, Top. Catal. 16 (2001) 83.
[99] P. Fornasiero, J. Kaspar and M. Graziani, Appl. Catal. B: Environ. 22 (1999) L11.
[100] R. Di Monte, J. Kaspar, P. Fornasiero, M. Graziani, J.J. Calvino,H. Bradshaw and C. Norman, *Design of Chemical and Textural Properties of CeO_2–ZrO_2 solid solutions*, communication presented at Europacat VI, Innsbruck (Austria) (2003).
[101] S. Bernal, J.J. Calvino, G.A. Cifredo, J.M. Rodriguez-Izquierdo, V. Perrichon and A. Laachir, J. Chem. Soc., Chem. Commun. (1992) 460.
[102] M. Niwa, Y. Furukawa and Y. Murakami; J. Coll. Interface Sci. 86 (1982) 260.
[103] A. Trovarelli, G. Dolcetti, C. de Leitenburg, J. Kaspar, P. Finetti and A. Santoni, J. Chem. Soc., Faraday Trans. 88 (1992) 1311.
[104] G. Ranga Rao, P. Fornasiero, R. Di Monte, J. Kaspar, G. Vlaic, G. Balducci, S. Meriani, G. Gubitosa, A. Cremona and M. Graziani, J. Catal. 162 (1996) 1.
[105] P. Fornasiero, N. Hickey, J. Kaspar, C. Dossi, D. Gava and M. Graziani, J. Catal. 189 (2000) 326.
[106] N. Hickey, P. Fornasiero, J. Kaspar, M. Graziani, G. Blanco and S. Bernal, Chem. Commun. (2000) 357.
[107] N. Hickey, P. Fornasiero, R. Di Monte, J. Kaspar, M. Graziani and G. Dolcetti, Catal. Lett. 72 (2001) 45.
[108] S. Salasc, V. Perrichon, M. Primet and N. Mouaddib-Moral, J. Catal. 206 (2002) 82.
[109] S. Salasc, V. Perrichon, M. Primet, M. Chevrier and N. Mouaddib-Moral, J. Catal. 189 (2000) 401.
[110] N. Hickey, P. Fornasiero, J. Kaspar, J.M. Gatica and S. Bernal, J. Catal. 200 (2001) 181.
[111] A. Laachir, V. Perrichon, S. Bernal, J.J. Calvino and G.A. Cifredo, J. Mol. Cat. 89 (1994) 391.
[112] C. Serre, F. Garin, G. Belot and G. Maire, J. Catal. 141 (1993) 1.
[113] C.E. Hori, H. Permana, K.Y.S. Ng, A. Brenner, K. More, K.M. Rahmoeller and D.N. Belton, Appl. Catal. B: Environ. 16 (1998) 105.
[114] C.E. Hori, A. Brenner, K.Y.S. Ng, K.M. Rahmoeller and D. Belton, Catal. Today 50 (1999) 299.
[115] M. Boaro, C. de Leitenburg, G. Dolcetti and A. Trovarelli, J. Catal. 193 (2000) 338.
[116] Y. Madier, C. Descorme, A.M. LeGovic and D. Duprez, J. Phys. Chem. B 103 (1999) 10999.
[117] M. Boaro, C. deLeitenburg, G. Dolcetti, A. Trovarelli and M. Graziani, Top. Catal. 16 (2001) 299.
[118] G. Avgouropoulos, T. Ioannides, H.K. Matralis, J. Batista and S. Hocevar, Catal. Lett. 73 (2001) 33.
[119] G. Sedmak, S. Hocevar and J. Levec, J. Catal. 213 (2003) 135.
[120] I.H. Son and A.M. Lane, Catal. Lett. 76 (2001) 151.
[121] L. Basini, A. Guarinoni and A. Aragno, J. Catal. 190 (2000) 284.
[122] W.S. Dong, K.W. Jun, H.S. Roh, Z.W. Liu and S.E. Park, Catal. Lett. 78 (2002) 215.
[123] H.S. Roh, K.W. Jun, W.S. Dong, J.S. Chang, S.E. Park and Y.I. Joe, J. Mol. Catal A Chem. 181 (2002) 137.
[124] P. Pantu, K. Kim and G.R. Gavalas, Appl. Catal. A: Gen. 193 (2000) 203.
[125] Q. Fu, A. Weber and M. Flytzani-Stephanopoulos, Catal. Lett. 77 (2001) 87.
[126] K. Li, Q. Fu and M. Flytzani-Stephanopoulos, Appl. Catal. B: Environ. 27 (2000) 179.
[127] R.W. McCabe and J.M. Kisenyi, Chem. Ind.-London (1995) 605.
[128] P. Fornasiero, J. Kaspar and M. Graziani, J. Catal. 167 (1997) 576.

Sixth Edition

ADVANCED INORGANIC CHEMISTRY

F. Albert Cotton

W. T. Doherty-Welch Foundation Distinguished Professor of Chemistry
Texas A&M University
College Station, Texas, USA

Geoffrey Wilkinson

Sir Edward Frankland Professor of Inorganic Chemistry
Imperial College of Science and Technology
University of London
London, England

Carlos A. Murillo

Professor
University of Costa Rica
Ciudad Universitaria, Costa Rica
Adjunct Professor
Texas A&M University
College Station, Texas, USA

Manfred Bochmann

Professor
School of Chemistry
University of Leeds
Leeds, England

A WILEY-INTERSCIENCE PUBLICATION
JOHN WILEY & SONS, INC.
New York • Chichester • Weinheim • Brisbane • Singapore • Toronto

Chapter 19

THE GROUP 3 ELEMENTS AND THE LANTHANIDES

19-1 Overview

The Group 3 elements are scandium, yttrium, and lanthanum. Strictly speaking actinium should also be included, but it is the general practice to associate it with the elements that follow it (the actinides) and treat them all separately, as we do in this book in Chapter 20.

There are fourteen elements that follow lanthanum and these are called the lanthanides. They are listed along with lanthanum in Table 19-1, where some of their principal characteristics are also listed. In passing from La to the last of the lanthanides, lutecium, Lu, the electron configuration goes from [Xe]$5d6s^2$ to [Xe]$4f^{14}5d6s^2$. That is, the fourteen $4f$ electrons are added, although as shown in Table 19-1, not without slight irregularities at several places. Among the Ln^{3+} ions (where Ln is a generic symbol for any one of the lanthanides) the progression is completely regular, from $4f^0$ (La), $4f^1$ (Ce), to $4f^{14}$ (Lu). The lanthanide metals, and La, are all relatively electropositive metals that strongly, although not exclusively, favor the tripositive oxidation state. Because of their very similar chemistries, they generally occur together in Nature and separating them is a non-trivial problem (see Section 19-3).

The lanthanide contraction is the name given to the phenomenon that is evident in the last column of Table 19-1, namely, that there is a steady decrease in the radii of the Ln^{3+} ions, from La to Lu, amounting overall to 0.17 Å. A similar contraction occurs for the metallic radii and is reflected in many smooth and systematic changes in the properties of the elements (Section 19-3). The lanthanide contraction also has consequences for all the elements following Lu. Thus, while the Zr atom is larger than the Ti atom with major consequences in differentiating their chemistries, Hf as well as Hf^{4+} are virtually identical in size to Zr and Zr^{4+} and their chemistries are very, very similar, although not identical. This sort of situation continues (i.e., for the pairs Nb/Ta, Mo/W, etc.) although the divergence in chemical properties progressively increases.

The lanthanide contraction used to be ascribed simply to the fact that while the $4f$ electrons have a considerable part of their wave function within the outer parts of the $4d$, $5s$, and $5p$ orbitals (i.e., the Xe core) thus making them unreactive, they still provide only incomplete shielding of the outer electrons from the steadily

Table 19-1 Some Properties of Lanthanide Atoms and Ions

Atomic number	Name	Symbol	Electronic configuration		$E^0(V)^a$	Radius M^{3+} (Å)
			Atom	M^{3+}		
57	Lanthanum	La	$5d6s^2$	[Xe]	−2.38	1.17
58	Cerium	Ce	$4f^15d^16s^2$	$4f^1$	−2.34	1.15
59	Praseodymium	Pr	$4f^36s^2$	$4f^2$	−2.35	1.13
60	Neodymium	Nd	$4f^46s^2$	$4f^3$	−2.32	1.12
61	Promethium	Pm	$4f^56s^2$	$4f^4$	−2.29	1.11
62	Samarium	Sm	$4f^66s^2$	$4f^5$	−2.30	1.10
63	Europium	Eu	$4f^76s^2$	$4f^6$	−1.99	1.09
64	Gadolinium	Gd	$4f^75d6s^2$	$4f^7$	−2.28	1.08
65	Terbium	Tb	$4f^96s^2$	$4f^8$	−2.31	1.06
66	Dysprosium	Dy	$4f^{10}6s^2$	$4f^9$	−2.29	1.05
67	Holmium	Ho	$4f^{11}6s^2$	$4f^{10}$	−2.33	1.04
68	Erbium	Er	$4f^{12}6s^2$	$4f^{11}$	−2.32	1.03
69	Thulium	Tm	$4f^{13}6s^2$	$4f^{12}$	−2.32	1.02
70	Ytterbium	Yb	$4f^{14}6s^2$	$4f^{13}$	−2.22	1.01
71	Lutetium	Lu	$4f^{14}5d6s^2$	$4f^{14}$	−2.30	1.00

[a] $Ln^{3+} + 3e = Ln$.

increasing nuclear charge. Therefore, the electron cloud as a whole steadily shrinks as the $4f$ shell is filled. In recent years there has been theoretical work suggesting that relativistic effects may also play a role.

The term *rare earth* elements is sometimes applied to the elements La–Lu plus yttrium. The convenience of including La, which, strictly speaking, is not a lanthanide, is obvious. The reason for including Y is that Y has radii (atomic, metallic, ionic) that fall close to those of erbium and holmium and all of its chemistry is in the trivalent state. Hence it resembles the later lanthanides very closely in its chemistry and occurs with them in Nature.

Scandium, on the other hand, is far smaller than any of the lanthanides (Sc^{3+} radius, 0.89 Å) and its chemical behavior deviates in many ways from that of the lanthanides, being in significant ways similar to that of aluminum or gallium.

Although the +3 oxidation state is by far the most common one for the rare earth elements, for some of them others (+2, +4) are of importance. Cerium, and to a much lesser extent Pr and Tb, can form Ln^{4+} ions (formally speaking) but these are strongly oxidizing. Sm, Eu, and to a lesser extent Yb form Ln^{2+} ions. These deviations from "normal" behavior (i.e., formation of only Ln^{3+}) are sometimes attributed to the special stability of empty, half-filled or filled shells: Ce^{4+} ($4f^0$), Eu^{2+} ($4f^7$), Yb^{2+} ($4f^{14}$), but Pr^{4+} ($4f^1$) and Sm^{2+} ($4f^6$) do not fully satisfy this criterion. This idea is better considered as a mnenonic than as an explanation.

Because ligand field stabilization energies are very small for the Ln^{3+} ions, the thermodynamic properties of their compounds as well as their electrode potentials can be fairly accurately correlated by equations based solely on the electrostatic consequences of charge and size.

CRC Handbook of Chemistry and Physics

A Ready-Reference Book of Chemical and Physical Data

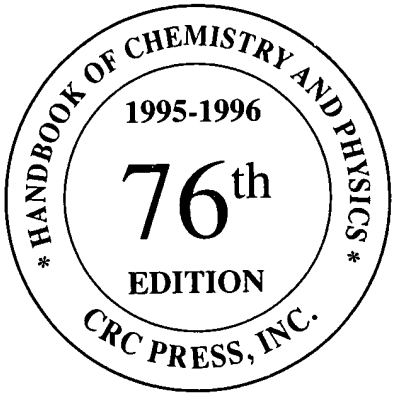

Editor-in-Chief

David R. Lide, Ph.D.

Former Director, Standard Reference Data
National Institute of Standards and Technology

Associate Editor

H. P. R. Frederikse, Ph.D.

(Retired)
Ceramics Division
National Institute of Standards and Technology

CRC Press

Boca Raton New York London Tokyo

PERIODIC TABLE OF THE ELEMENTS

1 Group IA	2 IIA	3 IIIA IIIB	4 IVA IVB	5 VA VB	6 VIA VIB	7 VIIA VIIB	8	9 VIIIA VIII	10	11 IB	12 IIB	13 IIIB IIIA	14 IVB IVA	15 VB VA	16 VIB VIA	17 VIIB VIIA	18 VIIIA	Shell
1 +1 H −1 1.00794 1																	2 0 He 4.0020602 2	K
3 +1 Li 6.941 2-1	4 +2 Be 9.012182 2-2											5 +3 B 10.811 2-3	6 +2 +4 −4 C 12.011 2-4	7 +1 +2 +3 +4 +5 −1 −2 −3 N 14.00674 2-5	8 −2 O 15.9994 2-6	9 −1 F 18.9984032 2-7	10 0 Ne 20.1797 2-8	K-L
11 +1 Na 22.989768 2-8-1	12 +2 Mg 24.3050 2-8-2											13 +3 Al 26.981539 2-8-3	14 +2 +4 −4 Si 28.0855 2-8-4	15 +3 +5 −3 P 30.97362 2-8-5	16 +4 +6 −2 S 32.066 2-8-6	17 +1 +5 +7 −1 Cl 35.4527 2-8-7	18 0 Ar 39.948 2-8-8	K-L-M
19 +1 K 39.0983 -8-8-1	20 +2 Ca 40.078 -8-8-2	21 +3 Sc 44.955910 -8-9-2	22 +2 +3 +4 Ti 47.867 -8-10-2	23 +2 +3 +4 +5 V 50.9415 -8-11-2	24 +2 +3 +6 Cr 51.9961 -8-13-1	25 +2 +3 +4 +7 Mn 54.93085 -8-13-2	26 +2 +3 Fe 55.845 -8-14-2	27 +2 +3 Co 58.93320 -8-15-2	28 +2 +3 Ni 58.6934 -8-16-2	29 +1 +2 Cu 63.546 -8-18-1	30 +2 Zn 65.39 -8-18-2	31 +3 Ga 69.723 -8-18-3	32 +2 +4 Ge 72.61 -8-18-4	33 +3 +5 −3 As 74.92159 -8-18-5	34 +4 +6 −2 Se 78.96 -8-18-6	35 +1 +5 −1 Br 79.904 -8-18-7	36 0 Kr 83.80 -8-18-8	K-L-M-N
37 +1 Rb 85.4678 -18-8-1	38 +2 Sr 87.62 -18-8-2	39 +3 Y 88.90585 -18-9-2	40 +4 Zr 91.224 -18-10-2	41 +3 +5 Nb 92.90638 -18-12-1	42 +6 Mo 95.94 -18-13-1	43 +4 +6 +7 Tc (98) -18-13-2	44 +3 Ru 101.07 -18-15-1	45 +3 Rh 102.90550 -18-16-1	46 +2 +4 Pd 106.42 -18-18-0	47 +1 Ag 107.8682 -18-18-1	48 +2 Cd 112.411 -18-18-2	49 +3 In 114.818 -18-18-3	50 +2 +4 Sn 118.710 -18-18-4	51 +3 +5 −3 Sb 121.760 -18-18-5	52 +4 +6 −2 Te 127.60 -18-18-6	53 +1 +5 +7 −1 I 126.90447 -18-18-7	54 0 Xe 131.29 -18-18-8	-M-N-O
55 +1 Cs 132.90543 -18-8-1	56 +2 Ba 137.327 -18-8-2	57* +3 La 138.9055 -18-9-2	72 +4 Hf 178.49 -32-10-2	73 +5 Ta 180.9479 -32-11-2	74 +6 W 183.84 -32-12-2	75 +4 +6 +7 Re 186.207 -32-13-2	76 +3 +4 Os 190.23 -32-14-2	77 +3 +4 Ir 192.217 -32-15-2	78 +2 +4 Pt 195.08 -32-17-1	79 +1 +3 Au 196.96654 -32-18-1	80 +1 +2 Hg 200.59 -32-18-2	81 +1 +3 Tl 204.3833 -32-18-3	82 +2 +4 Pb 207.2 -32-18-4	83 +3 +5 Bi 208.98037 -32-18-5	84 +2 +4 Po (209) -32-18-6	85 At (210) -32-18-7	86 0 Rn (222) -32-18-8	-N-O-P
87 +1 Fr (223) -18-8-1	88 +2 Ra 226.025 -18-8-2	89** +3 Ac 227.028 -18-9-2	104 +4 Unq (261) -32-10-2	105 Unp (262) -32-11-2	106 Unh (263) -32-12-2	107 Uns (262) -32-13-2	108 Uno (265) -32-14-2	109 Une (266) -32-15-2	110 Uun (269) -32-16-2									O P Q

*Lanthanides	58 +3 +4 Ce 140.115 -19-9-2	59 +3 Pr 140.90765 -21-8-2	60 +3 Nd 144.24 -22-8-2	61 +3 Pm (145) -23-8-2	62 +2 +3 Sm 150.36 -24-8-2	63 +2 +3 Eu 151.965 -25-8-2	64 +3 Gd 157.25 -25-9-2	65 +3 Tb 158.92534 -27-8-2	66 +3 Dy 162.50 -28-8-2	67 +3 Ho 164.93032 -29-8-2	68 +3 Er 167.26 -30-8-2	69 +3 Tm 168.93421 -31-8-2	70 +2 +3 Yb 173.04 -32-8-2	71 +3 Lu 174.967 -32-9-2				N O P
**Actinides	90 +4 Th 232.0381 -18-10-2	91 +5 +4 Pa 231.03588 -20-9-2	92 +3 +4 +5 +6 U 238.0289 -21-9-2	93 +3 +4 +5 +6 Np 237.048 -22-9-2	94 +3 +4 +5 +6 Pu (244) -24-8-2	95 +3 +4 +5 +6 Am (243) -25-8-2	96 +3 Cm (247) -25-9-2	97 +3 +4 Bk (247) -27-8-2	98 +3 Cf (251) -28-8-2	99 +3 Es (252) -29-8-2	100 +3 Fm (257) -30-8-2	101 +2 +3 Md (258) -31-8-2	102 +2 +3 No (259) -32-8-2	103 +3 Lr (260) -32-9-2				O P Q

KEY TO CHART

Atomic Number → 50 +2 ← Oxidation States
Symbol → Sn +4
1993 Atomic Weight → 118.71
18 18 4 ← Electron Configuration

New notation →
Previous IUPAC form →
CAS version →

The new IUPAC format numbers the groups from 1 to 18. The previous IUPAC numbering system and the system used by Chemical Abstracts Service (CAS) are also shown. For radioactive elements that do not occur in nature, the mass number of the most stable isotope is given in parentheses.

REFERENCES

1. G. J. Leigh, Editor, *Nomenclature of Inorganic Chemistry*, Blackwell Scientific Publications, Oxford, 1990.
2. *Chemical and Engineering News*, 63(5), 27, 1985.
3. Atomic Weights of the Elements, 1993, *Pure & Appl. Chem.*, 66, 2423, 1994

CRC Handbook of Chemistry and Physics

A Ready-Reference Book of Chemical and Physical Data

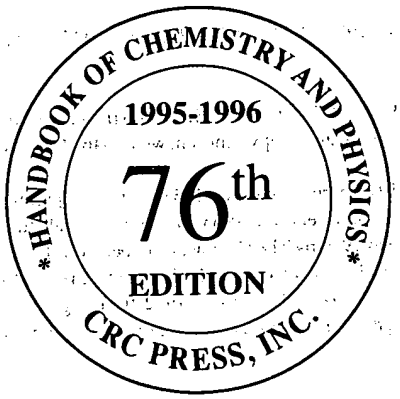

Editor-in-Chief

David R. Lide, Ph.D.

Former Director, Standard Reference Data
National Institute of Standards and Technology

Associate Editor

H. P. R. Frederikse, Ph.D.

(Retired)
Ceramics Division
National Institute of Standards and Technology

CRC Press

Boca Raton New York London Tokyo

industry with countless uses. Mixed with sand it hardens as mortar and plaster by taking up carbon dioxide from the air. Calcium from limestone is an important element in Portland cement. The solubility of the carbonate in water containing carbon dioxide causes the formation of caves with stalactites and stalagmites and is responsible for hardness in water. Other important compounds are the carbide (CaC_2), chloride ($CaCl_2$), cyanamide ($CaCN_2$), hypochlorite ($Ca(OCl)_2$), nitrate ($Ca(NO_3)_2$), and sulfide (CaS).

Californium — (State and University of California), Cf; at. wt. (251); at. no. 98. Californium, the sixth transuranium element to be discovered, was produced by Thompson, Street, Ghiorso, and Seaborg in 1950 by bombarding microgram quantities of ^{242}Cm with 35 MeV helium ions in the Berkeley 60-inch cyclotron. Californium (III) is the only ion stable in aqueous solutions, all attempts to reduce or oxidize californium (III) having failed. The isotope ^{249}Cf results from the beta decay of ^{249}Bk while the heavier isotopes are produced by intense neutron irradiation by the reactions:

$$^{249}Bk(n,\gamma) \rightarrow {}^{250}Bk \xrightarrow{-\beta} {}^{250}Cf \text{ and } {}^{249}Cf(n,\gamma) \rightarrow {}^{250}Cf$$

followed by

$$^{250}Cf(n,\gamma) \rightarrow {}^{251}Cf(n,\gamma) \rightarrow {}^{252}Cf$$

The existence of the isotopes ^{249}Cf, ^{250}Cf, ^{251}Cf, and ^{252}Cf makes it feasible to isolate californium in weighable amounts so that its properties can be investigated with macroscopic quantities. Californium-252 is a very strong neutron emitter. One microgram releases 170 million neutrons per minute, which presents biological hazards. Proper safeguards should be used in handling californium. In 1960 a few tenths of a microgram of californium trichloride, $CfCl_3$, californium oxychloride, CfOCl, and californium oxide, Cf_2O_3, were first prepared. Reduction of californium to its metallic state has not yet been accomplished. Because californium is a very efficient source of neutrons, many new uses are expected for it. It has already found use in neutron moisture gages and in well-logging (the determination of water and oil-bearing layers). It is also being used as a portable neutron source for discovery of metals such as gold or silver by on-the-spot activation analysis. ^{252}Cf is now being offered for sale by the O.R.N.L. at a cost of $10/μg. As of May 1975, more than 63 mg have been produced and sold. It has been suggested that californium may be produced in certain stellar explosions, called *supernovae*, for the radioactive decay of ^{254}Cf (55-day half-life) agrees with the characteristics of the light curves of such explosions observed through telescopes. This suggestion, however, is questioned.

Carbon — (L. *carbo*, charcoal), C; at. wt. 12.011; at. no. 6; m.p. ~3550°C; graphite sublimes at 3825°C; triple point, (graphite-liquid-gas), 4492°C at a pressure of 10.3 MPa and (graphite-diamond-liquid), 3830—3930° at a pressure of 12—13 GPa; sp. gr. amorphous 1.8 to 2.1, graphite 1.9 to 2.3, diamond 3.15 to 3.53 (depending on variety); gem diamond 3.513 (25°C); valence 2, 3, or 4. Carbon, an element of prehistoric discovery, is very widely distributed in nature. It is found in abundance in the sun, stars, comets, and atmospheres of most plants. Carbon in the form of microscopic diamonds is found in some meteorites. Natural diamonds are found in *kimberlite* of ancient volcanic "pipes," such as found in South Africa, Arkansas, and elsewhere. Diamonds are now also being recovered from the ocean floor off the Cape of Good Hope. About 30% of all industrial diamonds used in the U.S. are now made synthetically. The energy of the sun and stars can be attributed at least in part to the well-known carbon-nitrogen cycle. Carbon is found free in nature in three allotropic forms: amorphous, graphite, and diamond. A fourth form, known as "white" carbon, is now thought to exist. Graphite is one of the softest known materials while diamond is one of the hardest. Graphite exists in two forms: alpha and beta. These have identical physical properties, except for their crystal structure. Naturally occurring graphites are reported to contain as much as 30% of the rhombohedral (beta) form, whereas synthetic materials contain only the alpha form. The hexagonal alpha type can be converted to the beta by mechanical treatment, and the beta form reverts to the alpha on heating it above 1000°C. In 1969 a new allotropic form of carbon was produced during the sublimation of pyrolytic graphite at low pressures. Under free-vaporization conditions above ~2550 K, "white" carbon forms as small transparent crystals on the edges of the basal planes of graphite. The interplanar spacings of "white" carbon are identical to those of carbon form noted in the graphitic gneiss from the Ries (meteoritic) Crater of Germany. "White" carbon is a transparent birefringent material. Little information is presently available about this allotrope. In combination, carbon is found as carbon dioxide in the atmosphere of the earth and dissolved in all natural waters. It is a component of great rock masses in the form of carbonates of calcium (limestone), magnesium, and iron. Coal, petroleum, and natural gas are chiefly hydrocarbons. Carbon is unique among the elements in the vast number and variety of compounds it can form. With hydrogen, oxygen, nitrogen, and other elements, it forms a very large number of compounds, carbon atom often being linked to carbon atom. There are close to ten million known carbon compounds, many thousands of which are vital to organic and life processes. Without carbon, the basis for life would be impossible. While it has been thought that silicon might take the place of carbon in forming a host of similar compounds, it is now not possible to form stable compounds with very long chains of silicon atoms. The atmosphere of Mars contains 96.2% CO_2. Some of the most important compounds of carbon are carbon dioxide (CO_2), carbon monoxide (CO), carbon disulfide (CS_2), chloroform ($CHCl_3$), carbon tetrachloride (CCl_4), methane (CH_4), ethylene (C_2H_4), acetylene (C_2H_2), benzene (C_6H_6), ethyl alcohol (C_2H_5OH), acetic acid (CH_3COOH), and their derivatives. Carbon has seven isotopes. In 1961 the International Union of Pure and Applied Chemistry adopted the isotope carbon-12 as the basis for atomic weights. Carbon-14, an isotope with a half-life of 5715 years, has been widely used to date such materials as wood, archeological specimens, etc. Carbon-13 is now commercially available at a cost of $700/g.

Cerium — (named for the asteroid *Ceres*, which was discovered in 1801 only 2 years before the element), Ce; at. wt. 140.115; at. no. 58; m.p. 799°C; b.p. 3424°C; sp. gr. 6.770 (25°C); valence 3 or 4. Discovered in 1803 by Klaproth and by Berzelius and Hisinger; metal prepared by Hillebrand and Norton in 1875. Cerium is the most abundant of the metals of the so-called rare earths. It is found in a number of minerals including *allanite* (also known as *orthite*), *monazite*, *bastnasite*, *cerite*, and *samarskite*. Monazite and bastnasite are presently the two most important sources of cerium. Large deposits of monazite found on the beaches of Travancore, India, in river sands in Brazil, and deposits of *allanite* in the western United States, and *bastnasite* in Southern California will supply cerium, thorium, and the other rare-earth metals for many years to come. Metallic cerium is prepared by metallothermic reduction techniques, such as by reducing cerous fluoride with calcium, or by electrolysis of molten cerous chloride or other cerous halides. The metallothermic technique is used to produce high-purity cerium. Cerium is especially interesting because of its variable electronic

structure. The energy of the inner 4f level is nearly the same as that of the outer or valence electrons, and only small amounts of energy are required to change the relative occupancy of these electronic levels. This gives rise to dual valency states. For example, a volume change of about 10% occurs when cerium is subjected to high pressures or low temperatures. It appears that the valence changes from about 3 to 4 when it is cooled or compressed. The low temperature behavior of cerium is complex. Four allotropic modifications are thought to exist: cerium at room temperature and at atmospheric pressure is known as γcerium. Upon cooling to −16°C, γcerium changes to β cerium. The remaining γcerium starts to change to α cerium when cooled to −172°C, and the transformation is complete at −269°C. α Cerium has a density of 8.16; δ cerium exists above 726°C. At atmospheric pressure, liquid cerium is more dense than its solid form at the melting point. Cerium is an iron-gray lustrous metal. It is malleable, and oxidizes very readily at room temperature, especially in moist air. Except for europium, cerium is the most reactive of the "rare-earth" metals. It slowly decomposes in cold water, and rapidly in hot water. Alkali solutions and dilute and concentrated acids attack the metal rapidly. The pure metal is likely to ignite if scratched with a knife. Ceric salts are orange red or yellowish; cerous salts are usually white. Cerium is a component of misch metal, which is extensively used in the manufacture of pyrophoric alloys for cigarette lighters, etc. While cerium is not radioactive, the impure commercial grade may contain traces of thorium, which is radioactive. The oxide is an important constituent of incandescent gas mantles and it is emerging as a hydrocarbon catalyst in "self-cleaning" ovens. In this application it can be incorporated into oven walls to prevent the collection of cooking residues. As ceric sulfate it finds extensive use as a volumetric oxidizing agent in quantitative analysis. Cerium compounds are used in the manufacture of glass, both as a component and as a decolorizer. The oxide is finding increased use as a glass polishing agent instead of rouge, for it is much faster than rouge in polishing glass surfaces. Cerium, with other rare earths, is used in carbon-arc lighting, especially in the motion picture industry. It is also finding use as an important catalyst in petroleum refining and in metallurgical and nuclear applications. In small lots, 99.9% cerium costs about $125/kg.

Cesium — (L. *caesius*, sky blue), Cs; at. wt. 132.90543; at. no. 55; m.p. 28.44 ± 0.01°C; b.p. 671°C; sp. gr. 1.873 (20°C); valence 1. Cesium was discovered spectroscopically by Bunsen and Kirchhoff in 1860 in mineral water from Durkheim. Cesium, an alkali metal, occurs in *lepidolite*, *pollucite* (a hydrated silicate of aluminum and cesium), and in other sources. One of the world's richest sources of cesium is located at Bernic Lake, Manitoba. The deposits are estimated to contain 300,000 tons of pollucite, averaging 20% cesium. It can be isolated by electrolysis of the fused cyanide and by a number of other methods. Very pure, gas-free cesium can be prepared by thermal decomposition of cesium azide. The metal is characterized by a spectrum containing two bright lines in the blue along with several others in the red, yellow, and green. It is silvery white, soft, and ductile. It is the most electropositive and most alkaline element. Cesium, gallium, and mercury are the only three metals that are liquid at room temperature. Cesium reacts explosively with cold water, and reacts with ice at temperatures above −116°C. Cesium hydroxide, the strongest base known, attacks glass. Because of its great affinity for oxygen the metal is used as a "getter" in electron tubes. It is also used in photoelectric cells, as well as a catalyst in the hydrogenation of certain organic compounds. The metal has recently found application in ion propulsion systems. Cesium is used in atomic clocks, which are accurate to 5 s in 300 years. Its chief compounds are the chloride and the nitrate. Cesium has 32 isotopes (more than any element) with masses ranging from 114 to 145. The present price of cesium is about $30/g.

Chlorine — (Gr. *chloros*, greenish yellow), Cl; at. wt. 35.4527; at. no. 17; m.p. −101.5°C; b.p. −34.04°C; density 3.214 g/l; sp. gr. 1.56 (−33.6°C); valence 1, 3, 5, or 7. Discovered in 1774 by Scheele, who thought it contained oxygen; named in 1810 by Davy, who insisted it was an element. In nature it is found in the combined state only, chiefly with sodium as common salt (NaCl), *carnallite* ($KMgCl_3 \cdot 6H_2O$), and *sylvite* (KCl). It is a member of the halogen (salt-forming) group of elements and is obtained from chlorides by the action of oxidizing agents and more often by electrolysis; it is a greenish-yellow gas, combining directly with nearly all elements. At 10°C one volume of water dissolves 3.10 volumes of chlorine, at 30°C only 1.77 volumes. Chlorine is widely used in making many everyday products. It is used for producing safe drinking water the world over. Even the smallest water supplies are now usually chlorinated. It is also extensively used in the production of paper products, dyestuffs, textiles, petroleum products, medicines, antiseptics, insecticides, foodstuffs, solvents, paints, plastics, and many other consumer products. Most of the chlorine produced is used in the manufacture of chlorinated compounds for sanitation, pulp bleaching, disinfectants, and textile processing. Further use is in the manufacture of chlorates, chloroform, carbon tetrachloride, and in the extraction of bromine. Organic chemistry demands much from chlorine, both as an oxidizing agent and in substitution, since it often brings desired properties in an organic compound when substituted for hydrogen, as in one form of synthetic rubber. Chlorine is a respiratory irritant. The gas irritates the mucous membranes and the liquid burns the skin. As little as 3.5 ppm can be detected as an odor, and 1000 ppm is likely to be fatal after a few deep breaths. It was used as a war gas in 1915. Exposure to chlorine should not exceed 0.5 ppm (8-hour time-weighted average — 40 hour week.)

Chromium — (Gr. *chroma*, color), Cr; at. wt. 51.9961; at. no. 24; m.p. 1907°C; b.p. 2671°C; sp. gr. 7.18 to 7.20 (20°C); valence chiefly 2, 3, or 6. Discovered in 1797 by Vauquelin, who prepared the metal the next year, chromium is a steel-gray, lustrous, hard metal that takes a high polish. The principal ore is *chromite* ($FeCr_2O_4$), which is found in Zimbabwe, U.S.S.R., Transvaal, Turkey, Iran, Albania, Finland, Democratic Republic of Madagascar, and the Philippines. The metal is usually produced by reducing the oxide with aluminum. Chromium is used to harden steel, to manufacture stainless steel, and to form many useful alloys. Much is used in plating to produce a hard, beautiful surface and to prevent corrosion. Chromium is used to give glass an emerald green color. It finds wide use as a catalyst. All compounds of chromium are colored: the most important are the chromates of sodium and potassium (K_2CrO_4) and the dichromates ($K_2Cr_2O_7$) and the potassium and ammonium chrome alums, as $KCr(SO_4)_2 \cdot 12H_2O$. The dichromates are used as oxidizing agents in quantitative analysis, also in tanning leather. Other compounds are of industrial value; lead chromate is chrome yellow, a valued pigment. Chromium compounds are used in the textile industry as mordants, and by the aircraft and other industries for anodizing aluminum. The refractory industry has found chromite useful for forming bricks and shapes, as it has a high melting point, moderate thermal expansion, and stability of crystalline structure. Chromium compounds are toxic and should be handled with proper safeguards.

Cobalt — (*Kobald*, from the German, goblin or evil spirit, *cobalos*, Greek, mine), Co; at. wt. 58.93320; at. no. 27; m.p. 1495°C; b.p. 2927°C; sp. gr. 8.9 (20°C); valence 2 or 3. Discovered by Brandt about 1735. Cobalt occurs in the mineral *cobaltite*, *smaltite*, and *erythrite*, and is often associated with nickel, silver, lead, copper, and iron ores, from which it is most frequently obtained as a by-product. It is also present in meteorites. Important ore deposits are found in Zaire, Morocco, and Canada. The U.S. Geological Survey has announced that the bottom of the north central Pacific Ocean may have cobalt-rich deposits at relatively shallow depths in waters close to the Hawaiian Islands and other U.S. Pacific territories. Cobalt is a brittle, hard metal, closely resembling iron and nickel in appearance. It has a magnetic permeability of about two thirds that of iron. Cobalt tends to exist as

a mixture of two allotropes over a wide temperature range; the β-form predominates below 400°C; and the α above that temperature. The transformation is sluggish and accounts in part for the wide variation in reported data on physical properties of cobalt. It is alloyed with iron, nickel and other metals to make Alnico, an alloy of unusual magnetic strength with many important uses. Stellite alloys, containing cobalt, chromium, and tungsten, are used for high-speed, heavy-duty, high temperature cutting tools, and for dies. Cobalt is also used in other magnet steels and stainless steels, and in alloys used in jet turbines and gas turbine generators. The metal is used in electroplating because of its appearance, hardness, and resistance to oxidation. The salts have been used for centuries for the production of brilliant and permanent blue colors in porcelain, glass, pottery, tiles, and enamels. It is the principal ingredient in Sevre's and Thenard's blue. A solution of the chloride ($CoCl_2 \cdot 6H_2O$) is used as sympathetic ink. The cobalt amines are of interest; the oxide and the nitrate are important. Cobalt carefully used in the form of the chloride, sulfate, acetate, or nitrate has been found effective in correcting a certain mineral deficiency disease in animals. Soils should contain 0.13 to 0.30 ppm of cobalt for proper animal nutrition. Cobalt-60, an artificial isotope, is an important gamma ray source, and is extensively used as a tracer and a radiotherapeutic agent. Single compact sources of Cobalt-60 vary from about $1 to $10/curie, depending on quantity and specific activity. Exposure to cobalt (metal fumes and dust) should be limited to 0.05 mg/m^3 (8-hour time-weighted average, 40-hour week).

Columbium — See Niobium.

Copper — (L. *cuprum*, from the island of Cyprus), Cu; at. wt. 63.546; at. no. 29; m.p. 1084.62 ± 0.2°C; b.p. 2562°C; sp. gr. 8.96 (20°C); valence 1 or 2. The discovery of copper dates from prehistoric times. It is said to have been mined for more than 5000 years. It is one of man's most important metals. Copper is reddish colored, takes on a bright metallic luster, and is malleable, ductile, and a good conductor of heat and electricity (second only to silver in electrical conductivity). The electrical industry is one of the greatest users of copper. Copper occasionally occurs native, and is found in many minerals such as *cuprite, malachite, azurite, chalcopyrite*, and *bornite*. Large copper ore deposits are found in the U.S., Chile, Zambia, Zaire, Peru, and Canada. The most important copper ores are the sulfides, oxides, and carbonates. From these, copper is obtained by smelting, leaching, and by electrolysis. Its alloys, brass and bronze, long used, are still very important; all American coins are now copper alloys; monel and gun metals also contain copper. The most important compounds are the oxide and the sulfate, blue vitriol; the latter has wide use as an agricultural poison and as an algicide in water purification. Copper compounds such as Fehling's solution are widely used in analytical chemistry in tests for sugar. High-purity copper (99.999 + %) is available commercially.

Curium — (Pierre and Marie Curie), Cm; at. wt. (247); at. no. 96; m.p. 1345 ± 40°C; sp. gr. 13.51 (calc.); valence 3 and 4. Although curium follows americium in the periodic system, it was actually known before americium and was the third transuranium element to be discovered. It was identified by Seaborg, James, and Ghiorso in 1944 at the wartime Metallurgical Laboratory in Chicago as a result of helium-ion bombardment of ^{239}Pu in the Berkeley, California, 60-inch cyclotron. Visible amounts (30 μg) of ^{242}Cm, in the form of the hydroxide, were first isolated by Werner and Perlman of the University of California in 1947. In 1950, Crane, Wallmann, and Cunningham found that the magnetic susceptibility of microgram samples of CmF_3 was of the same magnitude as that of GdF_3. This provided direct experimental evidence for assigning an electronic configuration to Cm^{+3}. In 1951, the same workers prepared curium in its elemental form for the first time. Fourteen isotopes of curium are now known. The most stable, ^{247}Cm, with a half-life of 16 million years, is so short compared to the earth's age that any primordial curium must have disappeared long ago from the natural scene. Minute amounts of curium probably exist in natural deposits of uranium, as a result of a sequence of neutron captures and β decays sustained by the very low flux of neutrons naturally present in uranium ores. The presence of natural curium, however, has never been detected. ^{242}Cm and ^{244}Cm are available in multigram quantities. ^{248}Cm has been produced only in milligram amounts. Curium is similar in some regards to gadolinium, its rare-earth homolog, but it has a more complex crystal structure. Curium is silver in color, is chemically reactive, and is more electropositive than aluminum. CmO_2, Cm_2O_3, CmF_3, CmF_4, $CmCl_3$, $CmBr_3$, and CmI_3 have been prepared. Most compounds of trivalent curium are faintly yellow in color. ^{242}Cm generates about three watts of thermal energy per gram. This compares to one-half watt per gram of ^{238}Pu. This suggests use for curium as a power source. ^{244}Cm is now offered for sale at $100/mg. Curium absorbed into the body accumulates in the bones, and is therefore very toxic as its radiation destroys the red-cell forming mechanism. The maximum permissible total body burden of ^{244}Cm (soluble) in a human being is 0.3 μCi (microcurie).

Deuterium, an isotope of hydrogen — see Hydrogen.

Dysprosium — (Gr. *dysprositos*, hard to get at), Dy; at. wt. 162.50; at. no. 66; m.p. 1411°C; b.p. 2561°C; sp. gr. 8.551 (25°C); valence 3. Dysprosium was discovered in 1886 by Lecoq de Boisbaudran, but not isolated. Neither the oxide nor the metal was available in relatively pure form until the development of ion-exchange separation and metallographic reduction techniques by Spedding and associates about 1950. Dysprosium occurs along with other so-called rare-earth or lanthanide elements in a variety of minerals such as *xenotime, fergusonite, gadolinite, euxenite, polycrase*, and *blomstrandine*. The most important sources, however, are from *monazite* and *bastnasite*. Dysprosium can be prepared by reduction of the trifluoride with calcium. The element has a metallic, bright silver luster. It is relatively stable in air at room temperature, and is readily attacked and dissolved, with the evolution of hydrogen, by dilute and concentrated mineral acids. The metal is soft enough to be cut with a knife and can be machined without sparking if overheating is avoided. Small amounts of impurities can greatly affect its physical properties. While dysprosium has not yet found many applications, its thermal neutron absorption cross-section and high melting point suggest metallurgical uses in nuclear control applications and for alloying with special stainless steels. A dysprosium oxide-nickel cermet has found use in cooling nuclear reactor rods. This cermet absorbs neutrons readily without swelling or contracting under prolonged neutron bombardment. In combination with vanadium and other rare earths, dysprosium has been used in making laser materials. Dysprosium-cadmium chalcogenides, as sources of infrared radiation, have been used for studying chemical reactions. The cost of dysprosium metal has dropped in recent years since the development of ion-exchange and solvent extraction techniques, and the discovery of large ore bodies. The metal costs about $300/kg in purities of 99 + %.

Einsteinium — (Albert Einstein), Es; at. wt. (252); at. no. 99. Einsteinium, the seventh transuranic element of the actinide series to be discovered, was identified by Ghiorso and co-workers at Berkeley in December 1952 in debris from the first large thermonuclear explosion, which took place in the Pacific in November 1952. The isotope produced was the 20-day ^{253}Es isotope. In 1961, a sufficient amount of einsteinium was produced to permit separation of a macroscopic amount of ^{253}Es. This sample weighed about 0.01 μg. A special magnetic-type balance was used in making this determination. ^{253}Es so produced was used to produce mendelevium (Element 101). About 3 μg of einsteinium has been produced at Oak Ridge National Laboratories by irradiating for several years kilogram quantities of ^{239}Pu in a reactor to produce ^{242}Pu. This was then fabricated into pellets

the existence of Element 109 by four independent measurements. The newly formed atom recoiled from the target at a predicted velocity and was separated from smaller, faster nuclei by a newly developed velocity filter. The time of flight to the detector and the striking energy were measured and found to match predicted values. The nucleus of ^{266}X started to decay 5 ms after striking the detector. A high-energy α particle was emitted, producing $^{262}_{107}X$. This in turn emitted an α particle, becoming $^{258}_{105}Ha$, which in turn captured an electron and became $^{258}_{104}Rf$. This in turn decayed into other nuclides. This experiment demonstrated the feasibility of using fusion techniques as a method of making new, heavy nuclei.

Element 110 (ununnilium) — In 1987 it was reported that Organessian, et al., in Russia claimed discovery of Element 110 (UUN). Their experiments indicated a spontaneous fissioning nuclide with an atomic number of 110, a mass of 272, and a half-life of 10 ms.

Erbium — (*Ytterby*, a town in Sweden), Er; at. wt. 167.26; at. no. 68; m.p. 1529°C; b.p. 2862°C; sp. gr. 9.066 (25°C); valence 3, Erbium, one of the so-called rare-earth elements of the lanthanide series, is found in the minerals mentioned under dysprosium above. In 1842 Mosander separated "yttria," found in the mineral *gadolinite*, into three fractions which he called *yttria*, *erbia*, and *terbia*. The names *erbia* and *terbia* became confused in this early period. After 1860, Mosander's *terbia* was known as *erbia*, and after 1877, the earlier known *erbia* became *terbia*. The *erbia* of this period was later shown to consist of five oxides, now known as *erbia*, *scandia*, *holmia*, *thulia* and *ytterbia*. By 1905 Urbain and James independently succeeded in isolating fairly pure Er_2O_3. Klemm and Bommer first produced reasonably pure erbium metal in 1934 by reducing the anhydrous chloride with potassium vapor. The pure metal is soft and malleable and has a bright, silvery, metallic luster. As with other rare-earth metals, its properties depend to a certain extent on the impurities present. The metal is fairly stable in air and does not oxidize as rapidly as some of the other rare-earth metals. Naturally occurring erbium is a mixture of six isotopes, all of which are stable. Nine radioactive isotopes of erbium are also recognized. Recent production techniques, using ion-exchange reactions, have resulted in much lower prices of the rare-earth metals and their compounds in recent years. The cost of 99+% erbium metal is about $650/kg. Erbium is finding nuclear and metallurgical uses. Added to vanadium, for example, erbium lowers the hardness and improves workability. Most of the rare-earth oxides have sharp absorption bands in the visible, ultraviolet, and near infrared. This property, associated with the electronic structure, gives beautiful pastel colors to many of the rare-earth salts. Erbium oxide gives a pink color and has been used as a colorant in glasses and porcelain enamel glazes.

Europium — (Europe), Eu; at. wt. 151.965; at. no. 63; m.p. 822°C; b.p. 1596°C; sp. gr. 5.244 (25°C); valence 2 or 3. In 1890 Boisbaudran obtained basic fractions from samarium-gadolinium concentrates which had spark spectral lines not accounted for by samarium or gadolinium. These lines subsequently have been shown to belong to europium. The discovery of europium is generally credited to Demarcay, who separated the rare earth in reasonably pure form in 1901. The pure metal was not isolated until recent years. Europium is now prepared by mixing Eu_2O_3 with a 10%-excess of lanthanum metal and heating the mixture in a tantalum crucible under high vacuum. The element is collected as a silvery-white metallic deposit on the walls of the crucible. As with other rare-earth metals, except for lanthanum, europium ignites in air at about 150 to 180°C. Europium is about as hard as lead and is quite ductile. It is the most reactive of the rare-earth metals, quickly oxidizing in air. It resembles calcium in its reaction with water. *Bastnasite* and *monazite* are the principal ores containing europium. Europium has been identified spectroscopically in the sun and certain stars. Seventeen isotopes are now recognized. Europium isotopes are good neutron absorbers and are being studied for use in nuclear control applications. Europium oxide is now widely used as a phosphor activator and europium-activated yttrium vanadate is in commercial use as the red phosphor in color TV tubes. Europium-doped plastic has been used as a laser material. With the development of ion-exchange techniques and special processes, the cost of the metal has been greatly reduced in recent years. Europium is one of the rarest and most costly of the rare-earth metals. It is priced at about $7500/kg.

Fermium — (Enrico Fermi), Fm; at. wt. (257); at. no. 100. Fermium, the eighth transuranium element of the actinide series to be discovered, was identified by Ghiorso and co-workers in 1952 in the debris from a thermonuclear explosion in the Pacific in work involving the University of California Radiation Laboratory, the Argonne National Laboratory, and the Los Alamos Scientific Laboratory. The isotope produced was the 20-hour ^{255}Fm. During 1953 and early 1954, while discovery of elements 99 and 100 was withheld from publication for security reasons, a group from the Nobel Institute of Physics in Stockholm bombarded ^{238}U with ^{16}O ions, and isolated a 30-min α-emitter, which they ascribed to $^{250}100$, without claiming discovery of the element. This isotope has since been identified positively, and the 30-min half-life confirmed. The chemical properties of fermium have been studied solely with tracer amounts, and in normal aqueous media only the (III) oxidation state appears to exist. The isotope ^{254}Fm and heavier isotopes can be produced by intense neutron irradiation of lower elements such as plutonium by a process of successive neutron capture interspersed with beta decays until these mass numbers and atomic numbers are reached. Sixteen isotopes of fermium are known to exist. ^{257}Fm, with a half-life of about 100.5 days, is the longest lived. ^{250}Fm, with a half-life of 30 min, has been shown to be a product of decay of Element $^{254}102$. It was by chemical identification of ^{250}Fm that production of Element 102 (nobelium) was confirmed.

Fluorine — (L. and F. *fluere*, flow, or flux), F; at. wt. 18.9984032; at. no. 9; m.p. −219.62°C (1 atm); b.p. −188.12°C (1 atm); density 1.696 g/L (0°C, 1 atm); liq. den. at b.p. 1.50 g/cm^3; valence 1. In 1529, Georigius Agricola described the use of fluorspar as a flux, and as early as 1670 Schwandhard found that glass was etched when exposed to fluorspar treated with acid. Scheele and many later investigators, including Davy, Gay-Lussac, Lavoisier, and Thenard, experimented with hydrofluoric acid, some experiments ending in tragedy. The element was finally isolated in 1886 by Moisson after nearly 74 years of continuous effort. Fluorine occurs chiefly in *fluorspar* (CaF_2) and *cryolite* (Na_2AlF_6), but is rather widely distributed in other minerals. It is a member of the halogen family of elements, and is obtained by electrolyzing a solution of potassium hydrogen fluoride in anhydrous hydrogen fluoride in a vessel of metal or transparent fluorspar. Modern commercial production methods are essentially variations on the procedures first used by Moisson. Fluorine is the most electronegative and reactive of all elements. It is a pale yellow, corrosive gas, which reacts with practically all organic and inorganic substances. Finely divided metals, glass, ceramics, carbon, and even water burn in fluorine with a bright flame. Until World War II, there was no commercial production of elemental fluorine. The atom bomb project and nuclear energy applications, however, made it necessary to produce large quantities. Safe handling techniques have now been developed and it is possible at present to transport liquid fluorine by the ton. Fluorine and its compounds are used in producing uranium (from the hexafluoride) and more than 100 commercial fluorochemicals, including many well-known high-temperature plastics. Hydrofluoric acid is extensively used for etching the glass of light bulbs, etc. Fluorochloro hydrocarbons are extensively used in air conditioning and refrigeration. It has been suggested that fluorine can be substituted for hydrogen wherever it occurs in organic compounds, which could lead to an astronomical number of new fluorine compounds. The presence of fluorine as a soluble fluoride

in drinking water to the extent of 2 ppm may cause mottled enamel in teeth, when used by children acquiring permanent teeth; in smaller amounts, however, fluorides are said to be beneficial and used in water supplies to prevent dental cavities. Elemental fluorine has been studied as a rocket propellant as it has an exceptionally high specific impulse value. Compounds of fluorine with rare gases have now been confirmed. Fluorides of xenon, radon, and krypton are among those known. Elemental fluorine and the fluoride ion are highly toxic. The free element has a characteristic pungent odor, detectable in concentrations as low as 20 ppb, which is below the safe working level. The recommended maximum allowable concentration for a daily 8-hour time-weighted exposure is 1 ppm.

Francium — (France), Fr; at. no. 87; at. wt. (223); m.p. 27°C; b.p. 677°C; valence 1. Discovered in 1939 by Mlle. Marguerite Perey of the Curie Institute, Paris. Francium, the heaviest known member of the alkali metal series, occurs as a result of an alpha disintegration of actinium. It can also be made artificially by bombarding thorium with protons. While it occurs naturally in uranium minerals, there is probably less than an ounce of francium at any time in the total crust of the earth. It has the highest equivalent weight of any element, and is the most unstable of the first 101 elements of the periodic system. Thirty-three isotopes of francium are recognized. The longest lived ^{223}Fr(Ac, K), a daughter of ^{227}Ac, has a half-life of 22 min. This is the only isotope of francium occurring in nature. Because all known isotopes of francium are highly unstable, knowledge of the chemical properties of this element comes from radiochemical techniques. No weighable quantity of the element has been prepared or isolated. The chemical properties of francium most closely resemble cesium.

Gadolinium — (*gadolinite*, a mineral named for Gadolin, a Finnish chemist), Gd; at. wt. 157.25; at. no. 64; m.p. 1314 ± 1°C; b.p. 3264°C; sp. gr. 7.901 (25°C); valence 3. Gadolinia, the oxide of gadolinium, was separated by Marignac in 1880 and Lecoq de Boisbaudran independently isolated the element from Mosander's "yttria" in 1886. The element was named for the mineral *gadolinite* from which this rare earth was originally obtained. Gadolinium is found in several other minerals, including *monazite* and *bastnasite*, which are of commercial importance. The element has been isolated only in recent years. With the development of ion-exchange and solvent extraction techniques, the availability and price of gadolinium and the other rare-earth metals have greatly improved. Seventeen isotopes of gadolinium are now recognized; seven occur naturally. The metal can be prepared by the reduction of the anhydrous fluoride with metallic calcium. As with other related rare-earth metals, it is silvery white, has a metallic luster, and is malleable and ductile. At room temperature, gadolinium crystallizes in the hexagonal, close-packed α form. Upon heating to 1235°C, α gadolinium transforms into the β form, which has a body-centered cubic structure. The metal is relatively stable in dry air, but in moist air it tarnishes with the formation of a loosely adhering oxide film which spalls off and exposes more surface to oxidation. The metal reacts slowly with water and is soluble in dilute acid. Gadolinium has the highest thermal neutron capture cross-section of any known element (49,000 barns). Natural gadolinium is a mixture of seven isotopes. Two of these, ^{155}Gd and ^{157}Gd, have excellent capture characteristics, but they are present naturally in low concentrations. As a result, gadolinium has a very fast burnout rate and has limited use as a nuclear control rod material. It has been used in making gadolinium yttrium garnets, which have microwave applications. Compounds of gadolinium are used in making phosphors for color TV tubes. The metal has unusual superconductive properties. As little as 1% gadolinium has been found to improve the workability and resistance of iron, chromium, and related alloys to high temperatures and oxidation. Gadolinium ethyl sulfate has extremely low noise characteristics and may find use in duplicating the performance of amplifiers, such as the maser. The metal is ferromagnetic. Gadolinium is unique for its high magnetic moment and for its special Curie temperature (above which ferromagnetism vanishes) lying just at room temperature. This suggests uses as a magnetic component that senses hot and cold. The price of the metal is $485/kg.

Gallium — (L. *Gallia*, France; also from Latin, *gallus*, a translation of Lecoq, a cock), Ga; at. wt. 69.723; at. no. 31; m.p. 29.76°C; b.p. 2204°C; sp. gr. 5.904 (29.6°C) solid; sp. gr. 6.095 (29.6°C) liquid; valence 2 or 3. Predicted and described by Mendeleev as ekaaluminum, and discovered spectroscopically by Lecoq de Boisbaudran in 1875, who in the same year obtained the free metal by electrolysis of a solution of the hydroxide in KOH. Gallium is often found as a trace element in *diaspore*, *sphalerite*, *germanite*, *bauxite*, and *coal*. Some flue dusts from burning coal have been shown to contain as much as 1.5% gallium. It is the only metal, except for mercury, cesium, and rubidium, which can be liquid near room temperatures; this makes possible its use in high-temperature thermometers. It has one of the longest liquid ranges of any metal and has a low vapor pressure even at high temperatures. There is a strong tendency for gallium to supercool below its freezing point. Therefore, seeding may be necessary to initiate solidification. Ultra-pure gallium has a beautiful, silvery appearance, and the solid metal exhibits a conchoidal fracture similar to glass. The metal expands 3.1% on solidifying; therefore, it should not be stored in glass or metal containers, as they may break as the metal solidifies. Gallium wets glass or porcelain, and forms a brilliant mirror when it is painted on glass. It is widely used in doping semiconductors and producing solid-state devices such as transistors. High-purity gallium is attacked only slowly by mineral acids. Magnesium gallate containing divalent impurities such as Mn^{+2} is finding use in commercial ultraviolet activated powder phosphors. Gallium arsenide is capable of converting electricity directly into coherent light. Gallium readily alloys with most metals, and has been used as a component in low-melting alloys. Its toxicity appears to be of a low order, but should be handled with care until more data are forthcoming. The metal can be supplied in ultrapure form (99.99999+%). The cost is about $3/g.

Germanium — (L. *Germania*, Germany), Ge; at. wt. 72.61; at. no. 32; m.p. 938.25°C; b.p. 2833°C; sp. gr. 5.323 (25°C); valence 2 and 4. Predicted by Mendeleev in 1871 as ekasilicon, and discovered by Winkler in 1886. The metal is found in *argyrodite*, a sulfide of germanium and silver; in *germanite*, which contains 8% of the element; in zinc ores; in coal; and in other minerals. The element is frequently obtained commercially from flue dusts of smelters processing zinc ores, and has been recovered from the by-products of combustion of certain coals. Its presence in coal insures a large reserve of the element in the years to come. Germanium can be separated from other metals by fractional distillation of its volatile tetrachloride. The tetrachloride may then be hydrolyzed to give GeO_2; the dioxide can be reduced with hydrogen to give the metal. Recently developed zone-refining techniques permit the production of germanium of ultra-high purity. The element is a gray-white metalloid, and in its pure state is crystalline and brittle, retaining its luster in air at room temperature. It is a very important semiconductor material. Zone-refining techniques have led to production of crystalline germanium for semiconductor use with an impurity of only one part in 10^{10}. Doped with arsenic, gallium, or other elements, it is used as a transistor element in thousands of electronic applications. Its application as a semiconductor element now provides the largest use for germanium. Germanium is also finding many other applications including use as an alloying agent, as a phosphor in fluorescent lamps, and as a catalyst. Germanium and germanium oxide are transparent to the infrared and are used in infrared spectroscopes and other optical equipment, including extremely sensitive infrared detectors. Germanium oxide's high index of refraction and dispersion has made it useful as a component of glasses used in wide-angle camera

research, as its boiling point is close to absolute zero. Its use in the study of superconductivity is vital. Using liquid helium, Kurti and co-workers, and others, have succeeded in obtaining temperatures of a few microkelvins by the adiabatic demagnetization of copper nuclei, starting from about 0.01 K. Seven isotopes of helium are known. Liquid helium (He^4) exists in two forms: He^4I and He^4II, with a sharp transition point at 2.174 K (3.83 cm Hg). He^4I (above this temperature) is a normal liquid, but He^4II (below it) is unlike any other known substance. It expands on cooling; its conductivity for heat is enormous; and neither its heat conduction nor viscosity obeys normal rules. It has other peculiar properties. Helium is the only liquid that cannot be solidified by lowering the temperature. It remains liquid down to absolute zero at ordinary pressures, but it can readily be solidified by increasing the pressure. Solid ^3He and ^4He are unusual in that both can readily be changed in volume by more than 30% by application of pressure. The specific heat of helium gas is unusually high. The density of helium vapor at the normal boiling point is also very high, with the vapor expanding greatly when heated to room temperature. Containers filled with helium gas at 5 to 10 K should be treated as though they contained liquid helium due to the large increase in pressure resulting from warming the gas to room temperature. While helium normally has a 0 valence, it seems to have a weak tendency to combine with certain other elements. Means of preparing helium diflouride have been studied, and species such as HeNe and the molecular ions He^+ and He^{++} have been investigated. Helium is widely used as an inert gas shield for arc welding; as a protective gas in growing silicon and germanium crystals, and in titanium and zirconium production; as a cooling medium for nuclear reactors, and as a gas for supersonic wind tunnels. A mixture of helium and oxygen is used as an artificial atmosphere for divers and others working under pressure. Different ratios of He/O_2 are used for different depths at which the diver is operating. Helium is extensively used for filling balloons as it is a much safer gas than hydrogen. One of the recent largest uses for helium has been for pressuring liquid fuel rockets. A Saturn booster such as used on the Apollo lunar missions required about 13 million $ft^3$of helium for a firing, plus more for checkouts. Liquid helium's use in magnetic resonance imaging (MRI) continues to increase as the medical profession accepts and develops new uses for the equipment. This equipment is providing accurate diagnoses of problems where exploratory surgery has previously been required to determine problems. Another medical application that is being developed uses MRI to determine by blood analysis whether a patient has any form of cancer. Lifting gas applications are increasing. Various companies in addition to Goodyear, are now using "blimps" for advertising. The Navy and the Air Force are investigating the use of airships to provide early warning systems to detect low-flying cruise missiles. The Drug Enforcement Agency is using radar-equipped blimps to detect drug smugglers along the southern border of the U.S. In addition, NASA is currently using helium-filled balloons to sample the atmosphere in Antarctica to determine what is depleting the ozone layer that protects Earth from harmful U.V. radiation. Research on and development of materials which become superconductive at temperatures well above the boiling point of helium could have a major impact on the demand for helium. Less costly refrigerants having boiling points considerably higher could replace the present need to cool such superconductive materials to the boiling point of helium.

Holmium — (L. *Holmia*, for Stockholm), Ho; at. wt. 164.93032; at. no 67; m.p. 1472°C; b.p. 2694°C; sp. gr. 8.795 (25°C); valence + 3. The spectral absorption bands of holmium were noticed in 1878 by the Swiss chemists Delafontaine and Soret, who announced the existence of an "Element X". Cleve, of Sweden, later independently discovered the element while working on erbia earth. The element is named after Cleve's native city. Pure holmia, the yellow oxide, was prepared by Homberg in 1911. Holmium occurs in *gadolinite, monazite,* and in other rare-earth minerals. It is commercially obtained from monazite, occurring in that mineral to the extent of about 0.05%. It has been isolated by the reduction of its anhydrous chloride or fluoride with calcium metal. Pure holmium has a metallic to bright silver luster. It is relatively soft and malleable, and is stable in dry air at room temperature, but rapidly oxidizes in moist air and at elevated temperatures. The metal has unusual magnetic properties. Few uses have yet been found for the element. The element, as with other rare earths, seems to have a low acute toxic rating. The price of 99 + % holmium metal is about $10/g.

Hydrogen — (Gr. *hydro*, water, and *genes*, forming), H; at. wt. 1.00794; at. no. 1; m.p. –259.34°C; b.p. –252.87°C; density 0.08988 g/l; density (liquid) 70.8 g/l (–253°C); density (solid) 70.6 g/l (–262°C); valence 1. Hydrogen was prepared many years before it was recognized as a distinct substance by Cavendish in 1766. It was named by Lavoisier. Hydrogen is the most abundant of all elements in the universe, and it is thought that the heavier elements were, and still are, being built from hydrogen and helium. It has been estimated that hydrogen makes up more than 90% of all the atoms or three quarters of the mass of the universe. It is found in the sun and most stars, and plays an important part in the proton-proton reaction and carbon-nitrogen cycle, which accounts for the energy of the sun and stars. It is thought that hydrogen is a major component of the planet Jupiter and that at some depth in the planet's interior the pressure is so great that solid molecular hydrogen is converted into solid metallic hydrogen. In 1973, it was reported that a group of Russian experimenters may have produced metallic hydrogen at a pressure of 2.8 Mbar. At the transition the density changed from 1.08 to 1.3 g/cm^3. Earlier, in 1972, a Livermore (California) group also reported on a similar experiment in which they observed a pressure-volume point centered at 2 Mbar. It has been predicted that metallic hydrogen may be metastable; others have predicted it would be a superconductor at room temperature. On earth, hydrogen occurs chiefly in combination with oxygen in water, but it is also present in organic matter such as living plants, petroleum, coal, etc. It is present as the free element in the atmosphere, but only to the extent of less than 1 ppm by volume. It is the lightest of all gases, and combines with other elements, sometimes explosively, to form compounds. Great quantities of hydrogen are required commercially for the fixation of nitrogen from the air in the Haber ammonia process and for the hydrogenation of fats and oils. It is also used in large quantities in methanol production, in hydrodealkylation, hydrocracking, and hydrodesulfurization. It is also used as a rocket fuel, for welding, for production of hydrochloric acid, for the reduction of metallic ores, and for filling balloons. The lifting power of 1 ft^3 of hydrogen gas is about 0.076 lb at 0°C, 760 mm pressure. Production of hydrogen in the U.S. alone now amounts to about 3 billion cubic feet per year. It is prepared by the action of steam on heated carbon, by decomposition of certain hydrocarbons with heat, by the electrolysis of water, or by the displacement from acids by certain metals. It is also produced by the action of sodium or potassium hydroxide on aluminum. Liquid hydrogen is important in cryogenics and in the study of superconductivity, as its melting point is only a 20 degrees above absolute zero. The ordinary isotope of hydrogen, H, is known as *protium*. In 1932, Urey announced the preparation of a stable isotope, deuterium (^2H or D) with an atomic weight of 2. Two years later an unstable isotope, tritium (H), with an atomic weight of 3 was discovered. Tritium has a half-life of about 12.5 years. One atom of deuterium is found in about 6000 ordinary hydrogen atoms. Tritium atoms are also present but in much smaller proportion. Tritium is readily produced in nuclear reactors and is used in the production of the hydrogen bomb. It is also used as a radioactive agent in making luminous paints, and as a tracer. The current price of tritium, to authorized personnel, is about $2/Ci; deuterium gas is readily available, without permit, at about $1/l. Heavy water, deuterium oxide (D_2O), which is used as a

Carbon steel is an alloy of iron with carbon, with small amounts of Mn, S, P, and Si. Alloy steels are carbon steels with other additives such as nickel, chromium, vanadium, etc. Iron is the cheapest and most abundant, useful, and important of all metals.

Krypton — (Gr. *kryptos*, hidden), Kr; at. wt. 83.80; at. no. 36; m.p. −157.36°C; b.p. −153.22 ± 0.10°C; density 3.733 g/l (0°C); valence usually 0. Discovered in 1898 by Ramsay and Travers in the residue left after liquid air had nearly boiled away. Krypton is present in the air to the extent of about 1 ppm. The atmosphere of Mars has been found to contain 0.3 ppm of krypton. It is one of the "noble" gases. It is characterized by its brilliant green and orange spectral lines. Naturally occurring krypton contains six stable isotopes. Seventeen other unstable isotopes are now recognized. The spectral lines of krypton are easily produced and some are very sharp. In 1960 it was internationally agreed that the fundamental unit of length, the meter, should be defined in terms of the orange-red spectral line of ^{86}Kr. This replaced the standard meter of Paris, which was defined in terms of a bar made of a platinum-iridium alloy. In October 1983 the meter, which originally was defined as being one ten millionth of a quadrant of the earth's polar circumference, was again redefined by the International Bureau of Weights and Measures as being the length of path traveled by light in a vacuum during a time interval of 1/299,792,458 of a second. Solid krypton is a white crystalline substance with a face-centered cubic structure which is common to all the "rare gases". While krypton is generally thought of as a rare gas that normally does not combine with other elements to form compounds, it now appears that the existence of some krypton compounds is established. Krypton difluoride has been prepared in gram quantities and can be made by several methods. A higher fluoride of krypton and a salt of an oxyacid of krypton also have been reported. Molecule-ions of $ArKr^+$ and KrH^+ have been identified and investigated, and evidence is provided for the formation of KrXe or $KrXe^+$. Krypton clathrates have been prepared with hydroquinone and phenol. ^{85}Kr has found recent application in chemical analysis. By imbedding the isotope in various solids, *kryptonates* are formed. The activity of these kryptonates is sensitive to chemical reactions at the surface. Estimates of the concentration of reactants are therefore made possible. Krypton is used in certain photographic flash lamps for high-speed photography. Uses thus far have been limited because of its high cost. Krypton gas presently costs about $30/l.

Kurchatovium — see Element 104.

Lanthanum — (Gr. *lanthanein*, to lie hidden), La; at. wt. 138.9055; at. no. 57; m.p. 920°C; b.p. 3455°C; sp. gr. 6.145 (25°C); valence 3. Mosander in 1839 extracted a new earth *lanthana*, from impure cerium nitrate, and recognized the new element. Lanthanum is found in rare-earth minerals such as *cerite*, *monazite*, *allanite*, and *bastnasite*. Monazite and bastnasite are principal ores in which lanthanum occurs in percentages up to 25 and 38%, respectively. Misch metal, used in making lighter flints, contains about 25% lanthanum. Lanthanum was isolated in relatively pure form in 1923. Ion-exchange and solvent extraction techniques have led to much easier isolation of the so-called "rare-earth" elements. The availability of lanthanum and other rare earths has improved greatly in recent years. The metal can be produced by reducing the anhydrous fluoride with calcium. Lanthanum is silvery white, malleable, ductile, and soft enough to be cut with a knife. It is one of the most reactive of the rare-earth metals. It oxidizes rapidly when exposed to air. Cold water attacks lanthanum slowly, and hot water attacks it much more rapidly. The metal reacts directly with elemental carbon, nitrogen, boron, selenium, silicon, phosphorus, sulfur, and with halogens. At 310°C, lanthanum changes from a hexagonal to a face-centered cubic structure, and at 865°C it again transforms into a body-centered cubic structure. Natural lanthanum is mixture of two stable isotopes, ^{138}La and ^{139}La. Twenty three other radioactive isotopes are recognized. Rare-earth compounds containing lanthanum are extensively used in carbon lighting applications, especially by the motion picture industry for studio lighting and projection. This application consumes about 25% of the rare-earth compounds produced. La_2O_3 improves the alkali resistance of glass, and is used in making special optical glasses. Small amounts of lanthanum, as an additive, can be used to produce nodular cast iron. There is current interest in hydrogen sponge alloys containing lanthanum. These alloys take up to 400 times their own volume of hydrogen gas, and the process is reversible. Heat energy is released every time they do so; therefore these alloys have possibilities in energy conservation systems. Lanthanum and its compounds have a low to moderate acute toxicity rating; therefore, care should be taken in handling them. The metal costs about $5/g.

Lawrencium — (Ernest O. Lawrence, inventor of the cyclotron), Lr; at. no. 103; at. mass no. (262); valence + 3(?). This member of the 5f transition elements (actinide series) was discovered in March 1961 by A. Ghiorso, T. Sikkeland, A. E. Larsh, and R. M. Latimer.A 3-μg californium target, consisting of a mixture of isotopes of mass number 249, 250, 251, and 252, was bombarded with either ^{10}B or ^{11}B. The electrically charged transmutation nuclei recoiled with an atmosphere of helium and were collected on a thin copper conveyor tape which was then moved to place collected atoms in front of a series of solid-state detectors. The isotope of element 103 produced in this way decayed by emitting an 8.6-MeV alpha particle with a half-life of 8 s. In 1967. Flerov and associates of the Dubna Laboratory reported their inability to detect an alpha emitter with a half-life of 8 s which was assigned by the Berkeley group to $^{257}103$. This assignment has been changed to ^{258}Lr or ^{259}Lr. In 1965, the Dubna workers found a longer-lived lawrencium isotope, ^{256}Lr, with a half-life of 35 s. In 1968, Ghiorso and associates at Berkeley were able to use a few atoms of this isotope to study the oxidation behavior of lawrencium. Using solvent extraction techniques and working very rapidly, they extracted lawrencium ions from a buffered aqueous solution into an organic solvent, completing each extraction in about 30 s. It was found that lawrencium behaves differently from dipositive nobelium and more like the tripositive elements earlier in the actinide series.

Lead — (Anglo-Saxon *lead*), Pb (L. *plumbum*); at. wt. 207.2; at. no. 82; m.p. 327.46°C; b.p. 1749°C; sp. gr. 11.35 (20°C); valence 2 or 4. Long known, mentioned in Exodus. The alchemists believed lead to be the oldest metal and associated it with the planet Saturn. Native lead occurs in nature, but it is rare. Lead is obtained chiefly from *galena* (PbS) by a roasting process. *Anglesite* ($PbSO_4$), *cerussite* ($PbCO_3$), and *minim* (Pb_3O_4) are other common lead minerals. Lead is a bluish-white metal of bright luster, is very soft, highly malleable, ductile, and a poor conductor of electricity. It is very resistant to corrosion; lead pipes bearing the insignia of Roman emperors, used as drains from the baths, are still in service. It is used in containers for corrosive liquids (such as sulfuric acid) and may be toughened by the addition of a small percentage of antimony or other metals. Natural lead is a mixture of four stable isotopes: ^{204}Pb (1.48%), ^{206}Pb (23.6%), ^{207}Pb (22.6%), and ^{208}Pb (52.3%). Lead isotopes are the end products of each of the three series of naturally occurring radioactive elements: ^{206}Pb for the uranium series, ^{207}Pb for the actinium series, and ^{208}Pb for the thorium series. Twenty seven other isotopes of lead, all of which are radioactive, are recognized. Its alloys include solder, type metal, and various antifriction metals. Great quantities of lead, both as the metal and as the dioxide, are used in storage batteries. Much metal also goes into cable covering, plumbing, ammunition, and in the manufacture of lead tetraethyl. The metal is very effective as a sound absorber, is used as a radiation shield around X-ray equipment and nuclear reactors, and is used to absorb vibration. White lead, the basic carbonate, sublimed white lead ($PbSO_4$) chrome yellow ($PbCrO_4$),

red lead (Pb_3O_4), and other lead compounds are used extensively in paints, although in recent years the use of lead in paints has been drastically curtailed to eliminate or reduce health hazards. Lead oxide is used in producing fine "crystal glass" and "flint glass" of a high index of refraction for achromatic lenses. The nitrate and the acetate are soluble salts. Lead salts such as lead arsenate have been used as insecticides, but their use in recent years has been practically eliminated in favor of less harmful organic compounds. Care must be used in handling lead as it is a cumulative poison. Environmental concern with lead poisoning has resulted in a national program to eliminate the lead in gasoline.

Lithium — (Gr. *lithos*, stone), Li; at. wt. 6.941; at. no. 3; m.p. 180.5°C; b.p. 1342°C; sp. gr. 0.534 (20°C); valence 1. Discovered by Arfvedson in 1817. Lithium is the lightest of all metals, with a density only about half that of water. It does not occur free in nature; combined it is found in small amounts in nearly all igneous rocks and in the waters of many mineral springs. *Lepidolite*, *spodumene*, *petalite*, and *amblygonite* are the more important minerals containing it. Lithium is presently being recovered from brines of Searles Lake, in California, and from those in Nevada. Large deposits of spodumene are found in North Carolina. The metal is produced electrolytically from the fused chloride. Lithium is silvery in appearance, much like Na and K, other members of the alkali metal series. It reacts with water, but not as vigorously as sodium. Lithium imparts a beautiful crimson color to a flame, but when the metal burns strongly the flame is a dazzling white. Since World War II, the production of lithium metal and its compounds has increased greatly. Because the metal has the highest specific heat of any solid element, it has found use in heat transfer applications; however, it is corrosive and requires special handling. The metal has been used as an alloying agent, is of interest in synthesis of organic compounds, and has nuclear applications. It ranks as a leading contender as a battery anode material as it has a high electrochemical potential. Lithium is used in special glasses and ceramics. The glass for the 200-inch telescope at Mt. Palomar contains lithium as a minor ingredient. Lithium chloride is one of the most hygroscopic materials known, and it, as well as lithium bromide, is used in air conditioning and industrial drying systems. Lithium stearate is used as an all-purpose and high-temperature lubricant. Other lithium compounds are used in dry cells and storage batteries. The metal is priced at about $100/lb.

Lutetium — (Lutetia, ancient name for Paris, sometimes called *cassiopeium* by the Germans), Lu; at. wt. 174.967; at. no. 71; m.p. 1663°C; b.p. 3393°C; sp. gr. 9.841 (25°C); valence 3. In 1907, Urbain described a process by which Marignac's ytterbium (1879) could be separated into the two elements, ytterbium (neoytterbium)and lutetium. These elements were identical with "aldebaranium" and "cassiopeium," independently discovered by von Welsbach about the same time. Charles James of the University of New Hampshire also independently prepared the very pure oxide, *lutecia*, at this time. The spelling of the element was changed from *lutecium* to *lutetium* in 1949. Lutetium occurs in very small amounts in nearly all minerals containing yttrium, and is present in *monazite* to the extent of about 0.003%, which is a commercial source. The pure metal has been isolated only in recent years and is one of the most difficult to prepare. It can be prepared by the reduction of anhydrous $LuCl_3$ or LuF_3 by an alkali or alkaline earth metal. The metal is silvery white and relatively stable in air. While new techniques, including ion-exchange reactions, have been developed to separate the various rare-earth elements, lutetium is still the most costly of all rare earths. It is priced at about $75/g. ^{176}Lu occurs naturally (2.6%) with ^{175}Lu (97.4%). It is radioactive with a half-life of about 3×10^{10} years. Stable lutetium nuclides, which emit pure beta radiation after thermal neutron activation, can be used as catalysts in cracking, alkylation, hydrogenation, and polymerization. Virtually no other commercial uses have been found yet for lutetium. While lutetium, like other rare-earth metals, is thought to have a low toxicity rating, it should be handled with care until more information is available.

Magnesium — (*Magnesia*, district in Thessaly) Mg; at. wt. 24.3050; at. no. 12; m.p. 650°C; b.p. 1090°C; sp. gr. 1.738 (20°C); valence 2. Compounds of magnesium have long been known. Black recognized magnesium as an element in 1755. It was isolated by Davy in 1808, and prepared in coherent form by Bussy in 1831. Magnesium is the eighth most abundant element in the earth's crust. It does not occur uncombined, but is found in large deposits in the form of *magnesite*, *dolomite*, and other minerals. The metal is now principally obtained in the U.S. by electrolysis of fused magnesium chloride derived from brines, wells, and sea water. Magnesium is a light, silvery-white, and fairly tough metal. It tarnishes slightly in air, and finely divided magnesium readily ignites upon heating in air and burns with a dazzling white flame. It is used in flashlight photography, flares, and pyrotechnics, including incendiary bombs. It is one third lighter than aluminium, and in alloys is essential for airplane and missile contruction. The metal improves the mechanical, fabrication, and welding characteristics of aluminum when used as an alloying agent. Magnesium is used in producing nodular graphite in cast iron,and is used as an additive to conventional propellants. It is also used as a reducing agent in the production of pure uranium and other metals from their salts. The hydroxide (*milk of magnesia*), chloride, sulfate (*Epsom salts*), and citrate are used in medicine. Dead-burned magnesite is employed for refractory purposes such as brick and liners in furnaces and converters. Organic magnesium compounds (Grignard's reagents) are important. Magnesium is an important element in both plant and animal life. Chlorophylls are magnesium-centered porphyrins. The adult daily requirement of magnesium is about 300 mg/day, but this is affected by various factors. Great care should be taken in handling magnesium metal, especially in the finely divided state, as serious fires can occur. Water should not be used on burning magnesium or on magnesium fires.

Manganese — (L. *magnes*, magnet, from magnetic properties of pyrolusite; It. *manganese*, corrupt form of *magnesia*), Mn; at. wt. 54.93805; at. no. 25; m.p. 1246 ± 3°C; b.p. 2061°C; sp. gr. 7.21 to 7.44, depending on allotropic form; valence 1, 2, 3, 4, 6, or 7. Recognized by Scheele, Bergman, and others as an element and isolated by Gahn in 1774 by reduction of the dioxide with carbon. Manganese minerals are widely distributed; oxides, silicates, and carbonates are the most common. The discovery of large quantities of manganese nodules on the floor of the oceans holds promise as a source of manganese. These nodules contain about 24% manganese together with many other elements in lesser abundance. Most manganese today is obtained from ores found in the U.S.S.R., Brazil, Australia, Republic of So. Africa, Gabon, and India. *Pyrolusite* (MnO_2) and *rhodochrosite* ($MnCO_3$) are among the most common manganese minerals. The metal is obtained by reduction of the oxide with sodium, magnesium, aluminum, or by electrolysis. It is gray-white, resembling iron, but is harder and very brittle. The metal is reactive chemically, and decomposes cold water slowly. Manganese is used to form many important alloys. In steel, manganese improves the rolling and forging qualities, strength, toughness, stiffness, wear resistance, hardness, and hardenability. With aluminum and antimony, especially with small amounts of copper, it forms highly ferromagnetic alloys. Manganese metal is ferromagnetic only after special treatment. The pure metal exists in four allotropic forms. The alpha form is stable at ordinary temperature; gamma manganese, which changes to alpha at ordinary temperatures, is said to be flexible, soft, easily cut, and capable of being bent. The dioxide (pyrolusite) is used as a depolarizer in dry cells, and is used to "decolorize" glass that is colored green by impurities of iron. Manganese

by itself colors glass an amethyst color, and is responsible for the color of true amethyst. The dioxide is also used in the preparation of oxygen and chlorine, and in drying black paints. The permanganate is a powerful oxidizing agent and is used in quantitative analysis and in medicine. Manganese is widely distributed throughout the animal kingdom. It is an important trace element and may be essential for utilization of vitamin B_1. Exposure to manganese dusts, fume, and compounds (as Mn) should not exceed the ceiling value of 5 mg/m^3 for even short periods because of the toxicity of the element.

Mendelevium — (Dmitri Mendeleev), Md; at. wt. (258); at. no. 101; valence +2, +3. Mendelevium, the ninth transuranium element of the actinide series to be discovered, was first identified by Ghiorso, Harvey, Choppin, Thompson, and Seaborg early in 1955 as a result of the bombardment of the isotope ^{253}Es with helium ions in the Berkeley 60-inch cyclotron. The isotope produced was ^{256}Md, which has a half-life of 76 min. This first identification was notable in that ^{256}Md was synthesized on a one-atom-at-a-time basis. Fourteen isotopes are now recognized. ^{258}Md has a half-life of 2 months. This isotope has been produced by the bombardment of an isotope of einsteinium with ions of helium. It now appears possible that eventually enough ^{258}Md can be made so that some of its physical properties can be determined. ^{256}Md has been used to elucidate some of the chemical properties of mendelevium in aqueous solution. Experiments seem to show that the element possesses a moderately stable dipositive (II) oxidation state in addition to the tripositive (III) oxidation state, which is characteristic of actinide elements.

Mercury — (Planet *Mercury*), Hg (*hydrargyrum*, liquid silver); at. wt. 200.59; at. no. 80; m.p. −38.83°C; b.p. 356.73°C; sp. gr. 13.546 (20°C); valence 1 or 2. Known to ancient Chinese and Hindus; found in Egyptian tombs of 1500 B.C. Mercury is the only common metal liquid at ordinary temperatures. It only rarely occurs free in nature. The chief ore is *cinnabar* (HgS). Spain and Italy produce about 50% of the world's supply of the metal. The commercial unit for handling mercury is the "flask," which weighs 76 lb. The metal is obtained by heating cinnabar in a current of air and by condensing the vapor. It is a heavy, silvery-white metal; a rather poor conductor of heat, as compared with other metals, and a fair conductor of electricity. It easily forms alloys with many metals, such as gold, silver, and tin, which are called *amalgams*. Its ease in amalgamating with gold is made use of in the recovery of gold from its ores. The metal is widely used in laboratory work for making thermometers, barometers, diffusion pumps, and many other instruments. It is used in making mercury-vapor lamps and advertising signs, etc. and is used in mercury switches and other electrical apparatus. Other uses are in making pesticides, mercury cells for caustic soda and chlorine production, dental preparations, antifouling paint, batteries, and catalysts. The most important salts are mercuric chloride $HgCl_2$ (corrosive sublimate — a violent poison), mercurous chloride Hg_2Cl_2 (calomel, occasionally still used in medicine), mercury fulminate ($Hg(ONC)_2$), a detonator widely used in explosives, and mercuric sulfide (HgS, vermillion, a high-grade paint pigment). Organic mercury compounds are important. It has been found that an electrical discharge causes mercury vapor to combine with neon, argon, krypton, and xenon. These products, held together with van der Waals' forces, correspond to HgNe, HgAr, HgKr, and HgXe. Mercury is a virulent poison and is readily absorbed through the respiratory tract, the gastrointestinal tract, or through unbroken skin. It acts as a cumulative poison and dangerous levels are readily attained in air. Air saturated with mercury vapor at 20°C contains a concentration that exceeds the toxic limit many times. The danger increases at higher temperatures. *It is therefore important that mercury be handled with care.* Containers of mercury should be securely covered and spillage should be avoided. If it is necessary to heat mercury or mercury compounds, it should be done in a well-ventilated hood. Methyl mercury is a dangerous pollutant and is now widely found in water and streams. The triple point of mercury, −38.8344°C, is a fixed point on the International Temperature Scale (ITS-90).

Molybdenum — (Gr. *molybdos*; lead), Mo; at. wt. 95.94; at. no. 42; m.p. 2623°C; b.p. 4639°C; sp. gr. 10.22 (20°C); valence 2, 3, 4?, 5?, or 6. Before Scheele recognized molybdenite as a distinct ore of a new element in 1778, it was confused with graphite and lead ore. The metal was prepared in an impure form in 1782 by Hjelm. Molybdenum does not occur native, but is obtained principally from *molybdenite* (MoS_2). *Wulfenite* ($PbMoO_4$) and *Powellite* ($Ca(MoW)O_4$) are also minor commercial ores. Molybdenum is also recovered as a by-product of copper and tungsten mining operations. The metal is prepared from the powder made by the hydrogen reduction of purified molybdic trioxide or ammonium molybdate. The metal is silvery white, very hard, but is softer and more ductile than tungsten. It has a high elastic modulus, and only tungsten and tantalum, of the more readily available metals, have higher melting points. It is a valuable alloying agent, as it contributes to the hardenability and toughness of quenched and tempered steels. It also improves the strength of steel at high temperatures. It is used in certain nickel-based alloys, such as the "Hastelloys®" which are heat-resistant and corrosion-resistant to chemical solutions. Molybdenum oxidizes at elevated temperatures. The metal has found recent application as electrodes for electrically heated glass furnaces and foreheaths. The metal is also used in nuclear energy applications and for missile and aircraft parts. Molybdenum is valuable as a catalyst in the refining of petroleum. It has found application as a filament material in electronic and electrical applications. Molybdenum is an essential trace element in plant nutrition. Some lands are barren for lack of this element in the soil. Molybdenum sulfide is useful as a lubricant, especially at high temperatures where oils would decompose. Almost all ultra-high strength steels with minimum yield points up to 300,000 psi(lb/in.^{2}) contain molybdenum in amounts from 0.25 to 8%.

Neodymium — (Gr. *neos*, new, and *didymos*, twin), Nd; at. wt. 144.24; at. no. 60; m.p. 1016°C; b.p. 3066°C; sp. gr. 7.008 (25°C); valence 3. In 1841, Mosander, extracted from *cerite* a new rose-colored oxide, which he believed contained a new element. He named the element *didymium*, as it was *an inseparable twin brother of lanthanum*.. In 1885 von Welsbach separated didymium into two new elemental components, *neodymia* and *praseodymia*, by repeated fractionation of ammonium didymium nitrate. While the free metal is in *misch metal*, long known and used as a pyrophoric alloy for light flints, the element was not isolated in relatively pure form until 1925. Neodymium is present in misch metal to the extent of about 18%. It is present in the minerals *monazite* and *bastnasite*, which are principal sources of rare-earth metals. The element may be obtained by separating neodymium salts from other rare earths by ion-exchange or solvent extraction techniques, and by reducing anhydrous halides such as NdF_3 with calcium metal. Other separation techniques are possible. The metal has a bright silvery metallic luster. Neodymium is one of the more reactive rare-earth metals and quickly tarnishes in air, forming an oxide that spalls off and exposes metal to oxidation. The metal, therefore, should be kept under light mineral oil or sealed in a plastic material. Neodymium exists in two allotropic forms, with a transformation from a double hexagonal to a body-centered cubic structure taking place at 863°C. Natural neodymium is a mixture of seven stable isotopes. Fourteen other radioactive isotopes are recognized. Didymium, of which neodymium is a component, is used for coloring glass to make welder's goggles. By itself, neodymium colors glass delicate shades ranging from pure violet through wine-red and warm gray. Light transmitted through such glass shows unusually sharp absorption bands. The glass has been used in astronomical work to produce sharp bands by which spectral lines may be calibrated. Glass containing neodymium can be used as

a laser material to produce coherent light. Neodymium salts are also used as a colorant for enamels. The price of the metal is about $1/g. Neodymium has a low-to-moderate acute toxic rating. As with other rare earths, neodymium should be handled with care.

Neon — (Gr. *neos*, new), Ne; at. wt. 20.1797; at. no. 10; m.p. –248.59°C; b.p. –246.08°C (1 atm); density of gas 0.89990 g/l (1 atm, 0°C); density of liquid at b.p. 1.207 g/cm^3; valence 0. Discovered by Ramsay and Travers in 1898. Neon is a rare gaseous element present in the atmosphere to the extent of 1 part in 65,000 of air. It is obtained by liquefaction of air and separated from the other gases by fractional distillation. Natural neon is a mixture of three isotopes. Six other unstable isotopes are known. It is very inert element; however, it is said to form a compound with fluorine. It is still questionable if true compounds of neon exist, but evidence is mounting in favor of their existence. The following ions are known from optical and mass spectrometric studies: Ne^+, $(NeAr)^+$, $(NeH)^+$, and $(HeNe^+)$. Neon also forms an unstable hydrate. In a vacuum discharge tube, neon glows reddish orange. Of all the rare gases, the discharge of neon is the most intense at ordinary voltages and currents. Neon is used in making the common neon advertising signs, which accounts for its largest use. It is also used to make high-voltage indicators, lightning arrestors, wave meter tubes, and TV tubes. Neon and helium are used in making gas lasers. Liquid neon is now commercially available and is finding important application as an economical cryogenic refrigerant. It has over 40 times more refrigerating capacity per unit volume than liquid helium and more than three times that of liquid hydrogen. It is compact, inert, and is less expensive than helium when it meets refrigeration requirements. Neon costs about $2.00/l.

Neptunium — (Planet *Neptune*), Np; at. wt. (237); at. no. 93; m.p. 644°C; b.p. 3902°C (est.); sp. gr. 20.25 (20°C); valence 3, 4, 5, and 6. Neptunium was the first synthetic transuranium element of the actinide series discovered; the isotope ^{239}Np was produced by McMillan and Abelson in 1940 at Berkeley, California; as the result of bombarding uranium with cyclotron-produced neutrons. The isotope ^{237}Np (half-life of 2.14×10^6 years) is currently obtained in gram quantities as a by-product from nuclear reactors in the production of plutonium. Trace quantities of the element are actually found in nature due to transmutation reactions in uranium ores produced by the neutrons which are present. Neptunium is prepared by the reduction of NpF_3 with barium or lithium vapor at about 1200°C. Neptunium metal has a silvery appearance, is chemically reactive, and exists in at least three structural modifications: α-neptunium, orthorhombic, density 20.25 g/cm^3, β-neptunium (above 280°C), tetragonal, density (313°C) 19.36 g/cm^3; γ-neptunium (above 577°C), cubic, density (600°C) 18.0 g/cm^3. Neptunium has four ionic oxidation states in solution: Np^{+3} (pale purple), analogous to the rare earth ion Pm^{+3}, Np^{+4} (yellow green); NpO^+ (green blue); and NpO^{++} (pale pink). These latter oxygenated species are in contrast to the rare earths which exhibit only simple ions of the (II), (III), and (IV) oxidation states in aqueous solution. The element forms tri- and tetrahalides such as NpF_3, NpF_4, $NpCl_4$, $NpBr_3$, NpI_3, and oxides of various compositions such as are found in the uranium-oxygen system, including Np_3O_8 and NpO_2. Fifteen isotopes of neptunium are now recognized. The O.R.N.L. has ^{237}Np available for sale to its licensees and for export. This isotope can be used as a component in neutron detection instruments. It is offered at a price of $280/g.

Nickel — (Ger. *Nickel*, Satan or Old Nick's and from *kupfernickel*, Old Nick's copper), Ni; at. wt. 58.6934; at. no. 28; m.p. 1455°C; b.p. 2913°C; sp. gr. 8.902 (25°C); valence 0, 1, 2, 3. Discovered by Cronstedt in 1751 in kupfernickel (*niccolite*). Nickel is found as a constituent in most meteorites and often serves as one of the criteria for distinguishing a meteorite from other minerals. Iron meteorites, or *siderites*, may contain iron alloyed with from 5 to nearly 20% nickel. Nickel is obtained commercially from *pentlandite* and *pyrrhotite* of the Sudbury region of Ontario, a district that produces about 30% of the nickel for the Free World. Other deposits are found in New Caledonia, Australia, Cuba, Indonesia, and elsewhere. Nickel is silvery white and takes on a high polish. It is hard, malleable, ductile, somewhat ferromagnetic, and a fair conductor of heat and electricity. It belongs to the iron-cobalt group of metals and is chiefly valuable for the alloys it forms. It is extensively used for making stainless steel and other corrosion-resistant alloys such as Invar®, Monel®, Inconel®, and the Hastelloys®. Tubing made of a copper-nickel alloy is extensively used in making desalination plants for converting sea water into fresh water. Nickel is also now used extensively in coinage and in making nickel steel for armor plate and burglar-proof vaults, and is a component in Nichrome®, Permalloy®, and constantan. Nickel added to glass gives a green color. Nickel plating is often used to provide a protective coating for other metals, and finely divided nickel is a catalyst for hydrogenating vegetable oils. It is also used in ceramics, in the manufacture of Alnico magnets, and in the Edison® storage battery. The sulfate and the oxides are important compounds. Natural nickel is a mixture of five stable isotopes; nine other unstable isotopes are known. Exposure to nickel metal and soluble compounds (as Ni) should not exceed 0.05 mg/m^3 (8-hour time-weighted average — 40-hour week). Nickel sulfide fume and dust is recognized as having carcinogenic potential.

Niobium — (*Niobe*, daughter of Tantalus), Nb; or Columbium (*Columbia*, name for America); at. wt. 92.90638; at. no. 41; m.p. 2477 ± 10°C; b.p. 4744°C, sp. gr. 8.57 (20°C); valence 2, 3, 4?, 5. Discovered in 1801 by Hatchett in an ore sent to England more that a century before by John Winthrop the Younger, first governor of Connecticut. The metal was first prepared in 1864 by Blomstrand, who reduced the chloride by heating it in a hydrogen atmosphere. The name *niobium* was adopted by the International Union of Pure and Applied Chemistry in 1950 after 100 years of controversy. Many leading chemical societies and government organizations refer to it by this name. Most metallurgists, leading metal societies, and all but one of the leading U.S. commercial producers, however, still refer to the metal as "columbium". The element is found in *niobite* (or *columbite*), *niobite-tantalite*, *pyrochlore*, and *euxenite*. Large deposits of niobium have been found associated with *carbonatites* (carbon-silicate rocks), as a constituent of *pyrochlore*. Extensive ore reserves are found in Canada, Brazil, Nigeria, Zaire, and in the U.S.S.R. The metal can be isolated from tantalum, and prepared in several ways. It is a shiny, white, soft, and ductile metal, and takes on a bluish cast when exposed to air at room temperatures for a long time. The metal starts to oxidize in air at 200°C, and when processed at even moderate temperatures must be placed in a protective atmosphere. It is used in arc-welding rods for stabilized grades of stainless steel. Thousands of pounds of niobium have been used in advance air frame systems such as were used in the Gemini space program. The element has superconductive properties; superconductive magnets have been made with Nb-Zr wire, which retains its superconductivity in strong magnetic fields. This type of application offers hope of direct large-scale generation of electric power. Eighteen isotopes of niobium are known. Niobium metal (99.5% pure) is priced at about $75/lb.

Nitrogen — (L. *nitrum*, Gr. *nitron*, native soda; genes. *forming*, N; at. wt. 14.00674; at. no. 7; m.p. –210.00°C; b.p. –195.8°C; density 1.2506 g/l; sp. gr. liquid 0.808 (–195.8°C), solid 1.026 (–252°C); valence 3 or 5. Discovered by Daniel Rutherford in 1772, but Scheele, Cavendish, Priestley, and others about the same time studied "burnt or dephlogisticated air," as air without oxygen was then called. Nitrogen makes up 78% of the air, by volume. The atmosphere of Mars, by comparison, is 2.6% nitrogen. The estimated amount of this element in our atmosphere is more than 4000 trillion tons. From this inexhaustible source it can be obtained by liquefaction and fractional distillation. Nitrogen molecules give the orange-red, blue-green, blue-violet, and deep violet shades to the aurora. The element is so inert that Lavoisier named it *azote*, meaning without life, yet its compounds are so

in its use for fertilizers. Potassium is an essential constituent for plant growth and it is found in most soils. Potassium is never found free in nature, but is obtained by electrolysis of the hydroxide, much in the same manner as prepared by Davy. Thermal methods also are commonly used to produce potassium (such as by reduction of potassium compounds with CaC_2, C, Si, or Na). It is one of the most reactive and electropositive of metals. Except for lithium, it is the lightest known metal. It is soft, easily cut with a knife, and is silvery in appearance immediately after a fresh surface is exposed. It rapidly oxidizes in air and must be preserved in a mineral oil such as kerosene. As with other metals of the alkali group, it decomposes in water with the evolution of hydrogen. It catches fire spontaneously on water. Potassium and its salts impart a violet color to flames. Seventeen isotopes of potassium are known. Ordinary potassium is composed of three isotopes, one of which is ^{40}K (0.0118%), a radioactive isotope with a half-life of 1.28×10^9 years. The radioactivity presents no appreciable hazard. An alloy of sodium and potassium (NaK) is used as a heat-transfer medium. Many potassium salts are of utmost importance, including the hydroxide, nitrate, carbonate, chloride, chlorate, bromide, iodide, cyanide, sulfate, chromate, and dichromate. Metallic potassium is available commercially for about $40/lb in small quantities.

Praseodymium — (Gr. *prasios*, green, and *didymos*, twin), Pr; at. wt. 140.90765; at. no. 59; m.p. 931°C; b.p. 3510°C; sp. gr. 6.773; valence 3. In 1841 Mosander extracted the rare earth *didymia* from *lanthana*; in 1879, Lecoq de Boisbaudran isolated a new earth, *samaria*, from didymia obtained from the mineral *samarskite*. Six years later, in 1885, von Welsbach separated didymia into two others, *praseodymia* and *neodymia*, which gave salts of different colors. As with other rare earths, compounds of these elements in solution have distinctive sharp spectral absorption bands or lines, some of which are only a few Angstroms wide. The element occurs along with other rare-earth elements in a variety of minerals. *Monazite* and *bastnasite* are the two principal commercial sources of the rare-earth metals. Ion-exchange and solvent extraction techniques have led to much easier isolation of the rare earths and the cost has dropped greatly in the past few years. Praseodymium can be prepared by several methods, such as by calcium reduction of the anhydrous chloride of fluoride. Misch metal, used in making cigarette lighters, contains about 5% praseodymium metal. Praseodymium is soft, silvery, malleable, and ductile. It was prepared in relatively pure form in 1931. It is somewhat more resistant to corrosion in air than europium, lanthanum, cerium, or neodymium, but it does develop a green oxide coating that spalls off when exposed to air. As with other rare-earth metals it should be kept under a light mineral oil or sealed in plastic. The rare-earth oxides, including Pr_2O_3, are among the most refractory substances known. Along with other rare earths, it is widely used as a core material for carbon arcs used by the motion picture industry for studio lighting and projection. Salts of praseodymium are used to color glasses and enamels; when mixed with certain other materials, praseodymium produces an intense and unusually clean yellow color in glass. Didymium glass, of which praseodymium is a component, is a colorant for welder's goggles. The metal (99 + % pure) is priced at about $70/oz.

Promethium — (*Prometheus*, who, according to mythology, stole fire from heaven), Pm; at. no. 61; at. wt. (145); m.p. 1042°C; b.p. 3000°C (est.); sp. gr. 7.264 (25°C); valence 3. In 1902 Branner predicted the existence of an element between neodymium and samarium, and this was confirmed by Moseley in 1914. In 1941, workers at Ohio State University irradiated neodymium and praseodymium with neutrons, deuterons, and alpha particles, resp., and produced several new radioactivities, which most likely were those of element 61. Wu and Segre, and Bethe, in 1942, confirmed the formation; however, chemical proof of the production of element 61 was lacking because of the difficulty in separating the rare earths from each other at that time. In 1945, Marinsky, Glendenin, and Coryell made the first chemical identification by use of ion-exchange chromatography. Their work was done by fission of uranium and by neutron bombardment of neodymium. Searches for the element on earth have been fruitless, and it now appears that promethium is completely missing from the earth's crust. Promethium, however, has been identified in the spectrum of the star HR^{465} in Andromeda. This element is being formed recently near the star's surface, for no known isotope of promethium has a half-life longer than 17.7 years. Seventeen isotopes of promethium, with atomic masses from 134 to 155 are now known. Promethium-147, with a half-life of 2.6 years, is the most generally useful. Promethium-145 is the longest lived, and has a specific activity of 940 Ci/g. It is a soft beta emitter; although no gamma rays are emitted, X-radiation can be generated when beta particles impinge on elements of a high atomic number, and great care must be taken in handling it. Promethium salts luminesce in the dark with a pale blue or greenish glow, due to their high radioactivity. Ion-exchange methods led to the preparation of about 10 g of promethium from atomic reactor fuel processing wastes in early 1963. Little is yet generally known about the properties of metallic promethium. Two allotropic modifications exist. The element has applications as a beta source for thickness gages, and it can be absorbed by a phosphor to produce light. Light produced in this manner can be used for signs or signals that require dependable operation; it can be used as a nuclear-powered battery by capturing light in photocells which convert it into electric current. Such a battery, using ^{147}Pm, would have a useful life of about 5 years. Promethium shows promise as a portable X-ray source, and it may become useful as a heat source to provide auxiliary power for space probes and satellites. More than 30 promethium compounds have been prepared. Most are colored. Promethium-147 is available at a cost of about 50c/Ci.

Protactinium — (Gr. *protos*, first), Pa; at. wt. 231.03588; at. no. 91; m.p. 1572°C; sp. gr. 15.37 (calc.); valence 4 or 5. The first isotope of element 91 to be discovered was ^{234}Pa, also known as UX_2, a short-lived member of the naturally occurring ^{238}U decay series. It was identified by K. Fajans and O. H. Gohring in 1913 and they named the new element *brevium*. When the longer-lived isotope ^{231}Pa was identified by Hahn and Meitner in 1918, the name protoactinium was adopted as being more consistent with the characteristics of the most abundant isotope. Soddy, Cranson, and Fleck were also active in this work. The name *protoactinium* was shortened to *protactinium* in 1949. In 1927, Grosse prepared 2 mg of a white powder, which was shown to be Pa_2O_5. Later, in 1934, from 0.1 g of pure Pa_2O_5 he isolated the element by two methods, one of which was by converting the oxide to an iodide and "cracking" it in a high vacuum by an electrically heated filament by the reaction

$$2PaI_5 \rightarrow 2Pa + 5I_2$$

Protactinium has a bright metallic luster which it retains for some time in air. The element occurs in *pitchblende* to the extent of about 1 part ^{231}Pa to 10 million of ore. Ores from Zaire have about 3 ppm. Protactinium has 20 isotopes, the most common of which is ^{231}Pr with a half-life of 32,700 years. A number of protactinium compounds are known, some of which are colored. The element is superconductive below 1.4 K. The element is a dangerous toxic material and requires precautions similar to those used when handling plutonium. In 1959 and 1961, it was announced that the Great Britain Atomic Energy Authority extracted by a 12-stage process 125 g of 99.9% protactinium, the world's only stock of the metal for many years to come.

ores of the Sudbury, Ontario region. Although the quantity occurring here is very small, the large tonnages of nickel processed make the recovery commercially feasible. The annual world production of rhodium is only 7 or 8 tons. The metal is silvery white and at red heat slowly changes in air to the sesquioxide. At higher temperatures it converts back to the element. Rhodium has a higher melting point and lower density than platinum. Its major use is as an alloying agent to harden platinum and palladium. Such alloys are used for furnace windings, thermocouple elements, bushings for glass fiber production, electrodes for aircraft spark plugs, and laboratory crucibles. It is useful as an electrical contact material as it has a low electrical resistance, a low and stable contact resistance, and is highly resistant to corrosion. Plated rhodium, produced by electroplating or evaporation, is exceptionally hard and is used for optical instruments. It has a high reflectance and is hard and durable. Rhodium is also used for jewelry, for decoration, and as a catalyst. Exposure to rhodium (metal fume and dust, as Rh) should not exceed 1 mg/m^3 (8-hour time-weighted average, 40-hour wk.). Soluble salts should not exceed 0.01 mg/m^3. Rhodium costs about $1000/troy oz.

Rubidium — (L. *rubidus*, deepest red), Rb; at. wt. 85.4678; at. no. 37; m.p. 39.31°C; b.p. 688°C; sp. gr. (solid) 1.532 (20°C), (liquid) 1.475 (39°C); valence 1, 2, 3, 4. Discovered in 1861 by Bunsen and Kirchoff in the mineral *lepidolite* by use of the spectroscope. The element is much more abundant than was thought several years ago. It is now considered to be the 16th most abundant element in the earth's crust. Rubidium occurs in *pollucite*, *carnallite*, *leucite*, and *zinnwaldite*, which contains traces up to 1%, in the form of the oxide. It is found in lepidolite to the extent of about 1.5%, and is recovered commercially from this source. Potassium minerals, such as those found at Searles Lake, California, and potassium chloride recovered from brines in Michigan also contain the element and are commercial sources. It is also found along with cesium in the extensive deposits of *pollucite* at Bernic Lake, Manitoba. Rubidium can be liquid at room temperature. It is a soft, silvery-white metallic element of the alkali group and is the second most electropositive and alkaline element. It ignites spontaneously in air and reacts violently in water, setting fire to the liberated hydrogen. As with other alkali metals, it forms amalgams with mercury and it alloys with gold, cesium, sodium, and potassium. It colors a flame yellowish violet. Rubidium metal can be prepared by reducing rubidium chloride with calcium, and by a number of other methods. It must be kept under a dry mineral oil or in a vacuum or inert atmosphere. Twenty four isotopes of rubidium are known. Naturally occurring rubidium is made of two isotopes, ^{85}Rb and ^{87}Rb. Rubidium-87 is present to the extent of 27.85% in natural rubidium and is a beta emitter with a half-life of 4.9×10^{10} years. Ordinary rubidium is sufficiently radioactive to expose a photographic film in about 30 to 60 days. Rubidium forms four oxides: Rb_2O, Rb_2O_2, Rb_2O_3, Rb_2O_4. Because rubidium can be easily ionized, it has been considered for use in "ion engines" for space vehicles; however, cesium is somewhat more efficient for this purpose. It is also proposed for use as a working fluid for vapor turbines and for use in a thermoelectric generator using the magnetohydrodynamic principle where rubidium ions are formed by heat at high temperature and passed through a magnetic field. These conduct electricity and act like an armature of a generator thereby generating an electric current. Rubidium is used as a getter in vacuum tubes and as a photocell component. It has been used in making special glasses. $RbAg_4I_5$ is important, as it has the highest room conductivity of any known ionic crystal. At 20°C its conductivity is about the same as dilute sulfuric acid. This suggests use in thin film batteries and other applications. The present cost in small quantities in about $25/g.

Ruthenium — (L. *Ruthenia*, Russia), Ru; at. wt. 101.07; at. no. 44; m.p. 2334°C; b.p. 4150°C; sp. gr. 12.41 (20°C); valence 0, 1, 2, 3, 4, 5, 6, 7, 8. Berzelius and Osann in 1827 examined the residues left after dissolving crude platinum from the Ural mountains in *aqua regia*. While Berzelius found no unusual metals, Osann thought he found three new metals, one of which he named ruthenium. In 1844 Klaus, generally recognized as the discoverer, showed that Osann's ruthenium oxide was very impure and that it contained a new metal. Klaus obtained 6 g of ruthenium from the portion of crude platinum that is insoluble in *aqua regia*. A member of the platinum group, ruthenium occurs native with other members of the group in ores found in the Ural mountains and in North and South America. It is also found along with other platinum metals in small but commercial quantities in *pentlandite* of the Sudbury, Ontario, nickel-mining region, and in *pyroxinite* deposits of South Africa. The metal is isolated commercially by a complex chemical process, the final stage of which is the hydrogen reduction of ammonium ruthenium chloride, which yields a powder. The powder is consolidated by powder metallurgy techniques or by argon-arc welding. Ruthenium is a hard, white metal and has four crystal modifications. It does not tarnish at room temperatures, but oxidizes in air at about 800°C. The metal is not attacked by hot or cold acids or *aqua regia*, but when potassium chlorate is added to the solution, it oxidizes explosively. It is attacked by halogens, hydroxides, etc. Ruthenium can be plated by electrodeposition or by thermal decomposition methods. The metal is one of the most effective hardeners for platinum and plalladium, and is alloyed with these metals to make electrical contacts for severe wear resistance. A ruthenium-molybdenum alloy is said to be superconductive at 10.6 K. The corrosion resistance of titanium is improved a hundredfold by addition of 0.1% ruthenium. It is a versatile catalyst. Hydrogen sulfide can be split catalytically by light using an aqueous suspension of CdS particles loaded with ruthenium dioxide. It is thought this may have application to removal of H_2S from oil refining and other industrial processes. Compounds in at least eight oxidation states have been found, but of these, the +2, +3, and +4 states are the most common. Ruthenium tetroxide, like osmium tetroxide, is highly toxic. In addition, it may explode. Ruthenium compounds show a marked resemblance to those of osmium. The metal is priced at about $30/g.

Rutherfordium — See Element 104 (unnilquadium).

Samarium — (*Samarskite* a mineral), Sm; at. wt. 150.36; at. no. 62; m.p. 1072°C; b.p. 1790°C; sp. gr (α) 7.520 (25°C); valence 2 or 3. Discovered spectroscopically by its sharp absorption lines in 1879 by Lecoq de Boisbaudran in the mineral *samarskite*, named in honor of a Russian mine official, Col. Samarski. Samarium is found along with other members of the rare-earth elements in many minerals, including *monazite* and *bastnasite*, which are commercial sources. It occurs in monazite to the extent of 2.8%. While *misch metal* containing about 1% of samarium metal, has long been used, samarium has not been isolated in relatively pure form until recent years. Ion-exchange and solvent extraction techniques have recently simplified separation of the rare earths from one another; more recently, electrochemical deposition, using an electrolytic solution of lithium citrate and a mercury electrode, is said to be a simple, fast, and highly specific way to separate the rare earths. Samarium metal can be produced by reducing the oxide with barium or lanthanum. Samarium has a bright silver luster and is reasonably stable in air. Three crystal modifications of the metal exist, with transformations at 734 and 922°C. The metal ignites in air at about 150°C. Twenty one isotopes of samarium exist. Natural samarium is a mixture of several isotopes, three of which are unstable with long half-lives. Samarium, along with other rare earths, is used for carbon-arc lighting for the motion picture industry. The sulfide has excellent high-temperature stability and good thermoelectric efficiencies up to 1100°C. $SmCo_5$ has been used in making a new permanent magnet material with the highest resistance to demagnetization of any known material. It is said to have an intrinsic coercive

force as high as 2200 kA/m. Samarium oxide has been used in optical glass to absorb the infrared. Samarium is used to dope calcium fluoride crystals for use in optical masers or lasers. Compounds of the metal act as sensitizers for phosphors excited in the infrared; the oxide exhibits catalytic properties in the dehydration and dehydrogenation of ethyl alcohol. It is used in infrared absorbing glass and as a neutron absorber in nuclear reactors. The metal is priced at about $5/g. Little is known of the toxicity of samarium; therefore, it should be handled carefully.

Scandium — (L. *Scandia*, Scandinavia). Sc; at. wt. 44.955910; at. no. 21; m.p. 1541°C; b.p. 2830°C; sp. gr. 2.989 (25°C); valence 3. On the basis of the Periodic System, Mendeleev predicted the existence of *ekaboron*, which would have an atomic weight between 40 of calcium and 48 of titanium. The element was discovered by Nilson in 1878 in the minerals *euxenite* and *gadolinite*, which had not yet been found anywhere except in Scandinavia. By processing 10 kg of euxenite and other residues of rare-earth minerals, Nilson was able to prepare about 2 g of scandium oxide of high purity. Cleve later pointed out that Nilson's scandium was identical with Mendeleev's ekaboron. Scandium is apparently a much more abundant element in the sun and certain stars than here on earth. It is about the 23rd most abundant element in the sun, compared to the 50th most abundant on earth. It is widely distributed on earth, occurring in very minute quantities in over 800 mineral species. The blue color of beryl (aquamarine variety) is said to be due to scandium. It occurs as a principal component in the rare mineral *thortveitite*, found in Scandinavia and Malagasy. It is also found in the residues remaining after the extraction of tungsten from Zinnwald *wolframite*, and in *wiikite* and *bazzite*. Most scandium is presently being recovered from *thortveitite* or is extracted as a by-product from uranium mill tailings. Metallic scandium was first prepared in 1937 by Fischer, Brunger, and Grieneisen, who electrolyzed a eutectic melt of potassium, lithium, and scandium chlorides at 700 to 800°C. Tungsten wire and a pool of molten zinc served as the electrodes in a graphite crucible. Pure scandium is now produced by reducing scandium fluoride with calcium metal. The production of the first pound of 99% pure scandium metal was announced in 1960. Scandium is a silver-white metal which develops a slightly yellowish or pinkish cast upon exposure to air. It is relatively soft, and resembles yttrium and the rare-earth metals more than it resembles aluminum or titanium. It is a very light metal and has a much higher melting point than aluminum, making it of interest to designers of spacecraft. Scandium is not attacked by a 1:1 mixture of conc. HNO_3 and 48% HF. Scandium reacts rapidly with many acids. Twelve isotopes of scandium are recognized. The metal is expensive, costing about $130/g with a purity of about 99.9%. Scandium oxide costs about $75/g. About 20 kg of scandium (as Sc_2O_3) are now being used yearly in the U.S. to produce high-intensity lights, and the radioactive isotope ^{46}Sc is used as a tracing agent in refinery crackers for crude oil, etc. Scandium iodide added to mercury vapor lamps produces a highly efficient light source resembling sunlight, which is important for indoor or night-time color TV. Little is yet known about the toxicity of scandium; therefore, it should be handled with care.

Selenium — (Gr. *Selene*, moon). Se; at. wt. 78.96; at. no. 34; m.p. (gray) 221°C; b.p. (gray) 685°C; sp. gr. (gray) 4.79, (vitreous) 4.28; valence −2, +4, or +6. Discovered by Berzelius in 1817, who found it associated with tellurium, named for the earth. Selenium is found in a few rare minerals, such as *crooksite* and *clausthalite*. In years past it has been obtained from flue dusts remaining from processing copper sulfide ores, but the anode muds from electrolytic copper refineries now provide the source of most of the world's selenium. Selenium is recovered by roasting the muds with soda or sulfuric acid, or by smelting them with soda and niter. Selenium exists in several allotropic forms. Three are generally recognized, but as many as six have been claimed. Selenium can be prepared with either an amorphous or crystalline structure. The color of amorphous selenium is either red, in powder form, or black, in vitreous form. Crystalline monoclinic selenium is a deep red; crystalline hexagonal selenium, the most stable variety, is a metallic gray. Natural selenium contains six stable isotopes. Fifteen other isotopes have been characterized. The element is a member of the sulfur family and resembles sulfur both in its various forms and in its compounds. Selenium exhibits both photovoltaic action, where light is converted directly into electricity, and photoconductive action, where the electrical resistance decreases with increased illumination. These properties make selenium useful in the production of photocells and exposure meters for photographic use, as well as solar cells. Selenium is also able to convert a.c. electricity to d.c., and is extensively used in rectifiers. Below its melting point selenium is a p-type semiconductor and is finding many uses in electronic and solid-state applications. It is used in Xerography for reproducing and copying documents, letters, etc. It is used by the glass industry to decolorize glass and to make ruby-colored glasses and enamels. It is also used as a photographic toner, and as an additive to stainless steel. Elemental selenium has been said to be practically nontoxic and is considered to be an essential trace element; however, hydrogen selenide and other selenium compounds are extremely toxic, and resemble arsenic in their physiological reactions. Hydrogen selenide in a concentration of 1.5 ppm is intolerable to man. Selenium occurs in some soils in amounts sufficient to produce serious effects on animals feeding on plants, such as locoweed, grown in such soils. Exposure to selenium compounds (as Se) in air should not exceed 0.2 mg/m^3 (8-hour time-weighted average — 40-hour week). Selenium is priced at about $30/lb. It is also available in high-purity form at a somewhat higher cost.

Silicon — (L. *silex, silicis*, flint), Si; at. wt. 28.0855; at. no. 14; m.p. 1414°C; b.p. 3265°C; sp. gr. 2.33 (25°C); valence 4. Davy in 1800 thought silica to be a compound and not an element; later in 1811, Gay Lussac and Thenard probably prepared impure amorphous silicon by heating potassium with silicon tetrafluoride. Berzelius, generally credited with the discovery, in 1824 succeeded in preparing amorphous silicon by the same general method as used earlier, but he purified the product by removing the fluosilicates by repeated washings. Deville in 1854 first prepared crystalline silicon, the second allotropic form of the element. Silicon is present in the sun and stars and is a principal component of a class of meteorites known as "aerolites". It is also a component of *tektites*, a natural glass of uncertain origin. Silicon makes up 25.7% of the earth's crust, by weight, and is the second most abundant element, being exceeded only by oxygen. Silicon is not found free in nature, but occurs chiefly as the oxide and as silicates. *Sand, quartz, rock crystal, amethyst, agate, flint, jasper*, and *opal* are some of the forms in which the oxide appears. *Granite, hornblende, asbestos, feldspar, clay mica*, etc. are but a few of the numerous silicate minerals. Silicon is prepared commercially by heating silica and carbon in an electric furnace, using carbon electrodes. Several other methods can be used for preparing the element. Amorphous silicon can be prepared as a brown powder, which can be easily melted or vaporized. Crystalline silicon has a metallic luster and grayish color. The Czochralski process is commonly used to produce single crystals of silicon used for solid-state or semiconductor devices. Hyperpure silicon can be prepared by the thermal decomposition of ultra-pure trichlorosilane in a hydrogen atmosphere, and by a vacuum float zone process. This product can be doped with boron, gallium, phosphorus, or arsenic to produce silicon for use in transistors, solar cells, rectifiers, and other solid-state devices which are used extensively in the electronics and space-age industries. Hydrogenated amorphous silicon has shown promise in producing economical cells for converting solar energy into electricity. Silicon is a relatively inert element, but it is attacked by halogens and dilute alkali. Most acids except hydrofluoric, do not affect it. Silicones are important products of silicon. They may be prepared by hydrolyzing a silicon organic chloride, such as dimethyl silicon chloride. Hydrolysis and condensation

was bombarded by deuterons in the Berkeley cyclotron, and which E. Lawrence sent to these investigators. Technetium was the first element to be produced artificially. Since its discovery, searches for the element in terrestrial materials have been made without success. If it does exist, the concentration must be very small. Technetium has been found in the spectrum of S-, M-, and N-type stars, and its presence in stellar matter is leading to new theories of the production of heavy elements in the stars. Nineteen isotopes of technetium, with atomic masses ranging from 90 to 108, are known. ^{97}Tc has a half-life of 2.6×10^6 years. ^{98}Tc has a half-life of 4.2×10^6 years. The isomeric isotope ^{95m}Tc, with a half-life of 61 days, is useful for tracer work, as it produces energetic gamma rays. Technetium metal has been produced in kilogram quantities. The metal was first prepared by passing hydrogen gas at 1100°C over Tc_2S_7. It is now conveniently prepared by the reduction of ammonium pertechnetate with hydrogen. Technetium is a silvery-gray metal that tarnishes slowly in moist air. Until 1960, technetium was available only in small amounts and the price was as high as $2800/g. It is now commercially available to holders of O.R.N.L. permits at a price of $60/g. The chemistry of technetium is said to be similar to that of rhenium. Technetium dissolves in nitric acid, aqua regia, and conc. sulfuric acid, but is not soluble in hydrochloric acid of any strength. The element is a remarkable corrosion inhibitor for steel. It is reported that mild carbon steels may be effectively protected by as little as 55 ppm of $KTcO_4$ in aerated distilled water at temperatures up to 250°C. This corrosion protection is limited to closed systems, since technetium is radioactive and must be confined. ^{99}Tc has a specific activity of 6.2×10^8 Bq/g. Activity of this level must not be allowed to spread. ^{99}Tc is a contamination hazard and should be handled in a glove box. The metal is an excellent superconductor at 11 K and below.

Tellurium — (L. *tellus*, earth), Te; at. wt. 127.60; at. no. 52; m.p. 449.51 ± 0.3°C; b.p. 988°C; sp. gr. 6.24 (20°C); valence 2, 4, or 6. Discovered by Muller von Reichenstein in 1782; named by Klaproth, who isolated it in 1798. Tellurium is occasionally found native, but is more often found as the telluride of gold (*calaverite*), and combined with other metals. It is recovered commercially from the anode muds produced during the electrolytic refining of blister copper. The U.S., Canada, Peru, and Japan are the largest Free World producers of the element. Crystalline tellurium has a silvery-white appearance, and when pure exhibits a metallic luster. It is brittle and easily pulverized. Amorphous tellurium is formed by precipitating tellurium from a solution of telluric or tellurous acid. Whether this form is truly amorphous, or made of minute crystals, is open to question. Tellurium is a p-type semiconductor, and shows greater conductivity in certain directions, depending on alignment of the atoms. Its conductivity increases slightly with exposure to light. It can be doped with silver, copper, gold, tin, or other elements. In air, tellurium burns with a greenish-blue flame, forming the dioxide. Molten tellurium corrodes iron, copper, and stainless steel. Tellurium and its compounds are probably toxic and should be handled with care. Workmen exposed to as little as 0.01 mg/m^3 of air, or less, develop "tellurium breath," which has a garlic-like odor. Thirty isotopes of tellurium are known, with atomic masses ranging from 108 to 137. Natural tellurium consists of eight isotopes. Tellurium improves the machinability of copper and stainless steel, and its addition to lead decreases the corrosive action of sulfuric acid on lead and improves its strength and hardness. Tellurium is used as a basic ingredient in blasting caps, and is added to cast iron for chill control. Tellurium is used in ceramics. Bismuth telluride has been used in thermoelectric devices. Tellurium costs about $100/lb, with a purity of about 99.5%.

Terbium — (*Ytterby*, village in Sweden), Tb; at. wt. 158.92534; at. no. 65; m.p. 1359°C; b.p. 3221°C; sp. gr. 8.230; valence 3, 4. Discovered by Mosander in 1843. Terbium is a member of the lanthanide or "rare earth" group of elements. It is found in *cerite*, *gadolinite*, and other minerals along with other rare earths. It is recovered commercially from *monazite* in which it is present to the extent of 0.03%, from *xenotime*, and from *euxenite*, a complex oxide containing 1% of more of terbia. Terbium has been isolated only in recent years with the development of ion-exchange techniques for separating the rare-earth elements. As with other rare earths, it can be produced by reducing the anhydrous chloride or fluoride with calcium metal in a tantalum crucible. Calcium and tantalum impurities can be removed by vacuum remelting. Other methods of isolation are possible. Terbium is reasonably stable in air. It is a silver-gray metal, and is malleable, ductile, and soft enough to be cut with a knife. Two crystal modifications exist, with a transformation temperature of 1289°C. Twenty one isotopes with atomic masses ranging from 145 to 165 are recognized. The oxide is a chocolate or dark maroon color. Sodium terbium borate is used as a laser material and emits coherent light at 0.546 μm. Terbium is used to dope calcium fluoride, calcium tungstate, and strontium molybdate, used in solid-state devices. The oxide has potential application as an activator for green phosphors used in color TV tubes. It can be used with ZrO_2 as a crystal stabilizer of fuel cells which operate at elevated temperature. Few other uses have been found. The element is priced at about $30/g (99.9%). Little is known of the toxicity of terbium. It should be handled with care as with other lanthanide elements.

Thallium — (Gr. *thallos*, a green shoot or twig), Tl; at. wt. 204.3833; at. no. 81; m.p. 304°C; b.p. 1473 ± 10°C; sp. gr. 11.85 (20°C); valence 1, or 3. Thallium was discovered spectroscopically in 1861 by Crookes. The element was named after the beautiful green spectral line, which identified the element. The metal was isolated both by Crookes and Lamy in 1862 about the same time. Thallium occurs in *crooksite*, *lorandite*, and *hutchinsonite*. It is also present in *pyrites* and is recovered from the roasting of this ore in connection with the production of sulfuric acid. It is also obtained from the smelting of lead and zinc ores. Extraction is somewhat complex and depends on the source of the thallium. Manganese nodules, found on the ocean floor, contain thallium. When freshly exposed to air, thallium exhibits a metallic luster, but soon develops a bluish-gray tinge, resembling lead in appearance. A heavy oxide builds up on thallium if left in air, and in the presence of water the hydroxide is formed. The metal is very soft and malleable. It can be cut with a knife. Twenty five isotopic forms of thallium, with atomic masses ranging from 184 to 210 are recognized. Natural thallium is a mixture of two isotopes. The element and its compounds are toxic and should be handled carefully. Contact of the metal with skin is dangerous, and when melting the metal adequate ventilation should be provided. Exposure to thallium (soluble compounds) — skin, as Tl, should not exceed 0.1 mg/m^3 (8-hour time-weighted average — 40-hour week). Thallium is suspected of carcinogenic potential for man. Thallium sulfate has been widely employed as a rodenticide and ant killer. It is odorless and tasteless, giving no warning of its presence. Its use, however, has been prohibited in the U.S. since 1975 as a household insecticide and rodenticide. The electrical conductivity of thallium sulfide changes with exposure to infrared light, and this compound is used in photocells. Thallium bromide-iodide crystals have been used as infrared optical materials. Thallium has been used, with sulfur or selenium and arsenic, to produce low melting glasses which become fluid between 125 and 150°C. These glasses have properties at room temperatures similar to ordinary glasses and are said to be durable and insoluble in water. Thallium oxide has been used to produce glasses with a high index of refraction. Thallium has been used in treating ringworm and other skin infections; however, its use has been limited because of the narrow margin between toxicity and therapeutic benefits. A mercury-thallium alloy, which forms a eutectic at 8.5% thallium, is reported to freeze at −60°C, some 20° below the freezing point of mercury. Commercial thallium metal (99%) costs about $40/lb.

Thorium — (*Thor*, Scandinavian god of war), Th; at. wt. 232.0381; at. no. 90; m.p. 1750°C; b.p. 4788°C; sp. gr. 11.72; valence +2(?), +3(?), +4.

Discovered by Berzelius in 1828. Thorium occurs in *thorite* ($ThSiO_4$) and in *thorianite* ($ThO_2 + UO_2$). Large deposits of thorium minerals have been reported in New England and elsewhere, but these have not yet been exploited. Thorium is now thought to be about three times as abundant as uranium and about as abundant as lead or molybdenum. The metal is a source of nuclear power. There is probably more energy available for use from thorium in the minerals of the earth's crust than from both uranium and fossil fuels. Any sizable demand for thorium as a nuclear fuel is still several years in the future. Work has been done in developing thorium cycle converter-reactor systems. Several prototypes, including the HTGR (high-temperature gas-cooled reactor) and MSRE (molten salt converter reactor experiment), have operated. While the HTGR reactors are efficient, they are not expected to become important commercially for many years because of certain operating difficulties. Thorium is recovered commercially from the mineral *monazite*, which contains from 3 to 9% ThO_2 along with rare-earth minerals. Much of the internal heat the earth produces has been attributed to thorium and uranium. Several methods are available for producing thorium metal: it can be obtained by reducing thorium oxide with calcium, by electrolysis of anhydrous thorium chloride in a fused mixture of sodium and potassium chlorides, by calcium reduction of thorium tetrachloride mixed with anhydrous zinc chloride, and by reduction of thorium tetrachloride with an alkali metal. Thorium was originally assigned a position in Group IV of the periodic table. Because of its atomic weight, valence, etc., it is now considered to be the second member of the *actinide* series of elements. When pure, thorium is a silvery-white metal which is air-stable and retains its luster for several months. When contaminated with the oxide, thorium slowly tarnishes in air, becoming gray and finally black. The physical properties of thorium are greatly influenced by the degree of contamination with the oxide. The purest specimens often contain several tenths of a percent of the oxide. High-purity thorium has been made. Pure thorium is soft, very ductile, and can be cold-rolled, swaged, and drawn. Thorium is dimorphic; changing at 1400°C from a cubic to a body-centered cubic structure. Thorium oxide has a melting point of 3300°C, which is the highest of all oxides. Only a few elements, such as tungsten, and a few compounds, such as tantalum carbide, have higher melting points. Thorium is slowly attacked by water, but does not dissolve readily in most common acids, except hydrochloric. Powdered thorium metal is often pyrophoric and should be carefully handled. When heated in air, thorium turnings ignite and burn brilliantly with a white light. The principal use of thorium has been in the preparation of the Welsbach mantle, used for portable gas lights. These mantles, consisting of thorium oxide with about 1% cerium oxide and other ingredients, glow with a dazzling light when heated in a gas flame. Thorium is an important alloying element in magnesium, imparting high strength and creep resistance at elevated temperatures. Because thorium has a low work-function and high electron emission, it is sued to coat tungsten wire used in electronic equipment. The oxide is also used to control the grain size of tungsten used for electric lamps; it is also used for high-temperature laboratory crucibles. Glasses containing thorium oxide have a high refractive index and low dispersion. Consequently, they find application in high-quality lenses for cameras and scientific instruments. Thorium oxide has also found use as a catalyst in the conversion of ammonia to nitric acid, in petroleum cracking, and in producing sulfuric acid. Twenty five isotopes of thorium are known with atomic masses ranging from 212 to 236. All are unstable. ^{232}Th occurs naturally and has a half-life of 1.4×10^{10} years. It is an alpha emitter. ^{232}Th goes through six alpha and four beta decay steps before becoming the stable isotope ^{208}Pb. ^{232}Th is sufficiently radioactive to expose a photographic plate in a few hours. Thorium disintegrates with the production of "thoron" (^{220}Rn), which is an alpha emitter and presents a radiation hazard. Good ventilation of areas where thorium is stored or handled is therefore essential. Thorium metal (99.9%) costs about $150/oz.

Thulium — (*Thule*, the earliest name for Scandinavia), Tm; at. wt. 168.93421; at. no. 69; m.p. 1545°C; b.p. 1946°C; sp. gr. 9.321 (25°C); valence 3. Discovered in 1879 by Cleve. Thulium occurs in small quantities along with other rare earths in a number of minerals. It is obtained commercially from *monazite*, which contains about 0.007% of the element. Thulium is the least abundant of the rare earth elements, but with new sources recently discovered, it is now considered to be about as rare as silver, gold, or cadmium. Ion-exchange and solvent extraction techniques have recently permitted much easier separation of the rare earths, with much lower costs. Only a few years ago, thulium metal was not obtainable at any cost; in 1985 the oxide sold for $3400/kg. Thulium metal costs $50/g. Thulium can be isolated by reduction of the oxide with lanthanum metal or by calcium reduction of the anhydrous fluoride. The pure metal has a bright, silvery luster. It is reasonably stable in air, but the metal should be protected from moisture in a closed container. The element is silver-gray, soft, malleable, and ductile, and can be cut with a knife. Twenty five isotopes are known, with atomic masses ranging from 152 to 176. Natural thulium, which is 100% ^{169}Tm, is stable. Because of the relatively high price of the metal, thulium has not yet found many practical applications. ^{169}Tm bombarded in a nuclear reactor can be used as a radiation source in portable X-ray equipment. ^{171}Tm is potentially useful as an energy source. Natural thulium also has possible use in *ferrites* (ceramic magnetic materials) used in microwave equipment. As with other lanthanides, thulium has a low-to-moderate acute toxic rating. It should be handled with care.

Tin — (anglo-Saxon, *tin*), Sn (L. *stannum*); at. wt. 118.710; at. no. 50; m.p. 231.9°C; b.p. 2602°C; sp. gr. (gray) 5.75, (white) 7.31; valence 2, 4. Known to the ancients. Tin is found chiefly in *cassiterite* (SnO_2). Most of the world's supply comes from Malaya, Bolivia, Indonesia, Zaire, Thailand, and Nigeria. The U.S. produces almost none, although occurrences have been found in Alaska and California. Tin is obtained by reducing the ore with coal in a reverberatory furnace. Ordinary tin is composed of nine stable isotopes; 18 unstable isotopes are also known. Ordinary tin is a silver-white metal, is malleable, somewhat ductile, and has a highly crystalline structure. Due to the breaking of these crystals, a "tin cry" is heard when a bar is bent. The element has two allotropic forms at normal pressure. On warming, gray, or α tin, with a cubic structure, changes at 13.2°C into white, or β tin, the ordinary form of the metal. White tin has a tetragonal structure. When tin is cooled below 13.2°C, it changes slowly from white to gray. This change is affected by impurities such as aluminum and zinc, and can be prevented by small additions of antimony or bismuth. This change from the α to β form is called the tin pest. There are few if any uses for gray tin. Tin takes a high polish and is used to coat other metals to prevent corrosion or other chemical action. Such tin plate over steel is used in the so-called tin can for preserving food. Alloys of tin are very important. Soft solder, type metal, fusible metal, pewter, bronze, bell metal, Babbitt metal, White metal, die casting alloy, and phosphor bronze are some of the important alloys using tin. Tin resists distilled sea and soft tap water, but is attacked by strong acids, alkalis, and acid salts. Oxygen in solution accelerates the attack. When heated in air, tin forms SnO_2, which is feebly acid, forming stannate salts with basic oxides. The most important salt is the chloride ($SnCl_2 \cdot H_2O$), which is used as a reducing agent and as a mordant in calico printing. Tin salts sprayed onto glass are used to produce electrically conductive coatings. These have been used for panel lighting and for frost-free windshields. Most window glass is now made by floating molten glass on molten tin (float glass) to produce a flat surface (Pilkington process). Of recent interest is a crystalline tin-niobium alloy that is superconductive at very low temperatures. This promises to be important in the construction of superconductive magnets that generate enormous field strengths but use practically no power. Such magnets, made of tin-niobium wire, weigh but a few pounds and produce magnetic fields that, when started with a small battery, are comparable

Wolfram — see Tungsten.

Xenon — (Gr. *xenon*, stranger); Xe; at. wt. 131.29; at. no. 54; m.p. −111.75°C; b.p. −108.0°C; density (gas) 5.887 ± 0.009 g/l; sp. gr (liquid) 3.52 (−109°C); valence usually 0. Discovered by Ramsay and Travers in 1898 in the residue left after evaporating liquid air components. Xenon is a member of the so-called noble or "inert" gases. It is present in the atmosphere to the extent of about one part in twenty million. Xenon is present in the Martian atmosphere to the extent of 0.08 ppm. The element is found in the gases evolved from certain mineral springs, and is commercially obtained by extraction from liquid air. Natural xenon is composed of nine stable isotopes. In addition to these, 20 unstable isotopes have been characterized. Before 1962, it had generally been assumed that xenon and other noble gases were unable to form compounds. Evidence has been mounting in the past few years that xenon, as well as other members of the zero valence elements, do form compounds. Among the "compounds" of xenon now reported are xenon hydrate, sodium perxenate, xenon deuterate, difluoride, tetrafluoride, hexafluoride, and $XePtF_6$ and $XeRhF_6$. Xenon trioxide, which is highly explosive, has been prepared. More than 80 xenon compounds have been made with xenon chemically bonded to fluorine and oxygen. Some xenon compounds are colored. Metallic xenon has been produced, using several hundred kilobars of pressure. Xenon in a vacuum tube produces a beautiful blue glow when excited by an electrical discharge. The gas is used in making electron tubes, stroboscopic lamps, bactericidal lamps, and lamps used to excite ruby lasers for generating coherent light. Xenon is used in the atomic energy field in bubble chambers, probes, and other applications where its high molecular weight is of value. The perxenates are used in analytical chemistry as oxidizing agents. ^{133}Xe and ^{135}Xe are produced by neutron irradiation in air cooled nuclear reactors. ^{133}Xe has useful applications as a radioisotope. The element is available in sealed glass containers for about $20/l of gas at standard pressure. Xenon is not toxic, but its compounds are highly toxic because of their strong oxidizing characteristics.

Ytterbium — (Ytterby, village in Sweden), Yb; at. wt. 173.04; at. no. 70; m.p. 824°C; b.p. 1194°C; sp. gr (α) 6.903 (β) 6.966; valence 2, 3. Marignac in 1878 discovered a new component, which he called *ytterbia*, in the earth then known as *erbia*. In 1907, Urbain separated ytterbia into two components, which he called *neoytterbia* and *lutecia*. The elements in these earths are now known as *ytterbium* and *lutetium*, respectively. These elements are identical with *aldebaranium* and *cassiopeium*, discovered independently and at about the same time by von Welsbach. Ytterbium occurs along with other rare earths in a number of rare minerals. It is commercially recovered principally from *monazite sand*, which contains about 0.03%. Ion-exchange and solvent extraction techniques developed in recent years have greatly simplified the separation of the rare earths from one another. The element was first prepared by Klemm and Bonner in 1937 by reducing ytterbium trichloride with potassium. Their metal was mixed, however, with KCl. Daane, Dennison, and Spedding prepared a much purer form in 1953 from which the chemical and physical properties of the element could be determined. Ytterbium has a bright silvery luster, is soft, malleable, and quite ductile. While the element is fairly stable, it should be kept in closed containers to protect it from air and moisture. Ytterbium is readily attacked and dissolved by dilute and concentrated mineral acids and reacts slowly with water. Ytterbium has three allotropic forms with transformation points at −13° and 795°C. The beta form is a room-temperature, face-centered, cubic modification, while the high-temperature gamma form is a body-centered cubic form. Another body-centered cubic phase has recently been found to be stable at high pressures at room temperatures. The beta form ordinarily has metallic-type conductivity, but becomes a semiconductor when the pressure is increased above 16,000 atm. The electrical resistance increases tenfold as the pressure is increased to 39,000 atm and drops to about 80% of its standard temperature-pressure resistivity at a pressure of 40,000 atm. Natural ytterbium is a mixture of seven stable isotopes. Seven other unstable isotopes are known. Ytterbium metal has possible use in improving the grain refinement, strength, and other mechanical properties of stainless steel. One isotope is reported to have been used as a radiation source as a substitute for a portable X-ray machine where electricity is unavailable. Few other uses have been found. Ytterbium metal is commercially available with a purity of about 99+% for about $875/kg. Ytterbium has a low acute toxic rating.

Yttrium — (*Ytterby*, village in Sweden near Vauxholm), Y; at. wt. 88.90585; at. no. 39; m.p. 1526°C; b.p. 3336°C; sp. gr. 4.469 (25°C); valence 3. *Yttria*, which is an earth containing yttrium, was discovered by Gadolin in 1794. *Ytterby* is the site of a quarry which yielded many unusually minerals containing rare earths and other elements. This small town, near Stockholm, bears the honor of giving names to *erbium*, *terbium*, and *ytterbium* as well as *yttrium*. In 1843 Mosander showed that yttria could be resolved into the oxides (or earths) of three elements. The name yttria was reserved for the most basic one; the others were named *erbia* and *terbia*. Yttrium occurs in nearly all of the rare-earth minerals. Analysis of lunar rock samples obtained during the Apollo missions show a relatively high yttrium content. It is recovered commercially from *monazite sand*, which contains about 3%, and from *bastnasite*, which contains about 0.2%. Wohler obtained the impure element in 1828 by reduction of the anhydrous chloride with potassium. The metal is now produced commercially by reduction of the fluoride with calcium metal. It can also be prepared by other techniques. Yttrium has a silver-metallic luster and is relatively stable in air. Turnings of the metal, however, ignite in air if their temperature exceeds 400°C, and finely divided yttrium is very unstable in air. Yttrium oxide is one of the most important compounds of yttrium and accounts for the largest use. It is widely used in making YVO_4 europium, and Y_2O_3 europium phosphors to give the red color in color television tubes. Many hundreds of thousands of pounds are now used in this application. Yttrium oxide also is used to produce yttrium-iron-garnets, which are very effective microwave filters. Yttrium iron, aluminum, and gadolinium garnets, with formulas such as $Y_3Fe_5O_{12}$ and $Y_3Al_5O_{12}$, have interesting magnetic properties. Yttrium iron garnet is also exceptionally efficient as both a transmitter and transducer of acoustic energy. Yttrium aluminum garnet, with a hardness of 8.5, is also finding use as a gemstone (simulated diamond). Small amounts of yttrium (0.1 to 0.2%) can be used to reduce the grain size in chromium, molybdenum, zirconium, and titanium, and to increase strength of aluminum and magnesium alloys. Alloys with other useful properties can be obtained by using yttrium as an additive. The metal can be used as a deoxidizer for vanadium and other nonferrous metals. The metal has a low cross section for nuclear capture. ^{90}Y, one of the isotopes of yttrium, exists in equilibrium with its parent ^{90}Sr, a product of atomic explosions. Yttrium has been considered for use as a nodulizer for producing nodular cast iron, in which the graphite forms compact nodules instead of the usual flakes. Such iron has increased ductility. Yttrium is also finding application in laser systems and as a catalyst for ethylene polymerization. It has also potential use in ceramic and glass formulas, as the oxide has a high melting point and imparts shock resistance and low expansion characteristics to glass. Natural yttrium contains but one isotope, ^{89}Y. Nineteen other unstable isotopes have been characterized. Yttrium metal of 99.9% purity is commercially available at a cost of about $75/oz.

Zinc — (Ger. *Zink*, of obscure origin), Zn; at. wt. 65.39; at. no. 30; m.p. 419.53°C; b.p. 907°C; sp. gr. 7.133 (25°C); valence 2. Centuries before zinc was recognized as a distinct element, zinc ores were used for making brass. Tubal-Cain, seven generations from Adam, is mentioned as being an "instructor in every artificer in brass and iron." An alloy containing 87% zinc has been found in prehistoric ruins in Transylvania. Metallic zinc

Nanocrystalline Ceria-based Catalysts for Water-gas Shift

Qi Fu, Steven Fiore, Howard Saltsburg, Xiaomei Qi,
Maria Flytzani-Stephanopoulos
Department of Chemical and Biological Engineering
Tufts University
4 Colby Street, Medford, MA 02155, USA

Introduction:

Water-gas-shift is a mature industrial process, which is applied in the production of hydrogen for ammonia synthesis and for adjusting the CO/H_2 ratio for the subsequent synthesis of methanol. Presently, there is a renewed interest in the water gas shift reaction because of its potential use in conjunction with fuel cell power generation. Advanced catalysts for the water-gas shift reaction are being actively sought by the developers of fuel cells.

From the review of the water-gas shift reaction literature, cerium oxide-based catalysts are singled out as very promising for both low- and high-temperature application. Cerium oxide can supply its surface oxygen, thus catalyzing a variety of oxidation reactions, including WGS. Nanocrystalline ceria is much more reducible than well-crystallized materials [1]. The addition of platinum metals, gold and base metal oxides, such as copper oxide, can significantly enhance the reducibility and WGS activity of ceria [2-5]. Dopants such as La or Zr oxides are added to ceria to suppress its crystal growth at high temperatures, and to also increase its reducibility.

Preparation, characterization, and catalytic properties of Cu_xO- or Au- ceria catalysts prepared as nanostructured materials are reported in this paper. Catalysts were characterized by XRD, XPS, STEM/EDS, HREM, TPR, and oxygen storage capacity (OSC) measurements.

Experimental:

Catalyst preparation Bulk doped or undoped ceria and Cu_xO-ceria were synthesized by the urea gelation/coprecipitation method (UGC), as described in detail elsewhere [3]. The cerium salt used in UGC is $(NH_4)_2Ce(NO_3)_6$. In brief, aqueous metal nitrate solutions were mixed with urea and heated to 100 °C under vigorous stirring and addition of deionized water. The resulting gel was aged for 8 hours at 100 °C; after aging, the precipitate was filtered and washed. Further, the precipitate was dried at 100-120 °C and calcined in static air at 400 °C for 10 h or 650 oC for 4 h. A slow heating rate, 2 °C/min, was used to reach the desired calcination temperature. In all preparation methods used in this work, the same heat treatment procedure was followed.

Gold-ceria samples were prepared by coprecipitation (CP) and by deposition precipitation (DP) of gold on ceria made by the above UGC method. The CP method involves mixing an aqueous solution of $HAuCl_4$, cerium (III) nitrate and lanthanum nitrate with $(NH_4)_2CO_3$ at 60-70 °C, keeping a constant pH value of 8 and aging the precipitate at 60-70 °C for 1h. Deposition-precipitation took place by adding the desired amount of $HAuCl_4$ dropwise into an aqueous slurry of the prepared ceria. The pH of the aqueous slurry had already been adjusted to the value of 8 using $(NH_4)_2CO_3$. The resulting precipitate was aged at room temperature for 1h. A few gold-ceria samples were prepared by UGC, following the procedure described above.

Catalyst characterization The total sample surface area was measured by single-point BET N_2 adsorption/desorption on a Micromeritics Pulse ChemiSorb 2705.

X-ray powder diffraction (XRD) analysis of the samples was performed on a Rigaku 300 X-ray Diffractometer with Rotating Anode Generators and a monochromatic detector. Copper K_α radiation was used. High-resolution transmission electron microscopy (HREM) performed on a JEOL 2010 instrument with an ultimate point-to-point resolution of 1.9 Å and lattice resolution of 1.4 Å. A Kratos AXIS Ultra Imaging X-ray Photoelectron Spectrometer with a resolution of 0.1 eV was used to determine the atomic metal ratios of the surface region and the metal oxidation state of selected catalysts.

Activity tests Water-gas shift reaction tests were performed in a quartz-tube flow reactor. A simulated reformate feed gas mixture was used containing 11% CO, 11% CO_2, 26 % H_2, and 26 % H_2O in helium. The reactant and product gas streams were analyzed using a HP-6890 gas chromatograph equipped with a thermal conductivity detector (TCD).

Temperature-programmed reduction (TPR) Temperature-programmed reduction (TPR) of the as-prepared catalysts in fine powder form was carried out in a Micromeritics Pulse ChemiSorb 2705 instrument. The gas streams were monitored by TCD for H_2-TPR, while a mass-spectrometer (MKS-model RS-1) is used in CO-TPR. A 20% H_2/N_2 or 10%CO/He gas mixture (50 cm^3/min (NTP)) was used as reducing gas. The sample was heated at a rate of 5 °C/min from room temperature to 900 °C.

Oxygen storage capacity (OSC) measurements Oxygen storage capacity measurements were carried out in a flow reactor system, equipped with a switching valve for rapid introduction of step changes in gas streams of CO/He, He, and O_2/He. A total gas flow rate of 50 cm^3/min (NTP) was used. The sample was exposed to 10% CO/He and 10% O_2/He step changes at the desired test temperature. The steady-state signals of CO, CO_2 and O_2 were detected by mass spectrometry.

Results and Discussion:

The backbone of the catalyst is ceria, while the metal or metal oxide is the minor phase. The amount of La or Zr oxide used as dopant in ceria, was varied from 10 to 30 at. %. Physical properties of some materials are listed in **Table 1**.

As shown in **Table 1**, the ceria lattice parameter α increases with La content, while it decreases when Zr is used as dopant. The addition of copper oxide also decreased the lattice parameter of ceria.

Table 1. Physical properties of as-prepared materials

(Prepared by urea coprecipitation/gelation method, calcined at 400 °C)

Sample	BET S. A. (m^2/g)	CeO_2 lattice parameters α (Å)	CeO_2 particle size (nm)	
			<111>	<200>
CeO_2	140.5	5.417	6.2	5.5
$Ce(10La)O_x$	161.6	5.435	5.1	4.8
$Ce(30La)O_x$	175.0	5.461	4.3	3.9
$Ce(30Zr)O_x$	169.1	5.364	4.1	3.7
$10CuCeO_x$	177.7	5.417	4.8	4.5
$10CuCe(10La)O_x$	200.3	5.419	4.0	3.5
$10CuCe(30La)O_x$	176.1	5.422	4.3	3.3
$10CuCe(30Zr)O_x$	168.0	5.352	4.2	3.9
$0.5AuCe(10La)O_x$	--	5.432	4.2	3.8
$5AuCe(10La)O_x$	--	5.438	4.5	4.1
$10AuCe(10La)O_x$	158.1	5.439	4.5	4.4

The surface oxygen of ceria is substantially weakened by gold or copper oxide as found by H_2-TPR, **Figure 1**. OSC measurements using step pulses of CO were in agreement with the TPR results; the presence of gold or copper oxide greatly enhances the OSC of ceria, **Figure 2**. Carbon-containing species left on the

surface after the CO step, can be fully removed with O_2 or partially removed with H_2O [5].

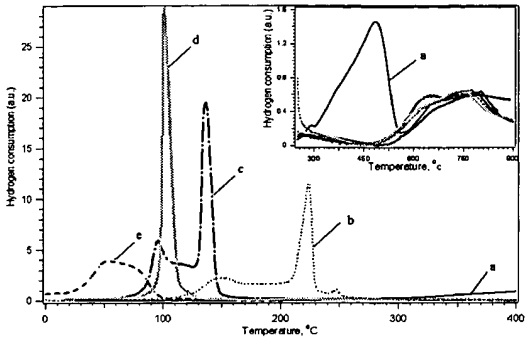

Figure 1. (a) CL (UGC) (b) 5Cu-CL (UGC); (c) 10Cu-CL (UGC); (d) 8Au-CL (UGC); (e) 4.5Au-CL(DP); all materials calcined at 400 °C, 10 h

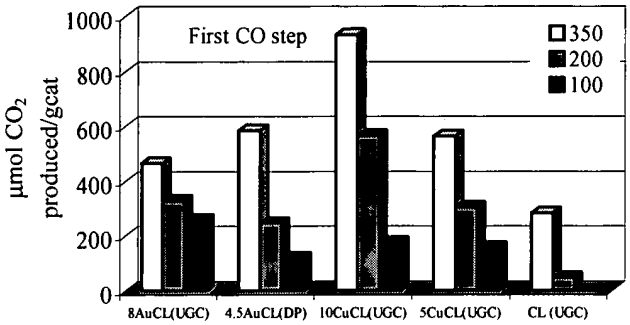

Figure 2. OSC of ceria-based catalysts at three different temperatures 350 °C, 200 °C and 100 °C; 10%CO/He, 10%O_2/He, 50cm^3/min (NTP), all materials calcined at 400 °C, 10 h;
CL: Ce(10La)O_x

The amount of CO_2 produced during the CO and O_2 steps in OSC is a strong function of the type of dopant used in ceria. This is shown in **Figure 3**.

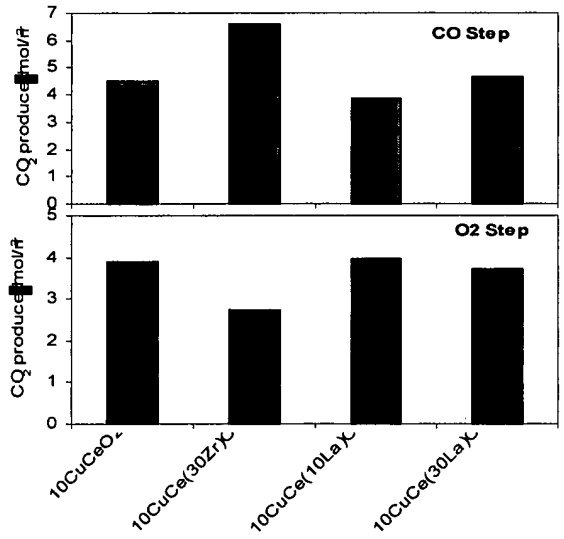

Figure 3. OSC of ceria-based catalysts with different dopants at 350 °C; 10%CO/He, 10%O_2/He, 50cm^3/min (NTP), all materials calcined at 400 °C, 10 h.

WGS rate measurements were conducted with simulated reformate gas mixtures. In 11%CO-7%CO_2-26%H_2O-26%H_2-He gas mixture, at 250 °C, the rate over 5-8%Au-ceria(La)O_x catalysts is 6-9 μmol/gcat*sec, while that over 10%CuCe(La)O_x is 3.2 μmol/gcat*sec. At 350 °C, the WGS reaction rate over the same gold and copper-ceria catalysts is 22-47.5 and 31 μmol/gcat*sec, respectively, **Figure4.**

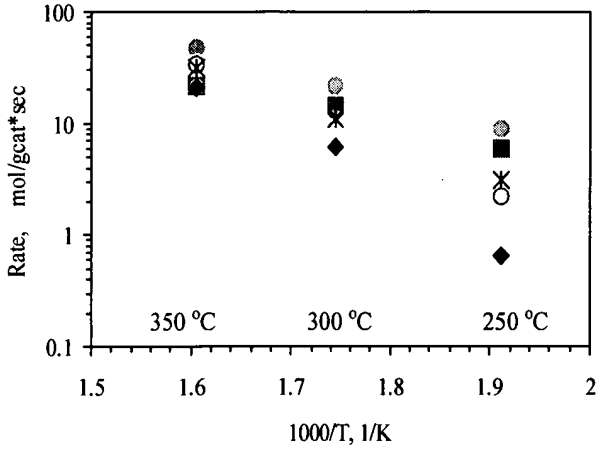

• 8Au-CL (UGC) ■ 4.5Au-CL(DP) * 10Cu-Ce(10La)O_x (UGC)
° 10Cu-Ce(30La)O_x(UGC) ♦ 10Cu-Ce(30Zr)O_x (UGC)

Figure 4 WGS rate over various ceria-based materials calcined at 400 °C, 10h; Simulated reformate gas mixture: 11% CO /7% CO_2/ 26% H_2 /26% H_2O /He

Conclusions:

Nanocrystalline ceria-based materials are active water-gas shift catalysts. Activity and reducibility greatly depend on the structural properties of these materials.

Acknowledgement:

The financial support of this work by NSF/EPA, Grant # CTS-9985305, and by the DOE/ Univ. Coal Res. Program, Grant # DE-FG2600-NT40819, is gratefully acknowledged.

References:

1. Chiang, Y. M.; Lavik, E.B.; Kosacki, I.; Tuller, H. L.; and Ying, J.Y.; *J. Electroceramics*, **1997**, 1, 7.
2. T. Bunluesin, R.J. Gorte, *Appl. Catal. B* 15 (1998) 107.
3. Li, Y.; Fu, Q.; Flytzani-Stephanopoulos, M.; *Appl. Catal. B:*, **2000**, 27, 179.
4. Fu, Q.; Weber, A.; Flytzani-Stephanopoulos, M.; *Catal. Letters*, **2001**, 77 (1/3) 87.
5. Fu, Q.; Kudriavtseva, S.; Saltsburg, H.; Flytzani-Stephanopoulos, M.; *Chem. Eng. J.*, in press.

ELSEVIER

Catalysis Today 77 (2003) 419–449

CATALYSIS TODAY

www.elsevier.com/locate/cattod

Automotive catalytic converters: current status and some perspectives

Jan Kašpar*, Paolo Fornasiero, Neal Hickey

Dipartimento di Scienze Chimiche, University of Trieste, via L. Giorgieri 1, I-34127 Trieste, Italy

Abstract

Automotive three-way catalysts (TWCs) have represented over the last 25 years one of the most successful stories in the development of catalysts. The aim of this paper is to illustrate the technology for abatement of exhaust emissions by analysing the current understanding of TWCs, the specific role of the various components, the achievements and the limitations. The challenges in the development of new automotive catalysts, which can meet future highly demanding pollution abatement requirements, are also discussed.

1. Introduction

Air pollution generated from mobile sources is a problem of general interest. In the last 60 years the world vehicle fleet has increased from about 40 million vehicles to over 700 million; this figure is projected to increase to 920 million by the year 2010 [1]. The environmental concern originated by mobile sources is due to the fact that the majority of engines employ combustion of fuels derived from crude oil as a source of energy. Burning of hydrocarbon (HC) ideally leads to the formation of water and carbon dioxide, however, due to non-perfect combustion control and the high temperatures reached in the combustion chamber, the exhaust contains significant amounts of pollutants which need to be transformed into harmless compounds. In this paper, the control strategies and achievements in automotive pollution control are discussed. Attention is focussed on recent developments in the field of the three-way type of catalysts, i.e. NM/CeO_2–ZrO_2–Al_2O_3 containing systems; insight on the lean-DeNO_x and diesel type of catalysts is also given. The paper is focussed essentially on the catalytic aspects of pollution abatement, even though the reader should consider that technological solutions such an electrically heated catalysts, etc., may heavily affect the converter performances [2]. A number of review papers have described the traditional CeO_2-based TWC technology, accordingly we refer the reader to these papers [2–13].

2. Emissions characteristics and control strategies

Engine exhausts consist of a complex mixture, the composition depending on a variety of factors such as: type of engine (two- or four-stroke, spark- or compression (diesel)-ignited), driving conditions, e.g. urban or extra-urban, vehicle speed, acceleration/deceleration, etc. Table 1 reports typical compositions of exhaust gases for some common engine types.

* Corresponding author. Fax: +39-40-5583903.
E-mail address: kaspar@units.it (J. Kašpar).

0920-5861/02/$ – see front matter © 2002 Elsevier Science B.V. All rights reserved.
PII: S0920-5861(02)00384-X

Table 1
Example of exhaust conditions for two- and four-stroke, diesel and lean-four-stroke engines [9,155,176,231]

Exhaust components and conditions[a]	Diesel engine	Four-stroke spark ignited-engine	Four-stroke lean-burn spark ignited-engine	Two-stroke spark ignited-engine
NO_x	350–1000 ppm	100–4000 ppm	≈1200 ppm	100–200 ppm
HC	50–330 ppm C	500–5000 ppm C	≈1300 ppm C	20,000–30,000 ppm C
CO	300–1200 ppm	0.1–6%	≈1300 ppm	1–3%
O_2	10–15%	0.2–2%	4–12%	0.2–2%
H_2O	1.4–7%	10–12%	12%	10–12%
CO_2	7%	10–13.5%	11%	10–13%
SO_x	10–100 ppm[b]	15–60 ppm	20 ppm	≈20 ppm
PM	65 mg/m^3			
Temperatures (test cycle)	r.t.–650 °C (r.t.–420 °C)	r.t.–1100 °C[c]	r.t.–850 °C	r.t.–1000 °C
GHSV (h^{-1})	30,000–100,000	30,000–100,000	30,000–100,000	30,000–100,000
λ (A/F)[d]	≈1.8 (26)	≈1 (14.7)	≈1.16 (17)	≈1 (14.7)[e]

[a] N_2 is remainder.
[b] For comparison: diesel fuels with 500 ppm of sulphur produce about 20 ppm of SO_2 [16].
[c] Close-coupled catalyst.
[d] λ defined as ratio of actual A/F to stoichiometric A/F, λ = 1 at stoichiometry (A/F = 14.7).
[e] Part of the fuel is employed for scavenging of the exhaust, which does not allow to define a precise definition of the A/F.

As shown in Table 1, the exhaust contains principally three primary pollutants,[1] unburned or partially burned hydrocarbons (HCs), carbon monoxide (CO) and nitrogen oxides (NO_x), mostly NO, in addition to other compounds such as water, hydrogen, nitrogen, oxygen, etc. Sulphur oxides, though polluting, are normally not removed by the post-combustion treatments, since the only effective way is to reduce them to elemental sulphur, which would accumulate in the system. Accordingly, it is preferred to minimise sulphur emissions by diminishing the sulphur content in the fuel. Given the different nature of the three classes of pollutants, i.e. reducing or oxidising agents, it is necessary to simultaneously carry out both reduction and oxidation reactions over the exhaust catalyst, which can occur by a variety of reactions. Some of these are summarised in Table 2. Importantly, this table reports only the desirable reactions, in that many other reactions could occur in the complex mixtures described in Table 1, such as, for example, reduction of NO_x to ammonia, partial oxidation of HC to give aldehydes and other toxic compounds, etc. Given the complexity of the exhaust media, a high selectivity is required in order to promote only the reactions reported in Table 2.

A perusal of the exhaust compositions reported in Table 1 for the different type of engines reveals some significant differences: (i) even if relatively diluted, the concentration of the various pollutants can change even by an order of magnitude, according to the type of engine; (ii) with the exception of the four-stroke spark ignited-engine, which, being equipped with a TWC, is run at stoichiometry, the other type of engines can be run under lean conditions, i.e. in excess of O_2; (iii) extremely high temperatures are reached in the four-stroke spark ignited-engine, particularly in the close-coupled catalyst (CCC).

In general, the emissions depend on air-to-fuel (A/F) ratio, as exemplified in Fig. 1. Tuning of the engine to rich feed gives the highest power output, which, however, occurs at expenses of high fuel consumption. Under lean conditions lower combustion

[1] The ability of the TWCs to simultaneously eliminate three classes of pollutants is at the origin of their name.

Table 2
Reactions occurring on the automotive exhaust catalysts, which may contribute to the abatement of exhaust contained pollutants [4]

Oxidation	$2CO + O_2 \rightarrow 2CO_2$ $HC + O_2 \rightarrow CO_2 + H_2O$[a]
Reduction/three-way	$2CO + 2NO \rightarrow 2CO_2 + N_2$ $HC + NO \rightarrow CO_2 + H_2O + N_2$[a] $2H_2 + 2NO \rightarrow 2H_2O + N_2$
WGS	$CO + H_2O \rightarrow CO_2 + H_2$
Steam reforming	$HC + H_2O \rightarrow CO_2 + H_2$[a]

[a] Unbalanced reaction.

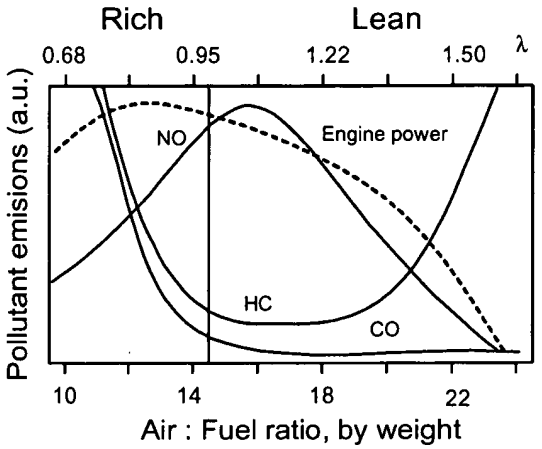

Fig. 1. Effect of A/F ratio (w/w) on engine emissions and engine power (after Ref. [3]).

temperatures lead to lower NO_x emissions, however, at very high A/F engine misfire occurs, leading again to high HC emissions. Under any A/F conditions catalytic abatement of pollutants is needed to comply with the legislation limits. Only at stoichiometric conditions are appropriate amounts of reducing and oxidising agents present in the exhaust to carry out the catalytic reactions as outlined in Table 2. Under such conditions TWCs effectively remove the pollutants.

In principle, there are several advantages in removing NO_x from the automotive exhaust under lean conditions, i.e. A/F > 14.7, compared to the stoichiometric feed (A/F = 14.7) of a traditional gasoline-fuelled engine, where the polluting components are abated using a TWC. The most important advantage of lean-burn engines is the significant fuel economy. In fact, an increase of fuel consumption of vehicles occurred in the 1990s, which was generally attributed to the introduction of TWCs and their requirement for a stoichiometric A/F ratio to achieve best performances. However, it should be noted that there are other factors that substantially contributed as well, such as the increase of vehicle weight due to implementation of security systems, the generalised use of vehicle air conditioning, etc. There is another advantage of lean NO_x engine, which is the fact that the highest exhaust temperatures are typically lower (≤800–850 °C) compared to the stoichiometric engines. In the latter engine, temperatures up to 1100 °C are met by the CCC, which may result in a disadvantage in terms of the catalyst durability.

Three types on engines can effectively run under lean-burn, i.e. diesel, four-stroke/lean-burn and two-stroke engine. The two-stroke engine is typically employed in small motorcycles, mopeds, chain saws and most recreational vehicles. This engine is characterised by high engine power output, compact design, and low construction costs, which makes it ideal for the above listed applications. However, it is noisy, it presents high fuel consumption and high levels of emitted HCs due to partial mixing of the combustion mixture with the exiting exhaust. It is estimated that up to 25–30% of fuel in the feed is emitted during the scavenging process of the exhaust mixture from the cylinder [14]. Accordingly, the HC emitted from this engine are predominantly C5–C6, in contrast to all other engines where C1–C3 constitute the majority of HC emitted. Even though various strategies of engine management were developed for limiting such high HC emissions, pollution control by catalytic methods is nowadays mandatory even for these engines, which may be achieved by introducing an oxidation catalyst for CO and HC removal, as the legislation is generally less demanding compared to four-wheel vehicles. Due to the intrinsically low NO_x emission levels (Table 1), EGR (exhaust gas re-circulation) technology can be employed for the reduction of emitted NO_x. Should legislation significantly increase the tightness of the present and forecasted limits, it may be expected that four-stroke engines, equipped with conventional TWCs could gradually replace two-stroke engines, as happened for four-wheel vehicles.

As for the exhausts originated by diesel and lean-burn engines, let us observe that even though both types of engines run in an excess of oxygen, typically 5–15% of O_2 is present in the exhausts compared to approximately 1% found in the engine fed at stoichiometry; the precise nature of the exhaust gases significantly differs between the two systems. In fact, both types of engine emit HC and NO_x at ppm levels (300–800 ppm) and large amounts of O_2 (5–15%), water and CO_2 (each 10–12%). However, as far as the HCs are concerned, there is an important difference in that very low levels are emitted from the diesel engine (≤NO_x), which makes necessary addition of a reducing agent to the exhaust in order to achieve appreciable reduction of the emitted NO_x. On the other

hand, diesel emissions are characterised by a significant level of particulate matter, which itself can be employed as a reducing agent for NO_x, or, vice versa, particulate can be abated by using NO_x as oxidant as in Johnson Matthey's continuously regenerating trap (CRT) [15]. In contrast, the issue of particulate matter is absent in the case of lean-burn engine powered by gasoline; moreover, higher contents of HC are emitted, which, in principle, allows direct selective catalytic NO_x removal to occur. In addition to these differences in the nature of the exhaust gases, the range of exhaust temperatures strongly differ between the two types of engine. For diesel exhaust, temperatures are on average in the range of 80–180 °C under the European urban driving cycle with some maxima up to 230 °C, while in the extra-urban part of the testing cycle a maximum temperature of 440 °C was observed, typical temperatures being in the range 180–280 °C [16]. This represents a serious problem, both in terms of need of activity at low temperatures and the difficulty in de-sulphurisation of the catalysts, which generally requires temperatures above 650 °C.

Let us now focus on the four-stroke spark ignition engines equipped with TWCs. As above reported, the required amounts of reducing and oxidising agents are present in the exhaust only under stoichiometric conditions. This leads to the typical dependency of the conversion patterns of the TWCs upon the A/F ratio (Fig. 2). Today the required conversion of pollutants is greater than 95%, which is attained only when a precise control of the A/F is maintained, i.e. within a narrow operating window. Accordingly, a complex integrated system is employed for the control of the exhaust emissions, which is aimed at maintaining the A/F ratio as close as possible to stoichiometry (Fig. 3). To obtain an efficient control of the A/F ratio the amount of air is measured and the fuel injection is controlled by a computerised system which uses an oxygen (λ) sensor located at the inlet of the catalytic converter. The signal from this λ sensor is used as a feedback for the fuel and air injection control loop. A second λ sensor is mounted at the outlet of the catalytic converter (Fig. 3). This configuration constitutes the basis of the so-called engine on-board diagnostics (OBD). By comparing the oxygen concentration before and after the catalyst, A/F fluctuations are detected. Extensive fluctuations of A/F at the outlet signal system failure. This OBD arrangement implicitly assumes that a

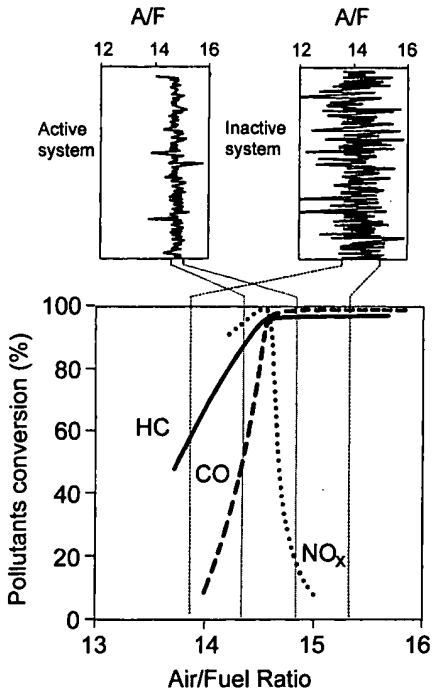

Fig. 2. Effect of A/F ratio on the conversion efficiency of three-way catalysts.

narrow A/F window at the stoichiometric point is the fingerprint of an effective TWC system.

The location of the catalytic converter is another critical point which determines the conversion efficiency. TWCs typically feature the so-called light-off type conversion vs. temperature behaviour. This curves is characterised by conversion which steadily increases from 0 to 100% conversion, the temperature

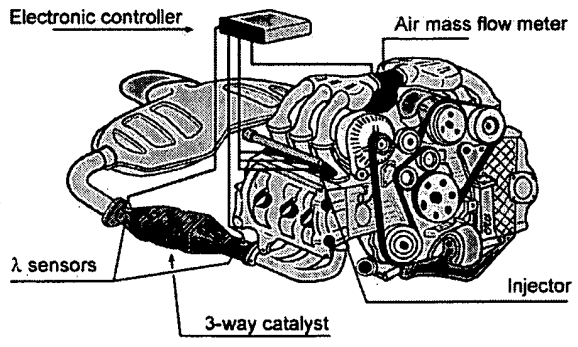

Fig. 3. Diagram of a modern TWC/engine/oxygen sensor (λ) control loop for engine exhaust control.

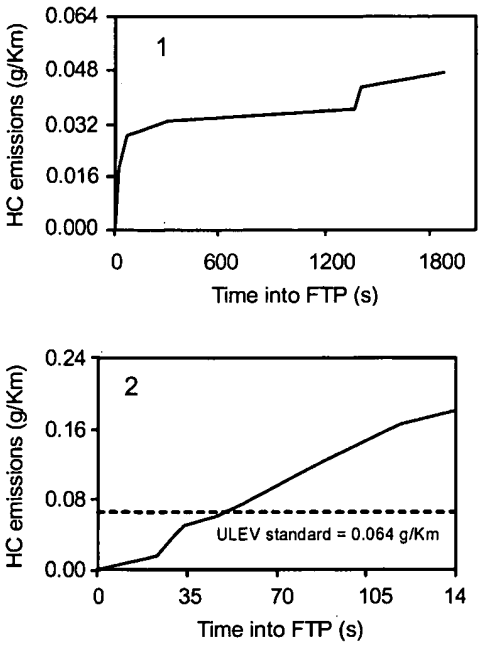

Fig. 4. Cumulative HC emissions measured during the federal test procedure (FTP cycle) on an US 1995 car: (1) tailpipe emissions with CCC; (2) engine-out emissions (after Ref. [11]).

of 50% of conversion being indicated as the light-off temperature. TWCs are characterised by a light-off temperature around 250–350 °C. This means that an under-floor catalyst is heated above the light-off temperature within 90–120 s. In contrast, when the catalyst is closely coupled to the engine (CCC) the heating time typically drops down to 10–20 s. This dramatically affects vehicle emissions immediately after the start-up of the engine (Fig. 4). As shown in this figure, the ULEV (Californian ultra-low emissions vehicle) limit (0.064 g HC emitted/km) is typically surpassed within 40 s after the engine start-up (Fig. 4(2)) [11]. To avoid this situation an almost instantaneous heating of the converter is required to achieve the required >95–98% conversion. CCCs minimise the heating time, however, temperatures up to 1100 °C are routinely met as a consequence of this location of the catalyst.

It must be realised that the latest US and European legislation (EURO phase V and US TIER II) limits for automotive emissions require application of the CCCs and OBD technologies in order to meet the emission standards. A high durability is also an important requirement for present and future TWCs, for example a durability up to 120,000 miles of the converter will be demanded by US tier II regulations in 2004. It should be considered that if a significant part of the vehicle fleet fails the periodical exhaust emission control test, converter replacement becomes mandatory for a vehicle manufacturer. Accordingly, an extremely efficient and robust catalyst is required for future vehicle application. In summary, catalytic converters suitable for 2005 and beyond must present the following characteristics:

- High activity and selectivity (conversions >98%) which increases up to 99% for Californian SULEV (super ultra-low emission vehicle).
- Very fast light-off (<10–20 s), i.e. high activity at low temperatures.

In the case of vehicles equipped with TWCs, two additional requirements should be considered:

- high thermal stability;
- high oxygen storage capacity.

Amazingly, problems and needs for improvements such as those above listed have been quoted for many years when discussing TWCs. A question arises: Why have they not been solved as yet? The reason is that as the performances of the TWCs improve, higher and higher targets, e.g. decrease of emissions and increase of durability, are pushed forward by the legislators, asking for further improvement of the de-pollution technology. For example, starting from 2003 the California SULEV legislation will require a 10-fold decrease in NO_x emissions compared to the already tight value of ULEV legislation (0.2 g/km), whereas HC emissions should drop by a factor of four, down to 0.01 g/km, with converter durability as high as 120,000 miles. Typically, cumulative tailpipe emissions exceed such stringent values within 3–15 s from the start of the engine! This means that catalyst must be effective a few seconds before this limit is reached and convert nearly 100% during the remaining period of the test procedure.

3. TWCS: principles and operation

A typical design of a modern three-way catalytic converter is reported in Fig. 5. Basically, it is a stainless

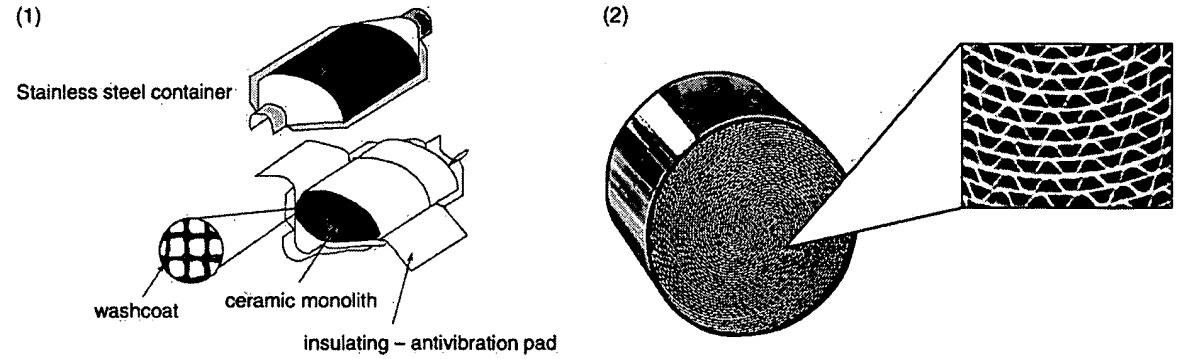

Fig. 5. Diagram of a typical catalytic converter (1) and a metallic honeycomb (a monolith from Emitec GmbH; adapted with permission) (2).

steel container which incorporates a honeycomb monolith made of cordierite ($2MgO{\cdot}2Al_2O_3{\cdot}5SiO_2$) or metal [9]. Although this aspect is sometimes neglected in the scientific literature, in must be underlined that the choice and geometrical characteristics of the honeycomb monolith play a key role in determining the efficiency of the converter. In fact, high conversion must be achieved in the converter and therefore the catalyst works under conditions where severe mass and heat transfer limitations apply. Typically, both metal and ceramic monoliths are employed nowadays. The major advantage of the metallic substrate is that the wall thickness is limited by the steel rolling mill's capabilities, not strength. In a typical automotive 400 cell/in.^{2} application, the frontal flow area in a ceramic monolith is 69% open (31% closed), while the metallic version has 91% open area. This is due to the higher wall thickness of ceramic monoliths (0.007 in. (0.178 mm)) compared to metallic ones (0.002 in. (0.050 mm)) [17,18]. However, even in this field there has been a strong improvement of the technology, cell densities as high as 900 cell/in.^{2} or even higher are now commonly available on the market for both types of monoliths [19]. Traditionally, cordierite monoliths have been employed quite extensively, primarily due to their lower production cost. However, a major advantage of the metal monoliths resides in their high thermal conductivity and low heat capacity, which allow very fast heating of the CCCs during the phase-in of the engine, minimising the light-off time.

The monolith is mounted in the container with a resilient matting material to ensure vibration resistance [10,20]. The active catalysts is supported (washcoated) onto the monolith by dipping it into a slurry containing the catalyst precursors. The excess of the deposited material (washcoat) is then blown out with hot air and the honeycomb is calcined to obtained the finished catalyst. This is clearly a very simplified and schematic description of the washcoating process as multiple layer technology, or multiple catalyst-bed converters are also employed [10,21]. The exact method of deposition and catalyst composition is therefore highly proprietary and specific for every washcoating company. For example, the metallic honeycombs are non-porous, which makes adhesion of the washcoat difficult. Accordingly a FeCrAl based alloy is employed, which contains up to 5 wt.% of aluminium; after an appropriate pre-treatment this element then acts as an anchoring centre for adhesion of the washcoat [19].

However, there are some common components, which represent the state-of-art of the washcoating composition:

- Alumina, which is employed as a high surface area support.
- CeO_2–ZrO_2 mixed oxides, principally added as oxygen storage promoters.
- Noble metals (NM = Rh, Pt and Pd) as active phases.
- Barium and/or lanthana oxides as stabilisers of the alumina surface area.

3.1. Al_2O_3

The choice of Al_2O_3 as carrier is dictated by the necessity of increasing the surface area of the honeycomb monolith which is typically below 2–4 m^2 l^{-1},

where the volume is that of the honeycomb [22]. This does not allow achievement of high NM dispersion. Alumina is chosen due to its high surface area and relatively good thermal stability under the hydrothermal conditions of the exhausts. In most of the studies γ-Al_2O_3 is employed due to its high surface area with respect to other transitional aluminas [23], however, also other high temperature aluminas such as δ- and θ-Al_2O_3 can be employed for high temperature applications such as in the CCCs because of their high thermal stability compared to γ-Al_2O_3. Since temperatures above 1000 °C can be met in the TWCs, stabilisation of transition aluminas is necessary to prevent their transformation to α-Al_2O_3, which typically features surface areas below $10\,m^2\,g^{-1}$. A number of stabilising agents have been reported in the literature, lanthanum, barium, strontium, cerium, and more recently, zirconium oxides or salts being the most investigated [24–31]. These additives are impregnated onto γ-Al_2O_3 or, sometimes, sol–gel techniques are employed to improve the stability of the surface area. The exact mechanism by which these additives stabilises transitional aluminas strongly depends on the amount of the stabilising agent and the synthesis conditions. This is exemplified in Fig. 6 for BaO doped aluminas; BaO and lanthana are the most used and effective stabilisers.

The effectiveness of each dopant on the stabilisation of alumina is difficult to predict, due to the variability of the factors involved in the synthesis. For example, CeO_2 was shown to thermally stabilise Al_2O_3, the maximum stabilisation effect being attained at a CeO_2 level of 5% [32]. However, Morterra et al. [33,34] found that little stabilisation of BET areas is attained by adding CeO_2 to γ-Al_2O_3, even though significant modification of surface properties were detected. In fact, using CO as a surface probe molecule of the surface Lewis acidity of the CeO_2–Al_2O_3 mixed systems, it was revealed that CeO_2 accumulates preferably on the flat patches of low-index crystal planes of the spinel structure, and that the presence of Ce cations stabilises, also at high temperatures, the most acidic Lewis centres. A possible rationale may be given by the recent observation that very efficient stabilisation of Al_2O_3 by addition of CeO_2 is achieved under reducing conditions compared to the oxidising ones, due to formation of $CeAlO_3$ [31]. Apparently, the stabilisation effect is more pronounced as long as dispersed Ce^{3+} species are present at the Al_2O_3 surface. The presence of such species has long been detected in CeO_2–Al_2O_3 provided that low CeO_2 loading is employed [35,36]. It is conceivable that CeO_2 stabilises γ-Al_2O_3 in a similar fashion to La^{3+}, i.e. formation of a surface perovskite-type of oxide $LaAlO_3$ [24], which may account for the conflicting observations reported in the literature. Under high temperature oxidising conditions, partial re-oxidation of Ce^{3+} sites may occur, with formation of CeO_2 particles which tends to agglomerate and grow over the Al_2O_3 surface, making stabilisation ineffective.

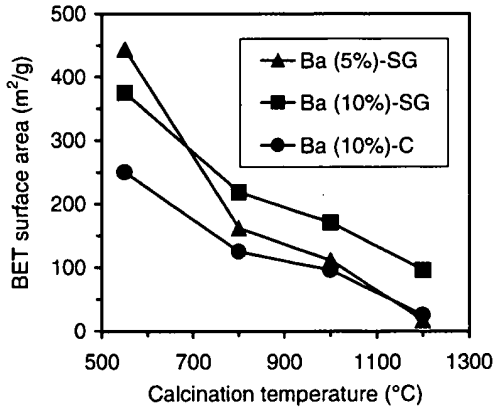

Fig. 6. Effect of synthesis method and BaO content of the stability of BET areas of Al_2O_3 after calcination at the indicated temperatures for 3 h. SG: sol–gel synthesis method; C: co-precipitated sample (after Ref. [29]).

Use of ZrO_2 has also been reported to effectively stabilise γ-Al_2O_3 at high temperatures [25]. In this case, however, the stabilisation of Al_2O_3 seems to be related to the ability of ZrO_2 to spread over the Al_2O_3 rather than formation of mixed oxides. Even though formation of ZrO_2–Al_2O_3 solid solution has been sometimes claimed, separation into ZrO_2 and Al_2O_3 occurs upon high temperature calcination, as dictated by the phase diagram [37]. The effectiveness of ZrO_2 in improving the thermal stability of Al_2O_3 surface area seems remarkable as surface areas as high as $50\,m^2\,g^{-1}$ were observed after calcination at 1200 °C [25]. Interestingly, ZrO_2 appears to be more effective than CeO_2 in stabilising Al_2O_3; consistently, ZrO_2-rich CeO_2–ZrO_2 mixed oxides more effectively stabilised Al_2O_3 compared to CeO_2-rich systems [30].

The overall picture concerning the development of Al_2O_3-based supports is that, at present, thermal

stability of the Al_2O_3 support is not an important issue for the next generation of TWCs in that the progress obtained so far makes these stabilised supports suitable even for high temperature applications such as in CCCs.

3.2. CeO_2–ZrO_2 mixed oxides

The beneficial effects of CeO_2-containing formulations of the TWC performances has long been recognised [38]. Many different promotional effects have been attributed to this component, such as the ability to:

- promote the noble metal dispersion;
- increase the thermal stability of the Al_2O_3 support;
- promote the water gas shift (WGS) and steam reforming reactions;
- favour catalytic activity at the interfacial metal-support sites;
- promote CO removal trough oxidation employing a lattice oxygen;
- store and release oxygen under, respectively, lean and rich conditions.

A detailed discussion of these roles and their relative importance is beyond the scope of this work and for this we refer the reader to earlier literature [4,12,13].

Among the different roles of CeO_2 in TWCs, the OSC is certainly the most important one, at least from the technological point of view. In fact, as above discussed, the OBD technology is based on monitoring of the efficiency of the OSC. This is due to the fact that unambiguous relationships between the TWC activity and OSC performances have been established [39]. For this reason, we will principally discuss thermal stability and the OSC property of the CeO_2–ZrO_2 mixed oxides, even though the reader should be aware that a variety of complex phenomena occur under the real exhaust conditions, originated mainly by the interaction of the NM- and CeO_2-based materials.

Starting from 1995, CeO_2–ZrO_2 mixed oxides have gradually replaced pure CeO_2 as OSC materials in the TWCs [40], even though some low purity CeO_2 materials may be employed for less demanding TWC technologies [41]. The principal reason for the introduction of CeO_2–ZrO_2 mixed oxides in place of CeO_2 is due to their higher thermal stability, as exemplified in Fig. 7, which reports the OSC and BET area of

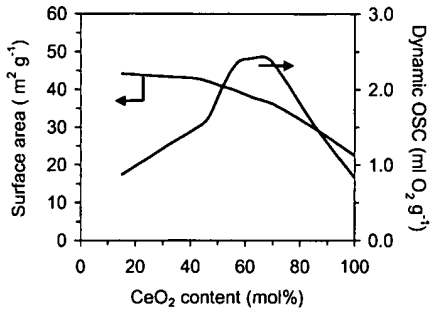

Fig. 7. Effect of CeO_2 content on the surface area stability and dynamic-OSC of CeO_2–ZrO_2 after calcination at 900 °C. OSC measured at 400 °C by alternatively pulsing 2.5% O_2 in He and 5% CO in He over the catalyst (after Ref. [42]).

CeO_2–ZrO_2 mixed oxides as a function of CeO_2 content [42]. Clearly, there is an important improvement of both OSC and BET area as soon as ZrO_2 is inserted into the CeO_2 lattice. At first glance, there appears to be a straightforward indication in Fig. 7, that is, CeO_2-rich compositions (around 60–70 mol%) are the most effective OSC promoters for TWC application. Unfortunately, this is a very simplified view of the problems related to the use of CeO_2–ZrO_2 mixed oxides in the TWCs, the real situation being much more complex, as described below.

3.2.1. Thermal stability of CeO_2–ZrO_2 mixed oxides

Thermal stability of the TWCs has always been a major issue in the development of the TWCs. The increase of the cruised mileage of passenger cars and higher exhaust temperatures observed nowadays compared to past [1], demanded for higher and higher thermal stability of the washcoat and particularly of the CeO_2 component. The relationship between the extent of surface area of CeO_2 and the OSC property, as detected by temperature programmed reduction (TPR), is well established (see Fig. 8 as an example). As below discussed, the ability of CeO_2 to undergo reduction, i.e. release of oxygen, at low temperatures (<500 °C) is well recognised as an immediate and useful tool to detect deactivation of the OSC and hence of TWC activity. Accordingly, the primary target in the development of high temperature OSC materials was always considered the resistance of CeO_2 towards sintering.

In principle, there are a number of different routes which may lead to enhanced thermal stability of the

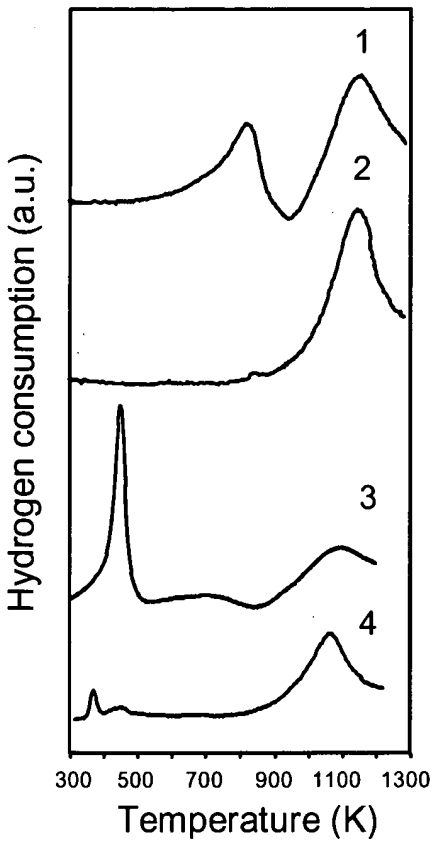

Fig. 8. TPR profiles of CeO_2 ((1) and (2)) and Rh/CeO_2 ((3) and (4)) with surface areas of, respectively, 190 $m^2 g^{-1}$ ((1) and (3)) and $<10\,m^2 g^{-1}$ ((2) and (4)).

CeO_2-based materials, which may be summarised as follows: (i) design of microstructure/textural properties by adopting an appropriate synthesis methodology, (ii) appropriate doping of CeO_2, (iii) dispersing of CeO_2 on a carrier. This last aspect has already been partially addressed since it is particularly related to the thermal stabilisation of Al_2O_3 (see above), as synergic stabilisation effects have been found for the CeO_2–ZrO_2–Al_2O_3 system [30]. Of course, any combination of these strategies can also be adopted, however, for sake of simplicity we prefer to discuss these aspects ((i) and (ii)) separately.

3.2.1.1. Design of microstructure/textural properties. The sinterability of any material is clearly related to its textural properties and in particular to its pore structure [43]. The pore structure, in turn, strongly depends on the synthesis conditions. For example, co-precipitation is typically employed to prepare mixed oxide catalysts. It has been shown that when the precipitated cake is treated at 80 °C in the presence of surfactants, extensive mesoporous texture develops in the CeO_2–ZrO_2 mixed oxides, leading to remarkably high surface areas compared to the traditional co-precipitation route [44]. On the other hand, the sintering mechanism at high temperature was apparently little affected, as comparable loss of surface area, in terms of relative loss of BET area, was observed in both samples, independently of the synthesis method [40]. Generally speaking, as the sintering at high temperatures proceeds, annihilation of small pores occurs first leading to decreases of the cumulative pore volume and BET area. On the other hand, large pores sinter with more difficulty as longer migration distances are needed for the matter to fill the pores and sinter the material. This concept is clearly illustrated by results of calcination of two $Ce_{0.2}Zr_{0.8}O_2$ samples where appropriate modifications of the conditions of sample processing were applied in a controlled way to obtain the initial pore distribution shown in Fig. 9. As a result of this pore distribution, sample A features a surface area of 27 $m^2 g^{-1}$ after calcination at 700 °C, which decreases by 85% after calcination at 1000 °C for 5 h, giving a BET area of 4 $m^2 g^{-1}$. This is not a surprising result since BET area of few square meters per gram are typically found after such a harsh calcination [45,46]. Sample B features much larger pores compared to sample A, leading to a BET surface area of 35 $m^2 g^{-1}$ after calcination at 700 °C. However, when the calcination temperature is increased to 1000 °C, a relatively small decrease of the BET area (37%) is observed, as the obtained product features a BET area of 22 $m^2 g^{-1}$. This is perfectly in line with the above reported comments on the sintering behaviour and indicates that extreme care should be taken before the effects of variation of CeO_2–ZrO_2 composition on textural stability can be assessed. Clearly, *meaningful comparison of properties of CeO_2–ZrO_2 mixed oxides can be obtained only when samples of comparable textural properties are compared.*

3.2.1.2. Doping of CeO_2–ZrO_2 mixed oxides with other elements. Even though the introduction of CeO_2–ZrO_2 mixed oxides into the TWCs represented a significant breakthrough point compared to the

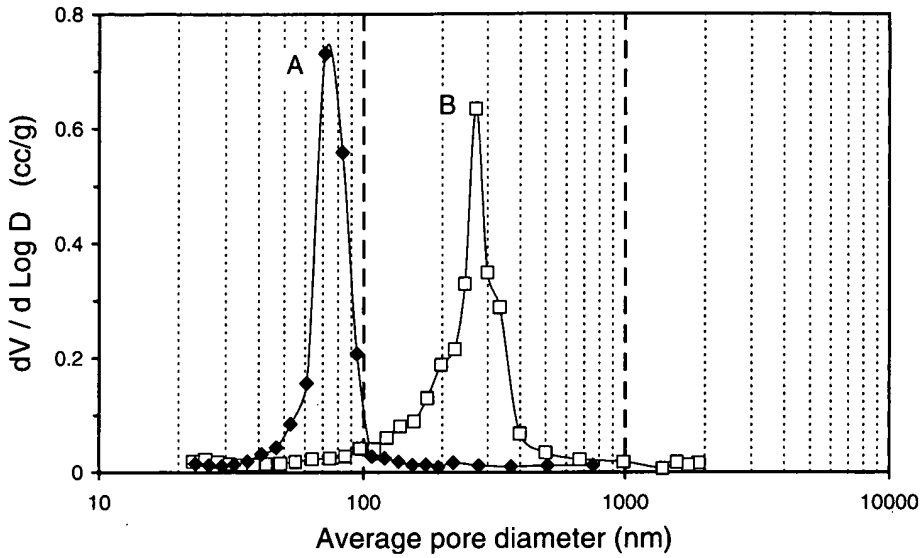

Fig. 9. Pore distribution in two samples of $Ce_{0.2}Zr_{0.8}O_2$ as detected from N_2 desorption isotherm using the BJH method: (A) surface area = 27 $m^2 g^{-1}$; (B) surface area = 35 $m^2 g^{-1}$.

CeO_2-based technology, it is now recognised that undoped CeO_2–ZrO_2 do not present sufficient thermal stability for application on the 2005 type of TWC converters. In fact, thermal stability in excess of 1000 °C cannot be achieved by simple CeO_2–ZrO_2 due to their metastable nature. As shown in the phase diagram reported in Fig. 10 [47–50], there are metastable (t' and t'') phases at intermediate CeO_2 compositions, which upon heating under oxidising conditions, lead to phase separation, CeO_2-rich (cubic: c-$Ce_{0.8}Zr_{0.2}O_2$) and ZrO_2-rich (tetragonal: t-$Ce_{0.2}Zr_{0.8}O_2$) phases being typically obtained [51,52]. In principle, TWCs must show high durability; accordingly phase separation is considered an undesirable feature of the CeO_2–ZrO_2 component since it may lead to unpredictable variations in the properties of the catalyst. By analogy with ZrO_2, trivalent dopants, such as yttria and lanthana, have been employed for the CeO_2–ZrO_2 mixed oxides [53–58]. However, to our knowledge no systematic study satisfying the above reported criterion of comparable textural properties for comparison of effects of composition has been reported so far. This makes difficult a rationalisation of the data reported in the literature on the effects of the doping agents.

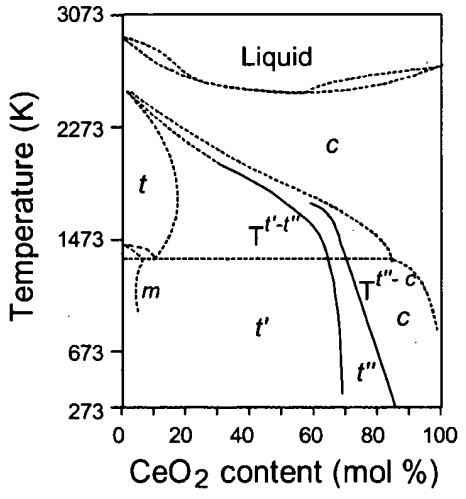

Fig. 10. Experimental phase diagram of the CeO_2–ZrO_2 system (after Ref. [70]).

Some qualitative and general comments can, however, be made for CeO_2–ZrO_2 systems: (i) CeO_2–ZrO_2 phase separation is favoured at the intermediate compositions and it is retarded or even prevented by addition of an appropriate low-valent dopant; (ii) phase separation is pronounced under oxidising conditions while under reducing conditions phase homogenisation is favoured [51,52]; (iii) sintering with decrease of surface area is very pronounced under reducing

conditions, particularly when compared to oxidising ones [59]. These general comments clearly point out the critical need for further research aimed at a rationalisation of the role of the dopant in affecting thermal stability of the CeO_2–ZrO_2 mixed oxides, in order to develop new products for high temperature applications.

3.2.2. Oxygen storage of CeO_2–ZrO_2 mixed oxides

A remarkable property of the CeO_2–ZrO_2 mixed oxides compared to CeO_2 is their ability to easily remove bulk oxygen species at moderate temperature even in highly sintered samples. Thus the reduction peak at approximately 900 °C (Fig. 8, trace 1), which is associated with reduction of CeO_2 in the bulk shifts down to approximately 400 °C when a 40 mol% of ZrO_2 was inserted into the CeO_2 lattice to prepare a highly sintered $Rh/Ce_{0.6}Zr_{0.4}O_2$ mixed oxide catalyst [60]. This was associated with the ability of ZrO_2 to modify the oxygen sub-lattice in the CeO_2–ZrO_2 mixed oxides, generating defective structures and highly mobile oxygen atoms in the lattice which can be released even at moderate temperatures [61,62]. These early findings indicated that improved efficiency of the OSC property can be achieved by using CeO_2–ZrO_2 mixed oxides instead of CeO_2 since, even if the sample sinters under the high temperature reaction conditions, it should be more effective then CeO_2 due to the high oxygen mobility in the bulk; lattice oxygen species could effectively participate in redox processes even under fluctuating exhaust feed-stream conditions. It is now well recognised that when the OSC property is investigated by the TPR technique, no appreciable distinction between the reduction in the bulk and at the surface can be observed in the CeO_2–ZrO_2 mixed oxides. Both reduction at the surface and in the bulk proceed with similar energetics and occur at mild temperatures [63,64]. Typically, a single peak reduction profile centred around is 500 °C is obtained for a single phase CeO_2–ZrO_2 solid solution, the presence of multiple peaks being taken as an indication of presence of phase impurities [40]. However, the changes in the TPR behaviour are even more subtle because other factors such as textural properties and even the pre-treatment can affect the TPR profile [65–68]. For example, a combination of TPR followed by mild oxidation leads to reduction phenomena occurring at low temperatures [65], whereas when a high temperature (severe) oxidation is included as a pre-treatment, these low temperature processes reversibly shift to high temperatures [66,67]. There has been some debate as to whether migration of oxygen species in the bulk is limiting the rate of the reduction of the CeO_2–ZrO_2, or whether the kinetics of redox phenomena are rather dictated by surface properties [45]. However, recent findings confirmed the important role of the bulk properties for redox phenomena occurring at low temperatures [68,69].

As above indicated, the TPR technique has been routinely applied to investigate the redox properties of the CeO_2–ZrO_2 mixed oxides. It should be noted, however, that under real exhaust conditions, the λ value oscillates between the oxidising and reducing conditions with a frequency of about 1 Hz. In principle, this makes the so-called dynamic-OSC more useful compared to the TPR technique [12,71], since this technique allows detection of the oxygen available for redox processes on a time scale of seconds. In fact, it should be noted that even favourable TPR profiles, i.e. featuring reduction peaks at low temperatures, may not necessarily be associated with effective OSC due to occurrence of in situ deactivation phenomena on increasing the temperature of the measurement [72]. However, a very recent report suggested that correlation between TPR profiles and effective dynamic-OSC exists in that texturally stable samples featuring a TPR behaviour independent of the pre-treatment, e.g. a mild or severe oxidation, are those giving the stable and effective dynamic-OSC, minimising the deactivation phenomena [73]. This confirms the importance of the stabilisation of the textural properties in the CeO_2–ZrO_2 mixed oxides and the need for further improvement of the thermal stability compared to typical temperatures so far investigated ($\approx$1000 °C).

3.3. Noble metals

Obviously, NMs represent the key component of the TWC, as the catalytic activity occurs at the noble metal centre. However, we purposely discuss the aspects related to the NM at this point, since its interaction with the various components of the washcoat critically affects the activity of the supported NM. In principle, the first aspect to be considered is the choice of the NM and its loading in the washcoat. Rh, Pd an Pt have long been employed in the TWCs and there is

a general agreement about the specificity of Rh to promote NO dissociation, thus enhancing the NO removal [4,6,74,75], even if alternative mechanistic pathways for NO reduction have also been proposed [7,76,77]. Pt and Pd are considered as metal of choice to promote the oxidation reaction, even though Rh also has a good oxidation activity. In particular, besides some initial use in 1975–1976, Pd has extensively been added to TWC formulations starting from mid-1990s due to its ability to promote HC oxidation [10,11]. In fact, better A/F control [78] and modification of the support provided high NO_x conversion, comparable to the traditional Rh/Pt catalyst [79]. The increase of the use of Pd in the TWC technology adversely affected Pd market price, which is now comparable to that of Pt.

In fact, there is a large demand for Pd due to the fact that the straightforward way to increase the efficiency of the TWCs at low temperatures is that of increasing the NM loading, and particularly that of Pd, which for long was the cheapest NM among the three employed (Fig. 11). On the other hand, use of high NM loading may favour sintering at high temperatures, leading to deactivation of the TWCs, in addition to the fact that cost-effective TWCs are required by the market. In summary, the choice and loading of the NM is a compromise between the required efficiency of the converter and the market price of the NM; ideally a car maker would prefer to have available a choice of TWCs with different formulations, which would allow a selection to be made according to price fluctuations of the NMs.

3.4. Deactivation of the TWCs

Generally speaking, sintering of NM, leading to decrease of the number of active sites, is a major pathway for the deactivation of TWCs. In addition to sintering, poisoning of the catalyst may contribute to their deactivation. The latter phenomenon is essentially related to the mileage travelled, quality of the fuel and the engine lubricating oil [22]. However, there are a number of other routes which can contribute to deactivation of the TWCs: (i) sintering of the OSC promoter leading to loss of OSC and, possibly, to encapsulation of the NM [80]; (ii) sintering of Al_2O_3 and, more important, deactivation of Rh due to migration of Rh^{3+} into the alumina lattice [22]. The comprehension of the relative importance of the different deactivation phenomena is difficult due to the variability of the reaction conditions, TWC preparation methods, etc. For example, when NM are supported on CeO_2–ZrO_2 mixed oxides and aged at high temperatures under redox conditions, encapsulation of Pd and Rh within the pores of the support occurs, while it does not occur for Pt [81].

Although it has received relatively scarce consideration [82], the issue of sulphur poisoning of TWC needs some consideration. As above discussed, inclusion of CeO_2-based promoters into the washcoat

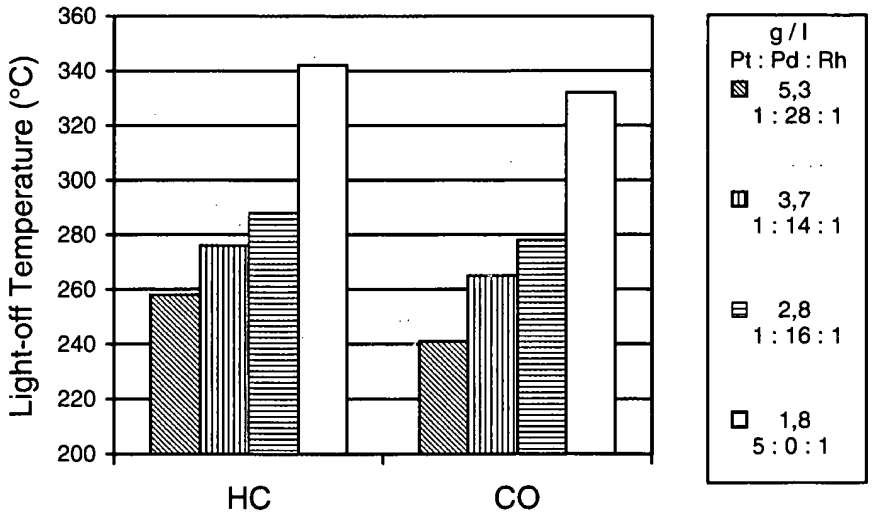

Fig. 11. Effect of NM loading on the light-off temperature in CCCs.

considerably enhances the conversion efficiency of the TWCs. On the other hand, both CeO_2 and ZrO_2 are known to easily adsorb SO_x species: sulphated ZrO_2 is a well-known solid acid catalyst [83], whereas CeO_2 is used as a $DeSO_x$ catalyst in cracking processes [84]. Investigation of reduced and oxidised CeO_2 revealed that SO_2 is adsorbed under various forms, with both surface and bulk-type of sulphates being observed [85,86], and it may even modify the microstructure of the CeO_2-based oxide [87]. Curiously, under oxidising conditions bulk sulphates decomposed by 600 °C, whereas surface sulphates persisted up to 700 °C [85]. Use of reducing conditions in the presence of H_2 favours elimination of sulphates as H_2S, which can be easily detected as rotten-egg odour [88], particularly in the presence of noble metal [89]. CO also promotes the reduction of sulphates to reduced oxy-sulphur species which unexpectedly increased the redox capability of the sulphated Pd/CeO_2 system compared to the sulphur-free analogue [90,91]. However, it was also observed that the OSC of CeO_2 is detrimentally affected by the presence of SO_2, while addition of ZrO_2 to CeO_2 increases the resistance of CeO_2 to sulphur poisoning, although more sulphur is adsorbed at the surface [82]. This may be associated with the generally higher OSC efficiency of the CeO_2–ZrO_2 mixed oxide compared to CeO_2 and the possibility that ZrO_2 acts as a sulphur scavenger. Ni containing oxides are sometimes added to the washcoat in the USA as sulphur scavengers, while their use in Europe is prohibited. In summary, adsorption of sulphur on the NM/CeO_2–ZrO_2-containing TWCs is rather complex and appears to be structure/adsorption conditions sensitive, which readily explains some contradictions in the literature. In terms of inhibition of the three-way activity it seems, however, that the issue of sulphur poisoning is much less stringent as compared, for example, to lean-$DeNO_x$ catalysts, due to the high temperatures achieved in the TWCs, which allow release of sulphur under driving conditions.

4. Future trends

4.1. Engine start-up emissions

As above discussed, TWCs represent a quite mature, highly effective technology for pollution abatement which, however, has some inherent limitations which need further improvement and development. These aspects are essentially related to: (i) low activity at low temperatures (start-up of the engine) and (ii) use of stoichiometric A/F. As far as the first aspect is concerned, it should be noted that roughly 50–80% of HC emissions during the test procedures are emitted before the TWC reaches the light-off temperature. When, in recent years, the emissions limits have been pushed down, it appeared clearly that minimisation of warm-up HC emissions was a major problem in automotive pollution abatement. This issue was been therefore addressed by introduction of the CCCs onto the market. This required development of TWCs featuring thermal stabilities well above 1000 °C [92].

In reality, the issue of the start-up emissions can be addressed by different approaches, some of which are listed in Fig. 12.

A first possibility is that of collecting the HC emitted during the warm-up of the converter in a HC trap, typically composed of hydrophobic zeolite. In an optimal trap, HC are trapped at low temperatures and as the temperature is increased above 250–300 °C, HC are released and converted on the TWCs [92]. A suitable trap must also feature very high thermal stability under hydrothermal conditions, which often is not the case for zeolite-based systems. We recall that temperatures as high as 850–900 °C may be reached in the under-floor catalysts. While such systems are still under investigation, alternative approaches have been indicated [92,93]. It must be recognised that to minimise the emissions, the catalysts must be heated-up in a minimum time. This can be achieved, for example, by electrically (Fig. 12) or combustion/chemically heated catalysts. In the latter case hydrogen and oxygen, or CO-rich feed is flowed over the catalysts [93]. Oxidation of both CO and H_2 are easy and exothermic reactions, which occur at low temperatures over the TWCs [94], leading to rapid heating of the catalyst. However, storage of H_2 on the vehicle or use of rich A/F which generates high CO and H_2 emissions, brings complexity to the de-pollution system. Large amounts of HC are in fact emitted at rich A/F, which require an additional HC trap.

Use of complex technology clearly pushes-up costs while the simplest technology is desirable. Accordingly, there has been a strong effort aimed at improving the thermal stability of the washcoat [42]. With

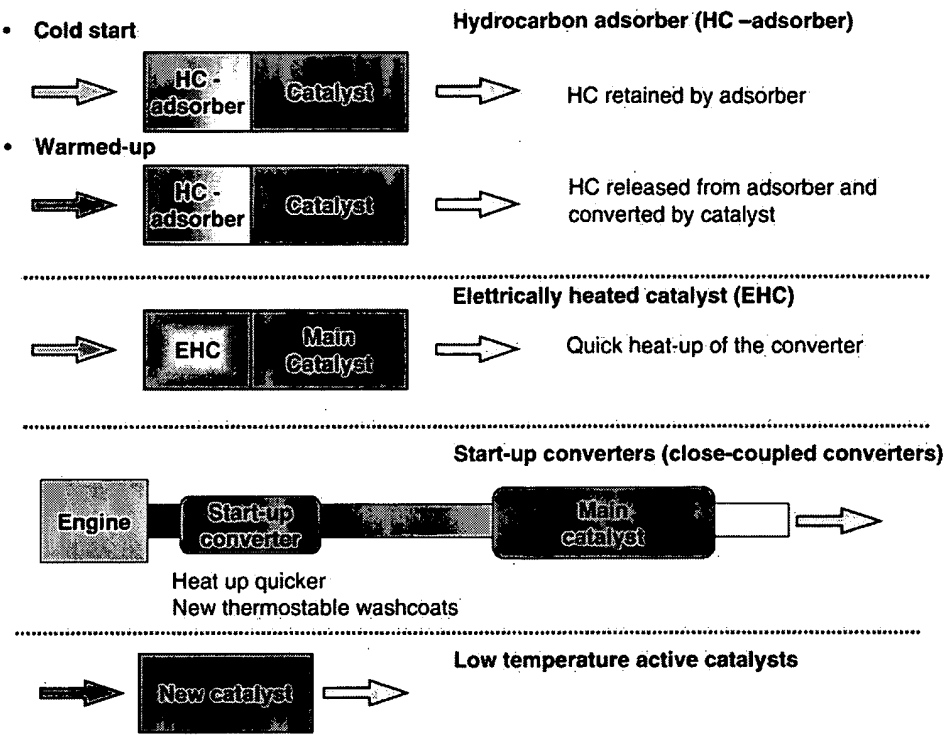

Fig. 12. Some strategies for the abatement of engine start-up emissions.

the availability of thermally stable washcoats, application of a start-up converter, i.e. converter that is closely coupled to the exhaust manifold, became feasible. This converter allows extremely rapid heating of the catalyst, leading to enhanced conversions during the warm-up of the engine. Metallic converter can be easily shaped into the exhaust manifold and are very convenient for such application also due to their low heat capacity. In general, the composition of the CCC is related to that of the typical TWC in that NM metals and particularly Pd are employed to promote HC conversion. The OSC promoter may be omitted from these formulations since it promotes CO conversion, leading to local overheating because of this highly exothermic reaction [92]. On the other hand, for the purpose of the OBD II technology, there is a necessity to monitor the OSC efficiency from the start-up of the engine. Accordingly, ZrO_2–rich doped CeO_2 promoters with very high thermal stabilities [42,73,95], are often added to this catalyst.

An alternative approach is that of developing new catalysts showing high conversion efficiency at low, nearly ambient, temperature [93]. A large part of these investigations have been triggered by the observation by Haruta et al. [96,97] that gold catalysts are able to efficiently oxidise CO even at subambient temperature provided that nano-dispersed Au particles are prepared on the support. Thus, light-off temperatures in the conversion of the exhausts as low as 100 °C could be achieved by depositing small Au particles on reducible oxides such as CeO_2 and TiO_2 [98]. However, the durability of gold catalysts under harsh conditions is still an issue, significant deactivation of cobalt oxide promoted Au catalysts was observed already after 157 h of reaction at 500 °C under simulated exhaust [99]. There is in fact a flourishing activity in the field of low temperatures catalysts [97,100,101], other noble metals, in addition to Au, being effective in low temperature oxidation reactions, provided that appropriate synthesis methodology is employed [100]. To our knowledge, however, due to the nano-dispersed nature of these catalysts, the issue of thermal stability, even at moderately high temperatures has not been solved as yet. Supported metal nano-particles are, in fact, quite

mobile on the surface, even at ambient temperature in the case of gold [101], which makes prevention of sintering phenomena difficult. We believe that thermal stabilisation of nano-dispersed metals may represent a new breakthrough point in the development of these environmental catalysts.

4.2. Lean DeNO$_x$ catalysts

The recently approved California legislation on automobile fuel consumption has prompted the necessity of developing new and more effective catalysts capable of removing NO_x even in excess of O_2. As indicated in Section 2, lean-burn gasoline and diesel engines, due to the high A/F used in the combustion process, can achieve significant fuel savings, however, under these conditions no TWC is effective in reducing NO_x due to the excess of O_2, which is competing for the reducing agent, in particular CO.

Studies on NO_x removal under oxidising conditions were triggered by the discovery in 1991 that HCs could act as selective reducing agents under excess of O_2 [102]. This discovery was followed by a feverish activity in the field of lean-DeNO$_x$ and more then 50 catalysts were reported in 1991–1992 [103]. Since then this topic has been reviewed by several researchers, even though a comprehensive knowledge of the exhaust lean technology is still missing [2,5,102–116]. As outlined in a report issued by MECA (Manufacturers of Emissions Controls Association) [117] there are two major strategies to control the NO_x emissions under oxidising conditions:

- DeNO$_x$ (lean-DeNO$_x$) catalysts;
- NO_x adsorbers (NO_x traps).

The former strategy employs a direct NO_x reduction catalyst, usually consisting of Pt/Al_2O_3 and a metal-loaded zeolite for NO_x reduction at, respectively, low and high temperature. The NO_x adsorber technology is sometimes called a NO_x storage/reduction (NSR) catalyst. In this case typically a $Pt/BaO/Al_2O_3$ catalyst is used to store NO_x under oxidising conditions as adsorbed "nitrate" species, which are then released and reduced on a traditional TWC by temporarily running the engine under rich conditions. Let us now examine in some detail these systems.

4.2.1. Pt/Al_2O_3 and derived systems

The activity of Pt/Al_2O_3 catalysts for NO_x reduction under lean exhaust conditions has been investigated in detail by Burch et al. [118–136]. They extensively analysed the effects of the nature of the noble metal, reducing agent, sulphur addition, nature of additives and of the support, and reaction mechanism.

A typical reaction profile for HC reduction over Pt/Al_2O_3 is reported in Fig. 13. This figure summarises some general features of Pt/Al_2O_3 lean-burn catalysts, that is: (i) a maximum of NO conversion at relatively low temperature, NO_x conversion peaking as the HC conversion reaches 100% in the case of C_3H_6; (ii) comparable starting temperatures for the NO reduction and HC oxidation; (iii) significant NO_2 formation at high temperatures when all the HC is burned-out; (iv) strong sensitivity of the NO conversion to the nature of the reducing agent (saturated vs. unsaturated HC); (v) poor selectivity towards di-nitrogen formation of the Pt catalyst, N_2O being the major product at low temperatures. As stated at point (iv), this general behaviour strongly depends on

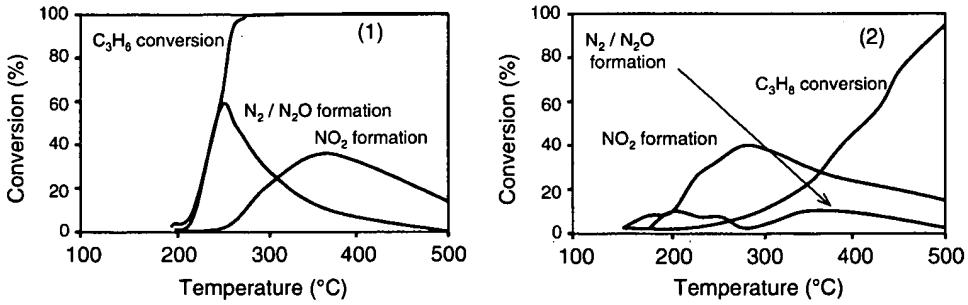

Fig. 13. Typical light-off behaviour for: (1) C_3H_6–NO–O_2 and (2) C_3H_8–NO–O_2 reactions over Pt/Al_2O_3. Pt: 1 wt.%, reactant feed: 1000 ppm C_3H_x, 500 ppm NO, 5% O_2. W/F = 4×10^{-4} g min ml^{-1} (GHSV 72,000 h^{-1}) (after Ref. [121]).

the nature of the reducing agent: non-reactive (short chain-saturated) HCs behave somewhat differently from reactive HCs such as alkenes or long-chain HC [127].

Let us discuss some important aspects of the above quoted properties of the Pt lean-DeNO$_x$ catalysts.

4.2.1.1. Light-off behaviour of the Pt catalysts. NO conversion typically shows a volcano shaped curve irrespective of the nature of the HC. This is due on one hand to the fact that NO$_x$ always initiates together with the HC oxidation and on the other hand to the fact that, with few exceptions, the maximum NO conversion corresponds to 100% HC conversion. At higher temperatures, when all the HC is consumed, significant NO$_2$ formation occurs by reaction of NO with excess O$_2$, the amount of NO$_2$ formed being limited by thermodynamic constrains. Note, however, that NO$_2$ concentration that apparently exceeded thermodynamic values were also reported for an Ag/Al$_2$O$_3$ system [137]. This fact was attributed to the presence organo-nitrite species as intermediates of the SCR process, which oxidation/decomposition led to NO$_2$ production.

The maximum of the NO$_x$ conversion is obviously affected by the space velocity (SV/GHSV). For a typical light-off curve, the reaction rate is kinetically limited only below the light-off temperature, while above light-off the reaction rate is limited either by heat or mass transfer. As a consequence, the maximum of the NO$_x$ conversion moves to low temperature and its intensity increases as SV decreases, however, this effect is not directly proportional to the decrease of the SV. Thus the maximum of the NO reduction peak moved from 200 °C (conversion 70%) to 215 °C (conversion 47%) as the SV was increased from 10,000 to 50,000 h^{-1}, while at intermediate SV = 25,000 h^{-1} a conversion of 57% was observed at approximately 210 °C [16]. From a practical point of view, exhaust emissions of a diesel engine were characterised by SV = 28,000–88,000 h^{-1} as the temperatures varied between 160 and 400 °C during the MVEuro2 driving cycle [16].

A corollary of this fact is that any comparison of activities simply based on light-off activities may be strongly misleading. Differences in light-off temperatures are in fact related to the number of active sites (Pt$_s$), total flow-rate (F) and kinetic law for the reaction by the following equation [138,139]:

$$\frac{1}{T_2} - \frac{1}{T_1} = \left(\frac{R}{E_a}\right) \ln \frac{f_2(c)\,\mathrm{Pt_s}\,F_2}{f_1(c)\,\mathrm{Pt_s}\,F_1} \quad (1)$$

For Eq. (1), a rate equation of the type $r = k(T)f(c)$ is assumed, where $k(T)$ is the rate constant for NO conversion, which depends on the temperature; and $f(c)$ represents the remaining factor of the rate equation, which depends on surface coverage and is independent of temperature [138,139]. An inspection of Eq. (1) reveals that upon comparison of the activities of two catalysts with different dispersions (i.e., there are two different Pt$_s$ terms) under equivalent reaction conditions (i.e., $F_1 = F_2$ and $f_1(c) = f_2(c)$), the higher the number of active sites the lower the light-off temperature. This means that the specific activity of two catalysts may be compared using the light-off behaviour only when an equal number of active sites is employed in the experiment. Unfortunately, very few investigations concerning lean-DeNO$_x$ have reported reaction rates, light-off temperature being generally shown, which makes direct comparison difficult. Note that when long-chain HC are investigated, which can easily generate coke at the catalysts surface, the light-off behaviour may not be relevant to the true catalytic activity as pseudo-steady states were observed below light-off temperature for short to medium periods (0.1–2 h) followed by a deactivation of the catalyst [131]. It is important to keep present these limitations when activity from different sources is compared.

Reaction rates and kinetic law for C$_3$H$_6$/NO/O$_2$ reaction were reported in the literature for Pt/Al$_2$O$_3$ and Rh/Al$_2$O$_3$ [140,141]. For Pt/Al$_2$O$_3$ the following expression were found experimentally at 230–236 °C (NO and C$_3$H$_6$ 250–4000 ppm, O$_2$ 0.5–12%, W/F = 0.0018 g s ml^{-1}, GHSV ≈ 100,000 h^{-1}, apparent activation energy 24±3 kcal mol^{-1}):

$$\text{reduction}: \quad r(\mathrm{NO}) = k_{\mathrm{red}} \frac{[\mathrm{O_2}]}{[\mathrm{C_3H_6}]^{0.5}}$$

$$\text{oxidation}: \quad r(\mathrm{C_3H_6}) = k_{\mathrm{ox}} \frac{[\mathrm{O_2}]}{[\mathrm{NO}]^{0.5}[\mathrm{C_3H_6}]^{0.5}}$$

For comparison, the kinetic expression for the combustion of C$_3$H$_6$ measured at 158 °C was

$$\text{combustion}: \quad r(\mathrm{C_3H_6}) = k_{\mathrm{comb}} \frac{[\mathrm{O_2}]}{[\mathrm{C_3H_6}]^{0.5}}$$

The apparent activation energies for NO reduction and C_3H_6 oxidation were measured as 22 and 24 kcal mol^{-1} over Pt (1.5 wt.%)/Al_2O_3 [141]. Interestingly, NO_x, even if present at ppm level, interferes with the HC oxidation. We recall that modification of CO oxidation kinetics in the presence of NO is typically assumed as a direct indication that NO removal occurs through the NO/CO reaction over TWCs [4]. In summary, independently of the reaction mechanism, the key factors in the light-off behaviour of Pt lean-DeNO_x catalysts is that a narrow maximum of activity is observed around 270–300 °C. The width and position of this maximum of activity depends on the reaction conditions and nature of the catalyst. As is shown below, also the nature of the HC also plays a fundamental role in the volcano shaped NO_x conversion curve because of the different HC reactivity.

4.2.1.2. The effect of the reducing agent and promoters on the reaction mechanism. The effect of the nature of the reducing agent was investigated in detail by researchers from Degussa (OMG) [142]. Even though the nature of the catalyst employed was not specified, except that a 50 g/ft^3 Pt honeycomb catalyst was used, the finding of this paper represent typical results observed over Pt/Al_2O_3 in subsequent papers. These findings can be summarised as follows:

- There is a remarkable difference in the response of the Pt catalyst to the nature of the HC reducing agent, e.g. the temperature of the maximum of HC and NO conversion is nearly independent of the type of linear alkene, while an increase of the length of the chain of the alkane significantly shifts down this temperature.
- At comparable HC chain length saturated HC are much less effective compared to unsaturated ones. Remarkably $C_{16}H_{34}$, which is a typical diesel fuel component, featured an activity comparable to that of C_3H_6.
- Use of alcohols resulted in high activity at low temperatures, the nature of the alcohol affecting the activity to a lesser extent compared to alkanes.
- Use of aromatic compounds as reducing agent showed a strong dependence of the conversion efficiency on the reactivity of the molecule.

The remarkable difference of the catalytic behaviour between the saturated and unsaturated HCs was rationalised in terms of the different reaction pathway for the NO reduction in the presence of either saturated or unsaturated HC (Fig. 14) [121,125]. It appears that reduction of the unsaturated HC can be depicted as a NO_x dissociation reaction occurring the metal centre, where the unsaturated HC is responsible for the removal of the adsorbed oxygen generated by the NO_x dissociation. In the presence of weakly adsorbed reducing agent, such as C_3H_8, adsorbed atomic oxygen is the dominant species on the metal surface under reaction conditions. The C_3H_8 oxidation is inhibited by both O_2 and in the facile oxidation of NO to NO_2. It is believed that the rate determining step in C_3H_8 oxidation by O_2 is the dissociative chemisorption of C_3H_8 involving the breaking of a C–H bond [123,125]. This is a difficult reaction and strongly depends on the nature of the HC, which accounts for the strong

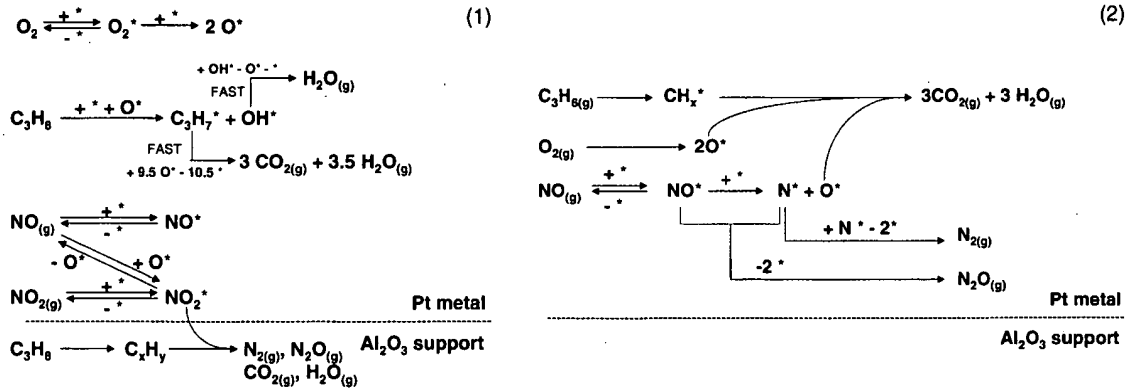

Fig. 14. Proposed reaction mechanism for lean-DeNO_x reaction over Pt/Al_2O_3 for alkane (1) and alkene (2) conversion (after Ref. [121]).

effect of the carbon chain length upon the $DeNO_x$ activity.

In addition, a comparison of different Pt/Al_2O_3 catalysts promoted by metal oxides (Ba, Ce, Co, Cs, Cu, K, La, Mg, Mo, Ti) or noble metals (Ag, Au, Pd, Rh) in the lean NO_x reaction, using C_3H_6 as a reducing agent, showed that even if the promoters have a significant effect (beneficial or otherwise) on the activity and temperature range of operation of Pt/Al_2O_3, they have no significant effect on the N_2/N_2O selectivity. The similarity in behaviour of the promoted catalysts and unpromoted Pt/Al_2O_3 suggests that the reaction mechanism was similar for all the catalysts tested [124]. The ability of the Al_2O_3 support to promote the interaction of the adsorbed/migrated NO_x/C_xH_y species generated from saturated HC, seems a particular property of this support, since changing the support to SiO_2 resulted in almost no reaction even with comparable Pt loading and dispersion. Finally, a comparison of different HCs as reducing agent revealed an unusual ability of aromatic HC (toluene) to promote high selectivity of the Pt catalysts towards formation of N_2 [122]. It should be also noted that when long-chain HCs are employed, the light-off activity may be very different from steady-state activity in that below or close to light-off temperature (generally chosen as 50% of conversion), catalysts poisoning with time-on-stream was observed [127]. By increasing the reaction temperature conversion of adsorbed carbonaceous species occurred, thus recovering the catalyst activity [130]. No deactivation was observed with small HC, formation of carbonaceous species being minimal in this case.

The effect of addition of SO_2 to the reaction feed appears in line with the above interpretation of the effect of the HC in that strong poisoning of activity was observed when C_3H_8 was employed as reducing agent due to the formation of aluminium sulphate. This is responsible for the poisoning of the catalytic sites at the support [128]. In contrast the activity was much less affected in the case of C_3H_6, which is in line with the smaller sensitivity of the Pt particles towards sulphur poisoning compared to the support.

Even though this reaction mechanism was questioned, in particular due to the lack of XPS evidence for reduced Pt sites [143], we believe that the major findings and suggestions reported by Burch and co-workers still provide an important guide-line for development of a new generation catalyst. In fact, despite the intensive research in the literature, the effect of the nature of the support has little been investigated [124,126,143–145], and most of the studies were carried out using C_3H_6 as reducing agent, where little or no effect of the support should be expected. In fact, we believe that in this case the major role of the support is to affect the Pt dispersion rather then other effects, thus modifying the activity of the supported metal. When saturated HCs are included in the feed, effects of support composition were detected [143], however, there is not enough evidence on a clear effect of the different supports in promoting Pt activity in lean-$DeNO_x$.

4.2.2. Other lean-$DeNO_x$ catalysts

Numerous other catalytic systems have been investigated as $DeNO_x$ catalysts, however, they appear much less applicability as next generation catalyst due to generally low activity and/or stability of such systems. For sake of convenience we will group all the catalysts in the following categories:

- Cu-ZSM5 and related systems;
- metal oxide catalysts.

As above written, Cu-ZSM5 represented the first major candidate for lean-$DeNO_x$ catalysts, even though it was quickly recognised that several problems affect the Cu-zeolite catalysts [103]. These include: (i) poor hydrothermal stability of Cu species and zeolite framework; (ii) appreciable activity only at high temperature (300–400 °C), which only allows the use of such system in conjunction with NM low temperature catalysts; (iii) generally poor activity under real exhaust and at high space velocities. The higher range of reaction temperatures compared to Pt catalysts makes these systems of potential interest for lean-burn gasoline engine, where such high temperatures are more easily met compared to the diesel engine.

With the aim of improving the thermal stability of the zeolite catalysts, a variety of supported and even unsupported metal oxides have been investigated. ZrO_2 itself was chosen as a possible candidate. Cu/ZrO_2 and other supported metal oxides, both sulphated and sulphur-free, have been investigated to some extent with the aim of improving the thermal

stability of the catalyst compared to the zeolitic system [146–154]. Even though some interesting activities were claimed, to our knowledge, there is not sufficient evidence for possible application of such systems under real exhaust conditions. In fact, even though some increase of thermal/hydrothermal stability could be achieved, the activity is generally poorer compared to the Cu-ZSM5 system. As a general comment, it seems that despite the Edisonian type of research on different metal oxides as $DeNO_x$ catalysts, the "high activities" sometimes claimed by the authors, withstand with difficulties the harsh exhaust conditions. A relatively recent comparative study of several types of "promising" lean-$DeNO_x$ catalysts under diesel conditions is very illustrative in this respect [155]: after testing nine different classes of catalysts (Pt/Al_2O_3, Rh/Al_2O_3, Ag/Al_2O_3, Pt-ZSM5, Cu-ZSM5, Pt/In-ZSM5, CeZSM5+Mn_2O_3, Co/Al_2O_3, and Au/Al_2O_3 + Mn_2O_3), the authors came to the conclusion that despite the fact that some high activities could be measured, particularly on the NM-containing catalysts, there is no single phase catalyst capable of satisfying the practical demand for NO_x removal from diesel exhaust.

Ag catalysts are also among those extensively studied since high activity were reported, particularly when alcohols are employed as reducing agents (see, for example [137,155–165]). A general comment concerning the Ag based catalysts is that, due to the low melting point of Ag, extensive sintering of the catalyst may be expected even at relatively low temperatures. The catalytic activity was shown to depend on the Ag particle size [166], high particle sizes favouring the unselective HC oxidation and N_2O formation at low temperatures (Fig. 15). On the contrary, highly dispersed Ag particles favour formation of N_2 but the reaction occurs at higher temperatures. This was explained by the different reaction pathway according to the nature of the supported Ag phase (Fig. 16).

The high sinterability of Ag may represent an important drawback for practical application unless particular synthesis methodology is employed [167,168]. As shown in Fig. 15, high activity and N_2 selectivity of the Ag catalysts is observed in the "high" range of temperatures; accordingly this catalyst may be considered as a substitute for the Cu-ZSM5 component in a full-range of temperatures operating lean-$DeNO_x$ catalyst [2,169]. To promote the activity at low temperatures, Ag could in principle be sintered, however this promotes the unselective HC oxidation [166]. An interesting way to promote the activity of these catalysts is to add another NM to the system [170,171].

Recently, we have shown that use of ZrO_2 or ZrO_2-rich CeO_2–ZrO_2 mixed oxides as supports for Ag strongly improves the activity at low temperatures (Fig. 17) [172]. As shown by comparison of activities of catalysts with different Ag dispersion

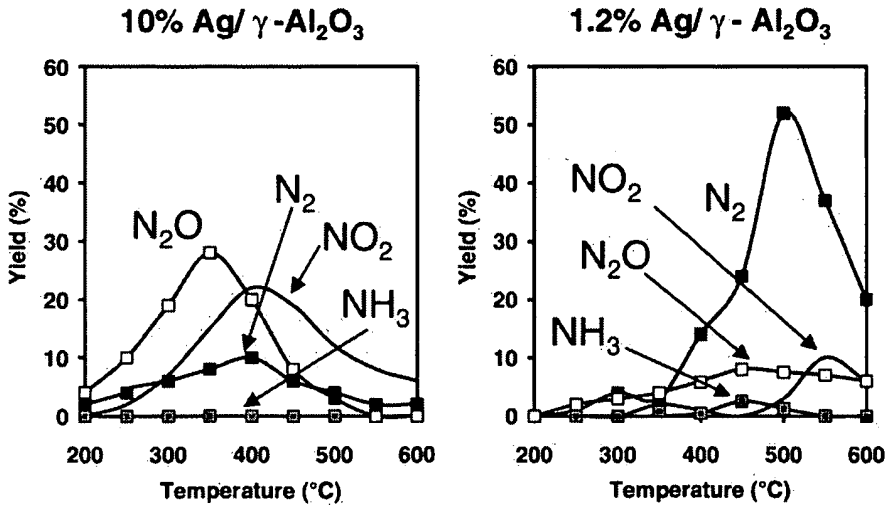

Fig. 15. Effect of Ag loading on the activity and product selectivity in Ag/Al_2O_3 catalysts (after Ref. [137]).

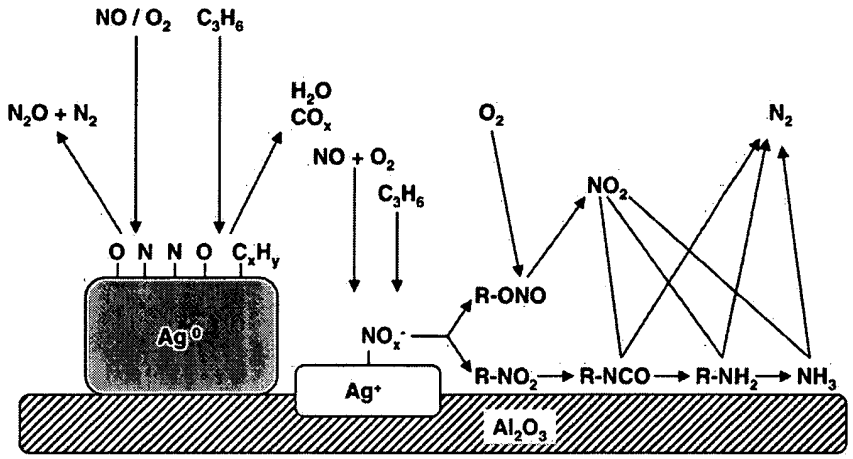

Fig. 16. Reaction mechanism(s) proposed for the lean-DeNO$_x$ reaction over Ag/Al$_2$O$_3$ catalysts (after Ref. [137]).

[172], the activity of Ag invariably occurs at lower temperatures on ZrO$_2$-containing supports compared to Al$_2$O$_3$ supports. More important is that the use of ZrO$_2$-containing supports remarkably facilitates the regeneration of the catalysts from SO$_x$ poisoning compared to Ag/Al$_2$O$_3$.

4.2.3. *Bi-functional lean-DeNO$_x$ catalysts*

The idea of bi-functionality to improve the activity of the lean-DeNO$_x$ catalysts has been pioneered by Misono and co-workers. These studies were recently reviewed [173], accordingly we refer the reader to this review. Of the several systems described, it is important to focus the mechanistic features of the authors' work. Essentially, the authors favour the reaction pathway which proceeds with formation of NO$_2$ as reaction intermediate, which then efficiently reacts with adsorbed HC to give surface intermediates. These intermediates then decompose leading to an overall reduction of NO$_x$. A redox type component such as Mn$_2$O$_3$ or SnO$_2$ is also added, which favours oxidation of NO to NO$_2$ (Fig. 18).

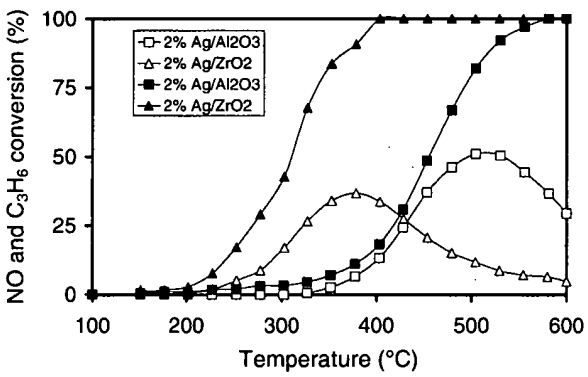

Fig. 17. Effect of the nature of the support on lean-DeNO$_x$ activity of Ag catalysts: NO$_x$ reduction (empty symbols), C$_3$H$_6$ oxidation (filled symbols). The 1000 ppm C$_3$H$_6$, 1000 ppm NO, 5% O$_2$, W/F = 0.05 g s ml^{-1} (after Ref. [172]).

An interesting aspect of these systems is that the presence of water, which normally deactivates the DeNO$_x$ catalysts, can even improve the catalytic activity (Fig. 19). This was attributed to the partial suppression of the direct HC oxidation at Mn$_2$O$_3$ (Fig. 18) that is responsible for non-selective HC oxidation.

Among the bi-functional systems, the NM/zeolite catalysts, containing particularly H-ZSM5, should also be quoted. A number of researchers have indeed employed both Pt/ZSM5 and Pd/ZSM5 as bi-functional systems for the lean-DeNO$_x$ (see, for example [147,173–180]). Typically, such catalysts and particularly those Pd-based were employed for lean-DeNO$_x$ using CH$_4$ as reducing agent. The bi-functionality of this type of catalyst is related to the necessity of acid sites, which apparently allow activation of the HC at the support leading to selective NO$_x$ reduction. In fact, using Na-ZSM5 as a support, no NO$_x$ reduction was detected. Several zeolites were employed for the CH$_4$/NO/O$_2$ reaction, however,

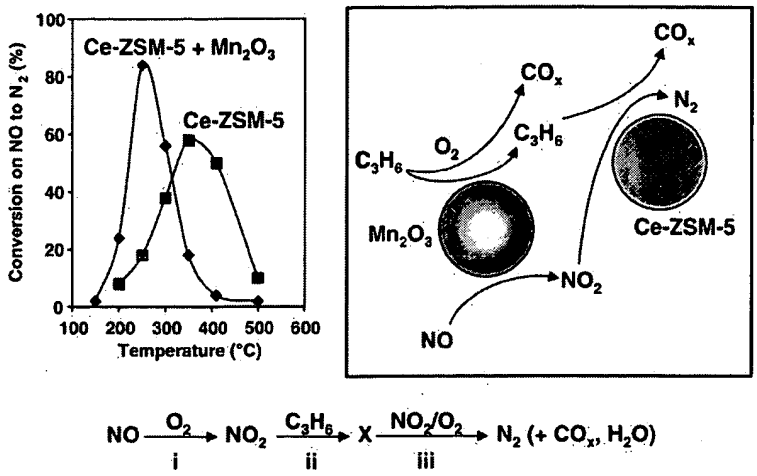

Fig. 18. Effect of addition of Mn_2O_3 (as physical mixture) on the $DeNO_x$ activity of Ce-ZSM5; and the proposed reaction mechanism (after Ref. [173]).

significant deactivation of the catalyst occurred in the presence of water and SO_x.

While a somewhat extensive description of the various attempts to develop efficient lean-$DeNO_x$ catalysts is reported here, it is important to outline that these systems do not ensure sufficient activity to foresee practical applications in a future. Development of new breakthrough strategies is an important target for the comming years to achieve significant environmental benefits from the use of lean, high-efficiency engines.

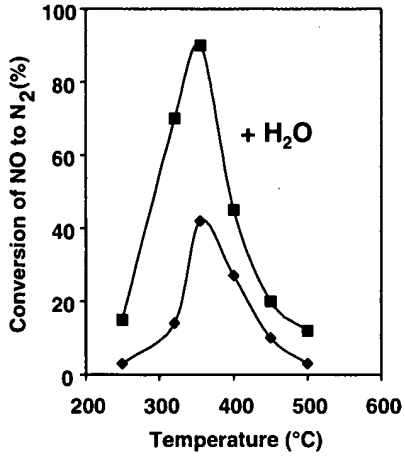

Fig. 19. Effect of addition of H_2O on the activity of Mn_2O_3/Sn-ZSM5 bi-functional catalyst (after Ref. [173]).

4.3. Lean NO_x traps

The discovery by Toyota researchers of the so-called NSR catalysts also triggered feverish activity in lean-$DeNO_x$ studies [181–183]. The principle of the reaction mechanism of these systems appears well established [183]. Under oxidising conditions NO_x are stored at the surface of a Ba-containing catalyst under various forms (surface nitrites/nitrates), which exact nature is still matter of debate [184–187] (Fig. 20). After a certain period, which length is an important factor and is correlated to the specific emission/catalyst characteristics, the A/F ratio is set to rich and the stored NO_x species are reduced over Pt or, more generally, TWC-type catalyst to N_2 [183].

The mechanism of NO_x adsorption and desorption/reduction has been investigated by a number of authors [112,184,185,187–197]. It appears now clearly the storage/reduction is rather complex process due to the complex nature of the exhaust mixture. For example, model studies performed on $Pt/BaO/Al_2O_3$ suggested that the first step is the oxidation of NO to NO_2, which is active species being adsorbed on the surface [190,191], even though kinetic studies could not distinguish whether surfaces nitrites are formed first and then oxidised to nitrates or whether both species are formed directly by a disproportionation mechanism [194]. However, the final species that is strongly held on the surface and accounts for the majority of NO_x

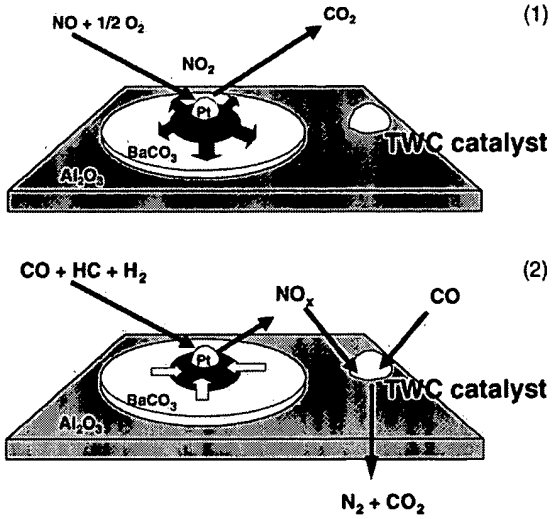

Fig. 20. Principle of operation of an NSR catalyst: NO_x are stored under oxidising conditions (1) and then reduced on a TWC when the A/F is temporarily switched to rich conditions (2).

stored appears to be a nitrate species, in particular at high temperature due to the low thermal stability of nitrite. Whatever is the true mechanism, it must be underlined that the kinetics and the extent of storage are heavily affected by the presence of water and CO_2 in the exhausts: CO_2 slows down the NO_x adsorption kinetics as the reaction can more appropriately be seen as a transformation of surface carbonates into nitrates, e.g. CO_2 strongly competes with NO_x for the adsorption sites [190,196]. This competition, on the other hand, increases the rate of NO_x releases under the rich-spike [188,189]. The effect of water is more controversial in that promotion of NO_x adsorption was observed below 250 °C by addition of small amounts of water (1%), whereas at higher temperature an inhibition effect was observed [194]. However, such promoting effect was not seen when both water CO_2 were co-fed.

The NSR technology is by far the most reliable and attractive lean-DeNO_x technology and it has been commercialised in Japan where low sulphur gasoline is available. In fact, the major drawback of the NSR catalyst is its sensitivity to SO_x due to the fact that surface sulphates are invariably more thermally stable compared to the nitrates [198]. The durability aspects of the NSR catalysts were addressed, for example, by researchers from OMG [199] and there seems to be general agreement that poisoning of the NO_x storage function is directly related to the amount of SO_2 passed over the catalyst. This is an important aspect since it suggests that for application of these catalysts to US or European markets, where higher sulphur contents are present in the fuel compared to Japan, appropriate strategies to develop sulphur resistant NO_x trap must be applied. In addition to the obvious requirement of lowering of sulphur content in the fuel, there are strategies that can be adopted for increasing sulphur tolerance of the converter: (i) adoption of an SO_x adsorber that protects the NO_x trap and is periodically regenerated; (ii) modification of the catalyst composition to promote of the removal efficiency of the adsorbed SO_x. An interesting example of such strategies was recently reported by Toyota [200,201]. In their system, TiO_2 was added to protect the barium-based trap from sulphur poisoning due to its high sulphur tolerance. LiO was added as it was observed that Li-promoted Al_2O_3 releases accumulated sulphur more easily compared to pure Al_2O_3. Rh/ZrO_2 was also employed to enhance the sulphur removal under reducing conditions due to its effectiveness as a steam reforming catalyst. In fact, an efficient H_2 generation under the rich-spike of the cycle strongly favours the removal of adsorbed SO_x. It should be noted that release of H_2S from the catalysts is undesirable, accordingly special schedules of the modulation of the A/F during the rich phases can be adopted, which pump additional oxygen during the rich-de-sulphation phase minimising H_2S release [202]. Finally, thermal deactivation due to sintering of the barium species and formation of barium aluminates may represent an issue in terms of durability of the catalyst [203]. Accordingly, thermally stable Ba-containing materials, such as doped aluminas or perovskites, has been investigated as NO_x absorbers [184,185,204].

It is worth of noting that the NSR strategy has also been applied to diesel engines. In this case generation of the rich conditions must be carefully considered as switching A/F to rich conditions easily generates typical black-smoke-containing emissions, often found in older vehicles. Low temperature smokeless combustion with a massive EGR or, more frequently, post-injection of fuel are employed to temporarily generate rich exhaust. The interesting point is that the NSR component may be deposited on the walls of the porous ceramic filter so that the precious metal can

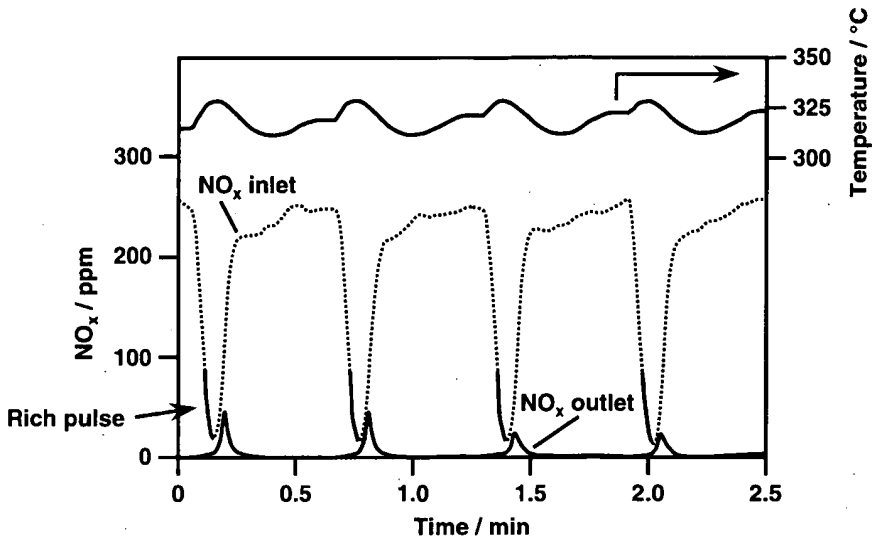

Fig. 21. Engine-out and tailpipe-out emissions from a 1.9 L diesel engine over an NSR catalysts deposited on a ceramic filter. Notice that similar efficiencies may be achieved over the NSR catalysts in the lean gasoline engines (after Ref. [205]).

contemporarily promote removal of the particulate [205]. Thus, very high pollutant conversion efficiency (ca. 80%) could be obtained in the engine test procedure (Fig. 21). Clearly, the issue of trap deactivation becomes even more stringent in the case of diesel vehicles due to the generally higher amounts of sulphur in the fuel and low operating temperatures that do not allow efficient trap regeneration. Rich conditions for several minutes and temperatures as high as 650–700 °C are typically needed to achieve effective trap de-sulphurisation [202].

4.4. Selective catalytic NO_x reduction using urea

Due to the limited success of HCs as efficient reducing agent under lean conditions, the use of urea as an alternative reducing agent for NO_x from heavy duty diesel[2] vehicles has received attention. Selective catalytic reduction of NO_x with NH_3 in the presence of excess O_2 is a well implemented technology for NO_x abatement from stationary sources [206]. Typically, vanadia supported on TiO_2, with different promoters (WO_3 and MoO_3) are employed in monolith type of catalysts. A sketch of an arrangement for the urea based NO_x abatement technology is shown in Fig. 22. Typically, the urea solution is vaporised and injected into a pre-heated zone where hydrolysis occurs according to the reaction:

$$H_2N\text{–}CO\text{–}NH_2 + H_2O \rightarrow CO_2 + 2NH_3$$

Ammonia then reacts with NO and NO_2 on the reduction catalyst via the following reactions:

$$4NO + 4NH_3 + O_2 \rightarrow 4N_2 + 6H_2O$$

$$6NO_2 + 8NH_3 \rightarrow 7N_2 + 12H_2O$$

This approach has proved to be quite successful and high NO_x (up to 80%) could be achieved on HD under driving conditions, even after reasonably high mileages (200,000–300,000 km), the activity decreased to about 75–80% of the initial value after over 500,000 km [207,208]. A major problem of such system is that extreme care must be exercised to develop a suitable urea injection strategy that avoids overloading of the system leading to ammonia slip [209].

[2] Light-duty (LD) diesel engines are generally defined as vehicles with an engine displacement of less than 4 l and power output of up to 100 kW, and are characterised by relatively high engine speeds. LD engines would normally be found in passenger vehicle and light commercial vehicle applications. Heavy duty (HD) diesel engines may be generally defined as of displacement greater than 8 l and power outputs of greater than 150 kW. HD engines are found in heavy road transport, industrial and marine applications. Medium duty engines fill the gap in the middle and are found in medium size trucks, buses and light industrial equipment.

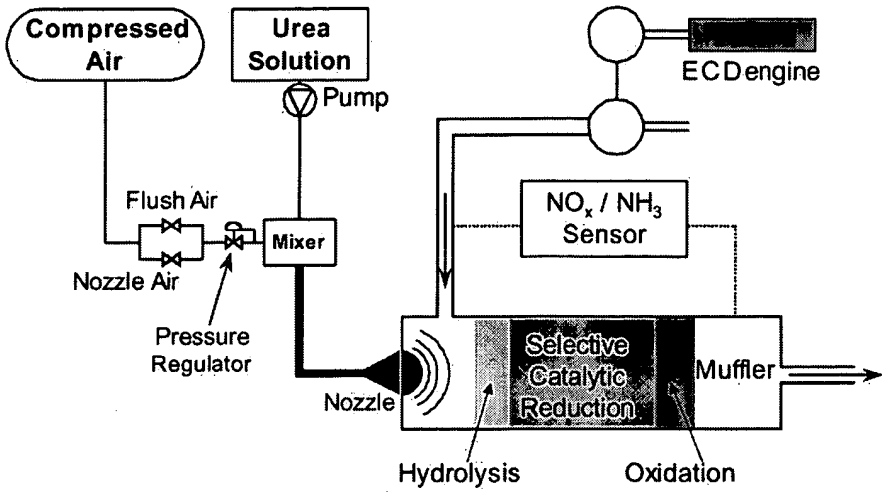

Fig. 22. A typical arrangement for abatement of NO_x from a heavy duty diesel engine using urea as reducing agent.

Typically, ammonia slip should not exceed 10 ppm. While the efficiency of urea-SCR technology is recognised [210], there are certainly still a number of issues concerning the catalyst efficiency at low temperatures, the design of compact converter systems that require higher conversion efficiency and, last but not least, the issue of generalised urea distribution when fuelling the vehicle.

Given the efficiency of such systems, the application of the urea-SCR technology to LD vehicles was also investigated [211]: while appreciable NO_x can be achieved, it must be recognised that a ratio of engine displacement-to-catalyst volume of 1:3 is typically employed for the urea-SCR systems that may represent a serious problem in compact LD vehicles. Clearly, an important improvement of the catalytic performances is needed before such systems can be effectively considered for LDV application.

4.5. Particulate matter removal

Even though this topic is specifically related to diesel engines, the general interest of these systems is related to the above quoted desire to use high-efficiency engines. Diesel particulate matter (DPM) is the most complex of diesel emissions. Diesel particulates, as defined by most emission standards, are sampled from diluted and cooled exhaust gases. This definition includes both solids, as well as liquid material which condenses during the dilution process. The basic fractions of DPM are elemental carbon, heavy HCs derived from the fuel and lubricating oil, and hydrated sulphuric acid derived from the fuel sulphur. DPM contains a large portion of the polynuclear aromatic hydrocarbons (PAH) found in diesel exhaust. Diesel particulates contains small nuclei with diameters below 0.04 μm, which agglomerate forming particles as large as 1 μm. The non-gaseous diesel emissions are grouped into three categories: soluble organic fraction (SOF), sulphate and soot [212].

Removal of the liquid fraction of PM is generally achieved by an oxidation catalyst. Oxidation catalysts have been fitted to US medium duty diesel vehicles since 1994 to reduce emissions of HC, the SOF content of DPM, and CO [212]. Typically, these catalysts are composed of $NM/CeO_2/Al_2O_3$ (NM = Pt) systems, where porosity of the catalysts often plays a key role since adsorption of the SOF at the support allows its conversion at catalytic sites and hence its removal before its desorption starts [212]. This is a critical aspect in the diesel exhaust removal due to the generally low temperatures (120–350 °C) of the diesel exhaust [213]. In fact, during the test cycle, the temperature of the catalyst may easily fall below the light-off temperature making necessary additions of an adsorbent, typically a zeolite. Oxidation catalysts promote the oxidation of HC and CO with oxygen in the exhaust to

form CO_2 and H_2O. Fuel sulphur levels of maximum 500 ppm are required to avoid excessive production of sulphate based PM and to minimise catalyst deactivation by sulphur poisoning. Lower levels of sulphur (50 ppm) can increase the effectiveness of oxidation catalysts by up to 50% and contribute to greater durability. Oxidation catalysts have not generally been used in heavy vehicles with the exception of urban buses, and are not considered necessary to meet HC and CO requirements of future HD emission regulations.

Removal of soot may be achieved by means of filtration (Fig. 23) [214]. Even though different types of filters can be employed [215], the filtration efficiency is generally high. However, the continuous use under the driving conditions leads to filter plugging. Regeneration of the filter is therefore a crucial step of the soot removal systems. This can be achieved thermally, by burning the soot deposits on the filter, using, for example a dual filter systems such as depicted in Fig. 23. However, such systems may be adopted only in the trucks where space requirements are less stringent compared to passenger cars. In addition, there are problems arising from the high temperatures achieved during the regeneration step when the deposited soot is burned off. In fact, local overheating can easily occur leading to sintering with consequent permanent plugging of the filter. To overcome these problems, development of catalytic filters has attracted the interested of many researchers (for a recent review, see Ref. [214]).

A comprehensive discussion of the diesel particulate abatement systems is beyond the scope of this paper, however, it is important to quote some emerging technologies in this field, one of the most important being those of the CRT [216] and use of fuel additives that favour combustion of the soot deposited on the filter [217,218]. The concept of the so-called CRT has been pioneered by researchers from Johnson Matthey [216] and is based on the observation that NO_2 is a more powerful oxidising agent towards the soot compared to O_2. The concept of CRT is illustrated in Fig. 24: a Pt catalysts is employed in front of the filtering device in order to promote NO oxidation; in the second part of CRT, DPM reacts with NO_2 favouring a continuous regeneration of the trap. A major drawback of these systems is related to the capability of Pt catalysts to promote SO_2 oxidation as well. The sulphate thus formed is then deposited on the particulate filter interfering with its regeneration. Moreover, the NO_2 reacts with the soot to reform NO whilst reduction of NO_2 to N_2 would be the desirable process. Accordingly, it is expected that as the NO_x emission limits will be pushed down by the legislation, less NO will be available in the exhaust for soot removal, unless the engine is tuned for high NO_x emission that are used in the CRT and then an additional $DeNO_x$ trap is located after the CRT device.

Use of fuel additives, particularly those based on CeO_2, is another area of interest [219]. Rhodia has introduced these additives on the market which now

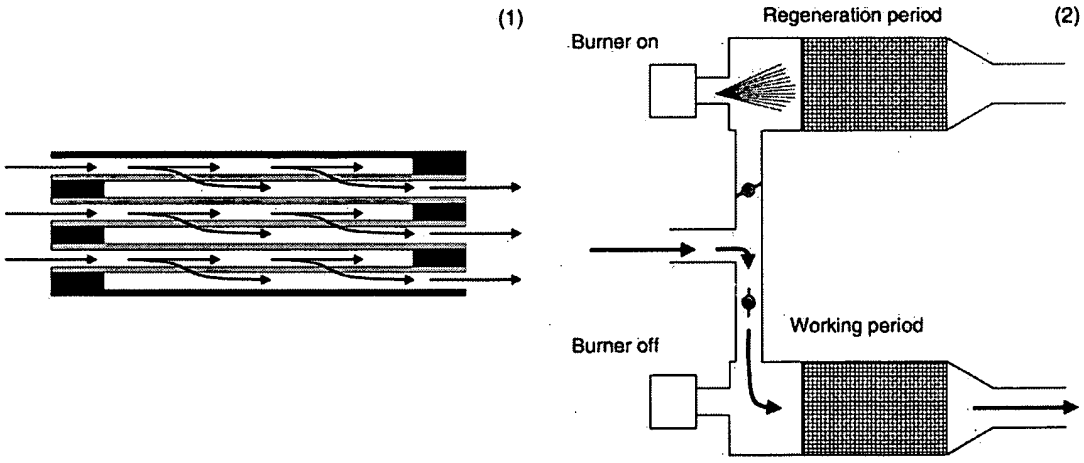

Fig. 23. Principle of filter operation (1) and filter re-generation (2) for a soot removal system, using fuel powered burners.

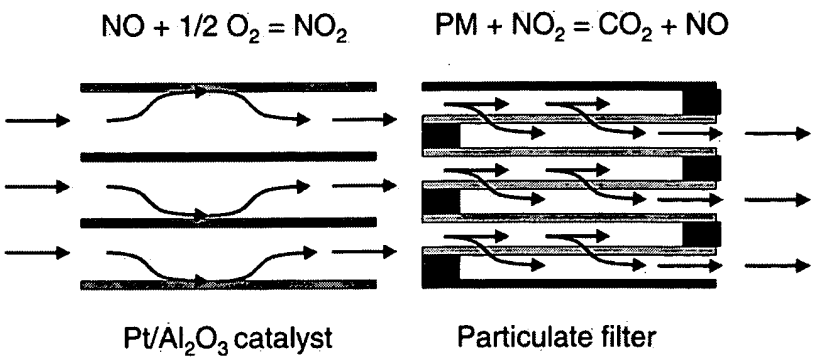

Fig. 24. The working principle of the continuously regenerating particulate trap.

have been applied in vehicles [217,218]. While there is a significant benefit in terms of promotion of the soot combustion from addition different additives even at very small concentrations [218], the environmental impact due the release of such additives into the atmosphere, following their widespread use, should be considered.

5. Conclusions

The development of automotive converters has proceeded by a continuous improvement of the catalytic performances and durability of the automotive catalysts over the past 25 years. Use of CeO_2–ZrO_2 technology represented a major improvement in terms of TWC durability in the last years, however, more and more demanding regulations are on the horizon. It is now clear that a TWC is a complex and integrated system that must be immediately effective and that its lifetime must be equivalent to that of the car. This demands new materials of extreme thermal stability, exceeding 1100 °C, which show extremely high conversions. The achievement of such targets require strong research efforts; a fundamental comprehension of the interactions between the NM and the other washcoat components and the deactivation phenomena is needed.

The requirements for more and more efficient engines highlights the problem of NO_x abatement under oxidising conditions. Even though huge efforts have been dedicated to development of lean-DeNO$_x$ catalysts, their durability and performances are still insufficient. Noticeably, of the different lean-DeNO$_x$ strategies for gasoline engines, the most effective and ready to use one is the so-called NSR concept which still uses a TWC to eliminate NO_x [112].

Technologies for control of particulate emissions from diesel engine will find increasing demand in the next years. In particular, catalytic filters will continue to be the subject of intense research.

Summarising, the end-of-pipe technologies for automotive pollution control, and in particular the TWC, have, and are, playing a key role in reducing air pollution. However, a new breakthrough point can be achieved only by adopting new strategies based more on prevention than on control. In this respect, it is important to highlight the great promise of hydrogen fuel cell technology [220]. The proton exchange membrane fuel cell—to make hydrogen from HCs—will be a major focus for research in electrocatalysis and catalytic fuel processing. It is worth noting that the targets obtained in the development of materials for TWCs constitutes an important scientific background for the design of new catalytic system for on-board hydrogen production. In fact, the on-board fuel reformer unit employs a number of catalytic steps involving reactions that routinely occur under the exhaust conditions and most of them appear to be promoted by the NM/CeO_2 interactions [13]. Consistently, M/CeO_2–ZrO_2 materials were reported to feature good activities for fuel reforming, WGS reaction and preferential CO oxidation [221–230]. However, further work is necessary to significantly enhance their performance, in order to obtain a miniaturisation of the system and therefore application in automobiles.

Acknowledgements

The authors gratefully thanks Dr. R. Di Monte, Prof. M. Graziani, University of Trieste, and Drs. P. Moles and C. Norman from MEL Chemicals for their valuable contribution to the development of the chemistry of CeO_2–ZrO_2 mixed oxides and helpful discussions. MEL Chemicals, University of Trieste, Fondo Trieste 1999, MURST-PRIN 2000 "Catalysis for the reduction of the environmental impact of mobile source emissions", CNR Agenzia 2000, INCA "Progetto Atmosfera Urbana" are gratefully acknowledged for financial support.

References

[1] J.C. Guibet, E. Faure-Birchem, Fuels and Engines: Technology, Energy, Environment, vol. 1, Editions Technip, Paris, 1999, pp. 1–385.
[2] R.J. Farrauto, R.M. Heck, Catal. Today 51 (1999) 351.
[3] M.L. Church, B.J. Cooper, P.J. Willson, SAE Paper 890815, 1989, p. 1.
[4] K.C. Taylor, Automobile catalytic converters, in: J.R. Anderson, M. Boudart (Eds.), Catalysis—Science and Technology, Springer, Berlin, 1984, Chapter 2, pp. 119–170.
[5] H. Bosch, Catal. Today 2 (1988) 369.
[6] K.C. Taylor, Catal. Rev.-Sci. Eng. 35 (1993) 457.
[7] M. Shelef, G.W. Graham, Catal. Rev.-Sci. Eng. 36 (1994) 433.
[8] M. Shelef, R.W. McCabe, Catal. Today 62 (2000) 35.
[9] P. Degobert, Automobiles and Pollution, Society of Automotive Engineers, Inc., Warrendale, PA, 1995.
[10] R.M. Heck, R.J. Farrauto, Catalytic Air Pollution Control: Commercial Technology, Van Nostrand Reinhold, New York, 1995, 1 pp.
[11] R.M. Heck, R.J. Farrauto, CATTECH 2 (1997) 117.
[12] A. Trovarelli, Catal. Rev.-Sci. Eng. 38 (1996) 439.
[13] J. Kaspar, M. Graziani, P. Fornasiero, Ceria-containing three way catalysts, in: K.A. Gschneidner Jr., L. Eyring (Eds.), Handbook on the Physics and Chemistry of Rare Earths: The Role of Rare Earths in Catalysis, Elsevier, Amsterdam, 2000, Chapter 184, pp. 159–267.
[14] M. Nuti, Emissions from Two-stroke Engines, Society of Automotive Engineers, Inc., Warrendale, PA, 1998, pp. 1–283.
[15] A. Walker, G. Chandler, J. Warren, C. Cooper, J. Harris, J. Thoss, A. Uusimeki, SAE Paper 01-0188, 2000.
[16] K.M. Adams, J.V. Cavataio, R.H. Hammerle, Appl. Catal. B 10 (1996) 157.
[17] M. Nonnenmann, SAE Paper 850131, 1985.
[18] S.T. Gulati, SAE Paper 850130, 1985.
[19] H. Bode (Ed.), Materials Aspects in Automotive Catalytic Converters, Wiley/VCH, Weinheim, Germany, 2002, pp. 1–281.
[20] S.T. Gulati, New developments in catalytic converter durability, in: A. Crucg (Ed.), Catalysis and Automotive Pollution Control, vol. II, Elsevier, Amsterdam, 1991, pp. 481–507.
[21] S. Eto, S. Yamamoto, Japan Patent N. JP-2000/26603 A2 155 9/5/2000.
[22] E.S.J. Lox, B.H. Engler, Environmental catalysis—mobile sources, in: G. Ertl, H. Knozinger, J. Weitkamp (Eds.), Environmental Catalysis, Wiley/VCH, Weinheim, Germany, 1999, Chapter 1, pp. 1–117.
[23] J.R. Anderson, Structure of Metallic Catalysts, Academic Press, London, 1975.
[24] F. Oudet, P. Courtine, A. Vejun, J. Catal. 114 (1988) 112.
[25] T. Horiuchi, Y. Teshima, T. Osaki, T. Sugiyama, K. Suzuki, T. Mori, Catal. Lett. 62 (1999) 107.
[26] F. Mizukami, K. Maeda, M. Watanabe, K. Masuda, T. Sano, K. Kuno, Preparation of thermostable high-surface-area aluminas and properties of the alumina-supported Pt catalysts, in: A. Crucg (Ed.), Catalysis and Automotive Pollution Control, vol. II, Elsevier, Amsterdam, 1991, pp. 557–568.
[27] L.L. Murrell, S.J. Tauster, Sols as precursors to transitional aluminas and these aluminas as host supports for CeO_2 and ZrO_2 microdomains, in: A. Crucg (Ed.), Catalysis and Automotive Pollution Control, vol. II, Elsevier, Amsterdam, 1991, pp. 547–555.
[28] N.A. Koryabkina, R.A. Shkrabina, V.A. Ushakov, M. Lausberg, F. Keptein, Z.R. Ismagilov, Kinet. Catal. 38 (1997) 112.
[29] Z.R. Ismagilov, R.A. Shkrabina, N.A. Koryabkina, D.A. Arendarskii, N.V. Shikina, Preparation of thermally stable washcoat aluminas for automotive catalysts, in: N. Kruse, A. Frennet, J.M. Bastin (Eds.), Catalysis and Automotive Pollution Control, vol. IV, Elsevier, Amsterdam, 1998, pp. 507–511.
[30] R. Di Monte, P. Fornasiero, J. Kaspar, M. Graziani, J.M. Gatica, S. Bernal, A. Gomez Herrero, Chem. Commun. (2000) 2167.
[31] A. Piras, A. Trovarelli, G. Dolcetti, Appl. Catal. B 28 (2000) L77.
[32] N.A. Koryabkina, R.A. Shkrabina, V.A. Ushakov, E.M. Moroz, M.F. Lansberg, Z.R. Ismagilov, Kinet. Catal. Engl. Transl. 37 (1996) 117.
[33] C. Morterra, G. Magnacca, V. Bolis, G. Cerrato, M. Barricco, A. Giachello, M. Fucale, Structural, morphological and surface chemical features of Al_2O_3 catalyst supports stabilized with CeO_2, in: A. Frennet, J.M. Bastin (Eds.), Catalysis and Automotive Pollution Control, vol. III, Elsevier, Amsterdam, 1995, pp. 361–373.
[34] C. Morterra, V. Bolis, G. Magnacca, J. Chem. Soc., Faraday Trans. 92 (1996) 1991.
[35] J.Z. Shyu, K. Otto, W.L.H. Watkins, G.W. Graham, R.K. Belitz, H.S. Gandhi, J. Catal. 114 (1988) 23.
[36] J.Z. Shyu, W.H. Weber, H.S. Gandhi, J. Phys. Chem. 92 (1988) 4964.
[37] J.M. Dominguez, J.L. Hernandez, G. Sandoval, Appl. Catal. A 197 (2000) 119.

[38] H.S. Gandhi, A.G. Piken, M. Shelef, R.G. Delosh, SAE Paper 760201, 1976, p. 55.
[39] M. Sideris, Methods for Monitoring and Diagnosing the Efficiency of Catalytic Converters: A Patent Oriented Survey, vol. 115, Elsevier, Amsterdam, 1997.
[40] J. Kaspar, P. Fornasiero, M. Graziani, Catal. Today 50 (1999) 285.
[41] R.W. McCabe, H.W. Jen, W. Chun, G.W. Graham, L.P. Haack, A. Straccia, D. Benson, Appl. Catal. A 184 (1999) 265.
[42] J.P. Cuif, G. Blanchard, O. Touret, A. Seigneurin, M. Marczi, E. Quémeré, SAE Paper 970463, 1997.
[43] W.D. Kingery, H.K. Bowen, D.R. Uhlmann, Grain growth, sintering and vitrification, in: Introduction to Ceramics, vol. 2, Wiley, New York, 1976, Chapter 10, pp. 448–515.
[44] D. Terribile, A. Trovarelli, J. Llorca, C. de Leitenburg, G. Dolcetti, Catal. Today 43 (1998) 79.
[45] C.E. Hori, H. Permana, K.Y.S. Ng, A. Brenner, K. More, K.M. Rahmoeller, D.N. Belton, Appl. Catal. B 16 (1998) 105.
[46] G.W. Graham, C.L. Roe, L.P. Haack, A.M. Straccia, J. Vac. Sci. Technol. A 18 (2000) 1093.
[47] P. Duwez, F. Odell, J. Am. Ceram. Soc. 33 (1950) 274.
[48] A.I. Leonov, E.K. Keler, A.B. Andreeva, Ogneupory 3 (1966) 42.
[49] A.I. Leonov, A.B. Andreeva, E.K. Keler, Izv. Akad. Nauk SSSR Neorg. Mater. 2 (1966) 137.
[50] E. Tani, M. Yoshimura, S. Somiya, J. Am. Ceram. Soc. 66 (1983) 506.
[51] G. Colon, M. Pijolat, F. Valdivieso, H. Vidal, J. Kaspar, E. Finocchio, M. Daturi, C. Binet, J.C. Lavalley, R.T. Baker, S. Bernal, J. Chem. Soc., Faraday Trans. 94 (1998) 3717.
[52] G. Colon, F. Valdivieso, M. Pijolat, R.T. Baker, J.J. Calvino, S. Bernal, Catal. Today 50 (1999) 271.
[53] T. Settu, R. Gobinathan, J. Eur. Ceram. Soc. 16 (1996) 1309.
[54] P. Vidmar, P. Fornasiero, J. Kaspar, G. Gubitosa, M. Graziani, J. Catal. 171 (1997) 160.
[55] G.L. Markaryan, L.N. Ikryannikova, G.P. Muravieva, A.O. Turakulova, B.G. Kostyuk, E.V. Lunina, V.V. Lunin, E. Zhilinskaya, A. Aboukais, Colloid Surf. A 151 (1999) 435.
[56] C.K. Narula, L.P. Haack, W. Chun, H.W. Jen, G.W. Graham, J. Phys. Chem. B 103 (1999) 3634.
[57] D. Terribile, A. Trovarelli, C. de Leitenburg, A. Primavera, G. Dolcetti, Catal. Today 47 (1999) 133.
[58] L.N. Ikryannikova, A.A. Aksenov, G.L. Markaryan, G.P. Muraveva, B.G. Kostyuk, A.N. Kharlanov, E.V. Lunina, Appl. Catal. A 210 (2001) 225.
[59] V. Perrichon, A. Laachir, S. Abouarnadasse, O. Touret, G. Blanchard, Appl. Catal. A 129 (1995) 69.
[60] G. Ranga Rao, J. Kaspar, R. Di Monte, S. Meriani, M. Graziani, Catal. Lett. 24 (1994) 107.
[61] P. Fornasiero, R. Di Monte, G. Ranga Rao, J. Kaspar, S. Meriani, A. Trovarelli, M. Graziani, J. Catal. 151 (1995) 168.
[62] G. Vlaic, P. Fornasiero, S. Geremia, J. Kaspar, M. Graziani, J. Catal. 168 (1997) 386.
[63] G. Balducci, J. Kaspar, P. Fornasiero, M. Graziani, M.S. Islam, J. Phys. Chem. B 102 (1998) 557.
[64] G. Balducci, M.S. Islam, J. Kaspar, P. Fornasiero, M. Graziani, Chem. Mater. 12 (2000) 677.
[65] G. Balducci, P. Fornasiero, R. Di Monte, J. Kaspar, S. Meriani, M. Graziani, Catal. Lett. 33 (1995) 193.
[66] N. Izu, T. Omata, S. Otsuka-Yao-Matsuo, J. Alloys Comp. 270 (1998) 107.
[67] R.T. Baker, S. Bernal, G. Blanco, A.M. Cordon, J.M. Pintado, J.M. Rodriguez-Izquierdo, F. Fally, V. Perrichon, Chem. Commun. (1999) 149.
[68] P. Fornasiero, J. Kaspar, M. Graziani, Appl. Catal. B 22 (1999) L11.
[69] M. Boaro, C. de Leitenburg, G. Dolcetti, A. Trovarelli, J. Catal. 193 (2000) 338.
[70] M. Yashima, H. Arashi, M. Kakihana, M. Yoshimura, J. Am. Ceram. Soc. 77 (1994) 1067.
[71] H.C. Yao, Y.F. Yu Yao, J. Catal. 86 (1984) 254.
[72] N. Hickey, P. Fornasiero, R. Di Monte, J. Kaspar, M. Graziani, G. Dolcetti, Catal. Lett. 72 (2001) 45.
[73] J. Kaspar, R. Di Monte, P. Fornasiero, M. Graziani, H. Bradshaw, C. Norman, Top. Catal. 16 (2001) 83.
[74] S.H. Oh, G.B. Fisher, J.E. Carpenter, D.W. Goodman, J. Catal. 100 (1986) 360.
[75] K.C. Taylor, J.C. Schlatter, J. Catal. 63 (1980) 53.
[76] B.K. Cho, J. Catal. 138 (1992) 255.
[77] B.K. Cho, J. Catal. 148 (1994) 697.
[78] R.W. McCabe, J.M. Kisenyi, Chem. Ind. London (1995) 605.
[79] J.C. Summers, W.B. Williamson, Palladium-only catalysts for closed-loop control, in: J.N. Armor (Ed.), Environmental Catalysis, American Chemical Society, Washington, DC, 1994, Chapter 9, pp. 95–113.
[80] D.D. Beck, J.W. Sommers, C.L. DiMaggio, Appl. Catal. B 11 (1997) 273.
[81] G.W. Graham, H.W. Jen, W. Chun, R.W. McCabe, J. Catal. 182 (1999) 228.
[82] M. Boaro, C. deLeitenburg, G. Dolcetti, A. Trovarelli, M. Graziani, Top. Catal. 16 (2001) 299.
[83] X.M. Song, A. Sayari, Catal. Rev.-Sci. Eng. 38 (1996) 329.
[84] A. Trovarelli, C. de Leitenburg, M. Boaro, G. Dolcetti, Catal. Today 50 (1999) 353.
[85] M. Waqif, P. Bazin, O. Saur, J.C. Lavalley, G. Blanchard, O. Touret, Appl. Catal. B 11 (1997) 193.
[86] S.H. Overbury, D.R. Mullins, D.R. Huntley, L. Kundakovic, J. Phys. Chem. B 103 (1999) 11308.
[87] A.E. Nelson, J. Yip, K.H. Schulz, Appl. Catal. B 30 (2001) 375.
[88] A.F. Diwell, R.R. Rajaram, H.A. Shaw, T.J. Truex, The role of ceria in three-way catalysts, in: A. Crucg (Ed.), Catalysis and Automotive Pollution Control, vol. II, Elsevier, Amsterdam, 1991, pp. 139–152.
[89] P. Bazin, O. Saur, J.C. Lavalley, G. Blanchard, V. Visciglio, O. Touret, Appl. Catal. B 13 (1997) 265.
[90] S. Hilaire, S. Sharma, R.J. Gorte, J.M. Vohs, H.W. Jen, Catal. Lett. 70 (2000) 131.
[91] T. Luo, J.M. Vohs, R.J. Gorte, J. Catal. 210 (2002) 397.
[92] R.M. Heck, R.J. Farrauto, Appl. Catal. A 221 (2001) 443.

[93] D.S. Lafyatis, G.P. Ansell, S.C. Bennett, J.C. Frost, P.J. Millington, R.R. Rajaram, A.P. Walker, T.H. Ballinger, Appl. Catal. B 18 (1998) 123.
[94] A.L. Boehman, S. Niksa, Appl. Catal. B 8 (1996) 41.
[95] J. Kaspar, P. Fornasiero, J. Solid State Chem. (2002), in press.
[96] M. Haruta, N. Yamada, T. Kobayashi, S. Iijima, J. Catal. 115 (1989) 301.
[97] M. Haruta, M. Date, Appl. Catal. A 222 (2001) 427.
[98] L.A. Petrov, Stud. Surf. Sci. Catal. C 130 (2000) 2345.
[99] J.R. Mellor, A. Palazov, B.S. Grigorova, J.F. Greyling, K. Reddy, M.P. Letsoalo, J.H. Marsh, Catal. Today 72 (2002) 145.
[100] S. Golunski, R. Rajaram, N. Hodge, G.J. Hutchings, C.J. Kiely, Catal. Today 72 (2002) 107.
[101] G.C. Bond, D.T. Thompson, Catal. Rev.-Sci. Eng. 41 (1999) 319.
[102] M. Iwamoto, H. Hamada, Catal. Today 10 (1991) 57.
[103] M. Shelef, Chem. Rev. 95 (1995) 209.
[104] K.A. Bethke, M.C. Kung, B. Yang, M. Shah, D. Alt, C. Li, H.H. Kung, Catal. Today 26 (1995) 169.
[105] J.N. Armor, Catal. Today 26 (1995) 147.
[106] Y. Traa, B. Burger, J. Weitkamp, Micropor. Mesopor. Mater. 30 (1999) 3.
[107] T.J. Truex, R.A. Searles, D.C. Sun, Plat. Met. Rev. 36 (1992) 2.
[108] J.N. Armor, Mobile engine emission control: an overview, in: J.N. Armor (Ed.), Environmental Catalysis, American Chemical Society, Washington, DC, 1994, Chapter 8, pp. 90–93.
[109] M.D. Amiridis, T.J. Zhang, R.J. Farrauto, Appl. Catal. B 10 (1996) 203.
[110] T. Kreuzer, E.S. Lox, D. Lindner, J. Leyrer, Catal. Today 29 (1996) 17.
[111] P. Zelenka, W. Cartellieri, P. Herzog, Appl. Catal. B 10 (1996) 3.
[112] A. Fritz, V. Pitchon, Appl. Catal. B 13 (1997) 1.
[113] P. Gilot, M. Guyon, B.R. Stanmore, Fuel 76 (1997) 507.
[114] H. Akama, K. Matsushita, Catal. Surv. Jpn. 3 (1999) 139.
[115] D.N. Belton, K.C. Taylor, Curr. Opin. Solid State Mater. Sci. 4 (1999) 97.
[116] M. Misono, T. Inui, Catal. Today 51 (1999) 369.
[117] The impact of sulfur in diesel fuel on catalyst emission control strategy, Report by Manufacturers of Emissions Controls Association, March 15, 1999, pp. 1–25.
[118] R. Burch, T.C. Watling, Catal. Lett. 37 (1996) 51.
[119] R. Burch, D. Ottery, Appl. Catal. B 9 (1996) L19.
[120] R. Burch, P.J. Millington, Catal. Today 29 (1996) 37.
[121] R. Burch, T.C. Watling, Catal. Lett. 43 (1997) 19.
[122] R. Burch, D. Ottery, Appl. Catal. B 13 (1997) 105.
[123] R. Burch, T.C. Watling, J. Catal. 169 (1997) 45.
[124] R. Burch, T.C. Watling, Appl. Catal. B 11 (1997) 207.
[125] R. Burch, J.A. Sullivan, T.C. Watling, Catal. Today 42 (1998) 13.
[126] R. Burch, P. Fornasiero, B.W.L. Southward, Chem. Commun. (1998) 625.
[127] R. Burch, P. Fornasiero, T.C. Watling, J. Catal. 176 (1998) 204.
[128] R. Burch, T.C. Watling, Appl. Catal. B 17 (1998) 131.
[129] R. Burch, E. Halpin, M. Hayes, K. Ruth, J.A. Sullivan, Appl. Catal. B 19 (1998) 199.
[130] R. Burch, P. Fornasiero, B.W.L. Southward, Chem. Commun. (1998) 739.
[131] R. Burch, P. Fornasiero, B.W.L. Southward, J. Catal. 182 (1999) 234.
[132] R. Burch, A.A. Shestov, J.A. Sullivan, J. Catal. 188 (1999) 69.
[133] R. Burch, J.A. Sullivan, J. Catal. 182 (1999) 489.
[134] R. Burch, A.A. Shestov, J.A. Sullivan, J. Catal. 186 (1999) 353.
[135] R. Burch, A.A. Shestov, J.A. Sullivan, J. Catal. 182 (1999) 497.
[136] A.A. Shestov, R. Burch, J.A. Sullivan, J. Catal. 186 (1999) 362.
[137] F.C. Meunier, J.P. Breen, V. Zuzaniuk, M. Olsson, J.R.H. Ross, J. Catal. 187 (1999) 493.
[138] B.K. Cho, J. Catal. 131 (1991) 74.
[139] J. Kaspar, C. de Leitenburg, P. Fornasiero, A. Trovarelli, M. Graziani, J. Catal. 146 (1994) 136.
[140] K.L. Roberts, M.D. Amiridis, Ind. Eng. Chem. Res. 36 (1997) 3528.
[141] A.A. Nikolopoulos, E.S. Stergioula, E.A. Efthimiadis, I.A. Vasalos, Catal. Today 54 (1999) 439.
[142] B.H. Engler, J. Leyrer, E.S. Lox, K. Ostgathe, Catalytic reduction of nitrogen oxides in diesel exhaust gas, in: A. Frennet, J.M. Bastin (Eds.), Catalysis and Automotive Pollution Control, vol. III, Elsevier, Amsterdam, 1995, pp. 529–547.
[143] V. Pitchon, A. Fritz, J. Catal. 186 (1999) 64.
[144] G.R. Bamwenda, A. Ogata, A. Obuchi, J. Oi, K. Mizuno, J. Skrzypek, Appl. Catal. B 6 (1995) 311.
[145] M. Inaba, Y. Kintaichi, H. Hamada, Catal. Lett. 36 (1996) 223.
[146] E. Guglielminotti, F. Boccuzzi, Appl. Catal. B 8 (1996) 375.
[147] J. Pasel, V. Speer, C. Albrecht, F. Richter, H. Papp, Appl. Catal. B 25 (2000) 105.
[148] G. Delahay, B. Coq, E. Ensuque, F. Figueras, Catal. Lett. 39 (1996) 105.
[149] Y. Liu, B. Zhong, S.Y. Peng, Q. Wang, T.D. Hu, Y.N. Xie, X. Ju, Catal. Today 30 (1996) 177.
[150] Y. Okamoto, H. Gotoh, H. Aritani, T. Tanaka, S. Yoshida, J. Chem. Soc., Faraday Trans. 93 (1997) 3879.
[151] Y. Okamoto, H. Gotoh, Catal. Today 36 (1997) 71.
[152] G. Delahay, E. Ensuque, B. Coq, F. Figueras, J. Catal. 175 (1998) 7.
[153] Y. Okamoto, T. Kubota, H. Gotoh, Y. Ohto, H. Aritani, T. Tanaka, S. Yoshida, J. Chem. Soc., Faraday Trans. 94 (1998) 3743.
[154] H. Aritani, S. Kawaguchi, T. Yamamoto, T. Tanaka, Y. Okamoto, S. Imamura, Chem. Lett. (2000) 532.
[155] A. Obuchi, I. Kaneko, J. Oi, A. Ohi, A. Ogata, G.R. Bamwenda, S. Kushiyama, Appl. Catal. B 15 (1998) 37.
[156] A. Abe, N. Aoyama, S. Sumiya, N. Kakuta, K. Yoshida, Catal. Lett. 51 (1998) 5.
[157] S. Kameoka, T. Chafik, Y. Ukisu, T. Miyadera, Catal. Lett. 51 (1998) 11.

[158] S. Kameoka, Y. Ukisu, T. Miyadera, Phys. Chem. Chem. Phys. 2 (2000) 367.
[159] M.F. Luo, X.X. Yuan, X.M. Zheng, Appl. Catal. A 175 (1998) 121.
[160] Y. Murata, S. Satokawa, K.I. Yamaseki, H. Yamamoto, H. Uchida, M. Yahagi, H. Yokota, AES 39 (1999) 447.
[161] S. Satokawa, Chem. Lett. (2000) 294.
[162] F.C. Meunier, J.P. Breen, J.R.H. Ross, Chem. Commun. (1999) 259.
[163] F.C. Meunier, V. Zuzaniuk, J.P. Breen, M. Olsson, J.R.H. Ross, Catal. Today 59 (2000) 287.
[164] F.C. Meunier, J.R.H. Ross, Appl. Catal. B 24 (2000) 23.
[165] V. Zuzaniuk, F.C. Meunier, J.R.H. Ross, Chem. Commun. (1999) 815.
[166] K.A. Bethke, H.H. Kung, J. Catal. 172 (1997) 93.
[167] T. Nakatsuji, T. Yasukawa, K. Tabata, K. Ueda, Assignee: JP 10244155 A2 (Issued: September 14, 1998); Priority: JP 97 47993 (Appl. Date: March 3, 1997), Sakai Chemical Industry Co. Ltd.
[168] E. Seker, J. Cavataio, E. Gulari, P. Lorpongpaiboon, S. Osuwan, Appl. Catal. A 183 (1999) 121.
[169] R.J. Farrauto, R.M. Heck, Catal. Today 55 (2000) 179.
[170] S. Naito, Y. Tanaka, Stud. Surf. Sci. Catal. 101 (1998) 1115.
[171] Q.W. Zhang, J. Li, X.X. Liu, Q.M. Zhu, Appl. Catal. A 197 (2000) 221.
[172] J.N. Hickey, P. Fornasiero, J. Kaspar, M. Graziani, G. Martra, S. Coluccia, S. Biella, L. Prati, M. Rossi, J. Catal. 209 (2002) 271.
[173] M. Misono, CATTECH 2 (1998) 53.
[174] T. Inui, S. Iwamoto, K. Matsuba, Y. Tanaka, Y. Yoshida, Catal. Today 26 (1995) 23.
[175] C. Rottlander, R. Andorf, C. Plog, B. Krutzsch, M. Baerns, Appl. Catal. B 11 (1996) 49.
[176] M. Iwamoto, H. Yahiro, H.K. Shin, M. Watanabe, J. Guo, M. Konno, T. Chikahisa, T. Murayama, Appl. Catal. B 5 (1994) L1.
[177] B.J. Adelman, W.M.H. Sachtler, Appl. Catal. B 14 (1997) 1.
[178] A. Ali, W. Alvarez, C.J. Loughran, D.E. Resasco, Appl. Catal. B 14 (1997) 13.
[179] H. Ohtsuka, T. Tabata, Appl. Catal. B 21 (1999) 133.
[180] H. Ohtsuka, T. Tabata, Appl. Catal. B 26 (2000) 275.
[181] S. Matsumoto, H. Watanabe, T. Tanaka, A. Isogai, K. Kasahara, Nippon Kagaku Kaishi 12 (1996) 997.
[182] N. Takahashi, H. Shinjoh, T. Iijima, T. Suzuki, K. Yamazaki, K. Yokota, H. Suzuki, N. Miyoshi, S. Matsumoto, T. Tanizawa, T. Tanaka, S. Tateishi, K. Kasahara, Catal. Today 27 (1996) 63.
[183] H. Shinjoh, N. Takahashi, K. Yokota, M. Sugiura, Appl. Catal. B 15 (1998) 189.
[184] S. Hodjati, P. Bernhardt, C. Petit, V. Pitchon, A. Kiennemann, Appl. Catal. B 19 (1998) 209.
[185] S. Hodjati, P. Bernhardt, C. Petit, V. Pitchon, A. Kiennemann, Appl. Catal. B 19 (1998) 221.
[186] S. Hodjati, C. Petit, V. Pitchon, A. Kiennemann, Appl. Catal. B 27 (2000) 117.
[187] H. Mahzoul, J.F. Brilhac, P. Gilot, Appl. Catal. B 20 (1999) 47.
[188] A. Amberntsson, H. Persson, P. Engstrom, B. Kasemo, Appl. Catal. B 31 (2001) 27.
[189] S. Balcon, C. Potvin, L. Salin, J.F. Tempere, G. Djega-Mariadassou, Catal. Lett. 60 (1999) 39.
[190] E. Fridell, M. Skoglundh, B. Westerberg, S. Johansson, G. Smedler, J. Catal. 183 (1999) 196.
[191] E. Fridell, H. Persson, B. Westerberg, L. Olsson, M. Skoglundh, Catal. Lett. 66 (2000) 71.
[192] E. Fridell, H. Persson, L. Olsson, B. Westerberg, A. Amberntsson, M. Skoglundh, Top. Catal. 16 (2001) 133.
[193] P.H. Han, Y.K. Lee, S.M. Han, H.K. Rhee, Top. Catal. 16 (2001) 165.
[194] L. Lietti, P. Forzatti, I. Nova, E. Tronconi, J. Catal. 204 (2001) 175.
[195] F. Prinetto, G. Ghiotti, I. Nova, L. Lietti, E. Tronconi, P. Forzatti, J. Phys. Chem. B 105 (2001) 12732.
[196] F. Rodrigues, L. Juste, C. Potvin, J.F. Tempere, G. Blanchard, G. Djega-Mariadassou, Catal. Lett. 72 (2001) 59.
[197] P.J. Schmitz, R.J. Baird, J. Phys. Chem. B 106 (2002) 4172.
[198] P. Engstrom, A. Amberntsson, M. Skoglundh, E. Fridell, G. Smedler, Appl. Catal. B 22 (1999) L241.
[199] U. Gobel, J. Hohne, E.S. Lox, W. Muller, A. Okumura, W. Strehlau, M. Hori, SAE Paper 99FL-103, 1999.
[200] H. Hirata, I. Hachisuka, Y. Ikeda, S. Tsuji, S. Matsumoto, Top. Catal. 16 (2001) 145.
[201] S. Matsumoto, Y. Ikeda, H. Suzuki, M. Ogai, N. Miyoshi, Appl. Catal. B 25 (2000) 115.
[202] J.R. Asik, D.A. Dobson, G.M. Meyer, Soc. Automot. Eng. SP-1573 (2001) 111.
[203] B.H. Jang, T.H. Yeon, H.S. Han, Y.K. Park, J.E. Yie, Catal. Lett. 77 (2001) 21.
[204] S. Hodjati, K. Vaezzadeh, C. Petit, V. Pitchon, A. Kiennemann, Appl. Catal. B 26 (2000) 5.
[205] K. Nakatani, S. Hirota, S. Takeshima, K. Itoh, K. Tanaka, K. Dohmae, Soc. Automot. Eng. SP-1674 (2002) 57.
[206] P. Forzatti, Appl. Catal. A 222 (2001) 221.
[207] B. Amon, G. Keefe, Soc. Automot. Eng. SP-1626 (2001) 1.
[208] B. Amon, S. Fischer, L. Hofmann, R. Zurbig, Top. Catal. 16 (2001) 187.
[209] R. van Helden, M. van Genderen, M. van Aken, R. Verbeek, J.A. Patchett, J. Kruithof, T. Straten, C. Gerentet de Saluneaux, Soc. Automot. Eng. SP-1674 (2002) 15.
[210] T.V. Johnson, Soc. Automot. Eng. SP-1581 (2001) 23.
[211] S.M. Choi, Y.K. Yoon, S.J. Kim, G.K. Yeo, H.S. Han, Soc. Automot. Eng. SP-1581 (2001) 171.
[212] R.J. Farrauto, K.E. Voss, Appl. Catal. B 10 (1996) 29.
[213] J.C. Clerc, Appl. Catal. B 10 (1996) 99.
[214] B.A.A.L. van Setten, M. Makkee, J.A. Moulijn, Catal. Rev.-Sci. Eng. 43 (2001) 489.
[215] P. Ciambelli, P. Corbo, V. Palma, P. Russo, S. Vaccaro, B. Vaglieco, Top. Catal. 16 (2001) 279.
[216] R. Allansson, P.G. Blakeman, B.J. Cooper, H. Hess, P.J. Silcock, A.P. Walker, SAE Paper SP-1673, 2002, 2002-01-428.
[217] E. AbiAad, R. Cousin, C. Pruvost, D. Courcot, R. Noirot, C. Rigaudeau, A. Aboukais, Top. Catal. 16 (2001) 263.
[218] S.J. Jelles, M. Makkee, J.A. Moulijn, Top. Catal. 16 (2001) 269.

[219] J.C. Summers, S. VanHoutte, D. Psaras, Appl. Catal. B 10 (1996) 139.
[220] D.L. Trimm, Z.I. Onsan, Catal. Rev.-Sci. Eng. 43 (2001) 31.
[221] G. Avgouropoulos, T. Ioannides, H.K. Matralis, J. Batista, S. Hocevar, Catal. Lett. 73 (2001) 33.
[222] I.H. Son, A.M. Lane, Catal. Lett. 76 (2001) 151.
[223] L. Basini, A. Guarinoni, A. Aragno, J. Catal. 190 (2000) 284.
[224] W.S. Dong, K.W. Jun, H.S. Roh, Z.W. Liu, S.E. Park, Catal. Lett. 78 (2002) 215.
[225] P. Pantu, K. Kim, G.R. Gavalas, Appl. Catal. A 193 (2000) 203.
[226] T. Bunluesin, R.J. Gorte, G.W. Graham, Appl. Catal. B 15 (1998) 107.
[227] J.A. Montoya, E. RomeroPascual, C. Gimon, P. DelAngel, A. Monzon, Catal. Today 63 (2000) 71.
[228] Q. Fu, A. Weber, M. Flytzani-Stephanopoulos, Catal. Lett. 77 (2001) 87.
[229] K. Li, Q. Fu, M. Flytzani-Stephanopoulos, Appl. Catal. B 27 (2000) 179.
[230] T.L. Zhu, M. Flytzani-Stephanopoulos, Appl. Catal. A 208 (2001) 403.
[231] P. Ciambelli, P. Corbo, M. Gambino, G. Minelli, G. Moretti, P. Porta, Catal. Today 26 (1995) 33.

Catalysis Letters 70 (2000) 35–41

The role of lanthanum oxide on Pd-only three-way catalysts prepared by co-impregnation and sequential impregnation methods

Do Heui Kim [a], Seong Ihl Woo [a,*], Jin Man Lee [b] and O-Bong Yang [b]

[a] *Department of Chemical Engineering, Korea Advanced Institute of Science and Technology, Taejon 305-701, Korea*
E-mail: siwoo@mail.kaist.ac.kr

[b] *School of Chemical Engineering and Technology, Chonbuk National University, Chonju, Chonbuk 561-756, Korea*

Received 22 March 2000; accepted 20 September 2000

The effect of lanthanum oxides on the catalytic performance and the physicochemical properties of Pd-only three-way catalysts prepared by co-impregnation and sequential impregnation methods was studied by using hydrogen chemisorption, BET surface area, X-ray diffraction and X-ray photoelectron spectroscopy. It was found that the roles of La closely depended on the order of La introduction in the preparation of the Pd catalysts. Pd–La/Al_2O_3 prepared by co-impregnation of La and Pd, kept its superior activity in spite of the significant loss of surface area of the alumina support after thermal aging at 1273 K, indicating that the primary role of La was a Pd stabilizer through the intimate interaction between La and Pd. However, on $Pd/La/Al_2O_3$, in which Pd was consecutively impregnated after the impregnation of La, La preferentially interacted with the alumina support as a form of $La_xAl_yO_2$, resulting in the stabilization of the alumina support during thermal aging. XPS results indicated that lanthanum oxide suppressed the formation of PdO interacting with alumina during thermal aging. In the case of $Pd/La–Ce/Al_2O_3$, the formation of the solid solution of $(Ce_xLa_{1-x})O_2$ was not strong enough to maintain the high activity and the good textural property after thermal aging.

Keywords: Pd-only three-way catalyst, lanthanum oxide, cerium oxide, co-impregnation, XPS, XRD, thermal aging

1. Introduction

Palladium as an active metal in a three-way catalyst (TWC) has been known to have a good resistance to thermal sintering, a lower price than Rh and a higher activity for the oxidation of hydrocarbons and CO [1]. Pd-only TWC has been intensively studied as a new generation three-way catalyst even in applications where catalyst temperature occasionally reaches 1273 K [2]. However, Pd-only TWC shows a relatively low activity for the NO removal in oxygen-rich conditions. It is well known that the Rh component in the conventional Pt/Rh catalyst is responsible for that role [3]. Lanthanide oxides such as La and Ce [4], and base metal oxides such as Co, Ba and Zr [5–8] have been used as promoters to improve the catalytic activity of Pd-only TWC. Especially La_2O_3 is known to act as a good promoter to increase the dispersion and the thermal stability [9], and improve the oxidation activity of Pd [10]. In addition, CeO_2 plays an important role as an oxygen storage capacitor (OSC) which stores the oxygen during lean conditions and releases it during rich conditions [11], provides the activity for water–gas shift reaction [12], maintains the dispersion of the catalytic active metals [13,14], and stabilizes the surface area of the alumina washcoat [15,16].

There are a few reports on the interaction between Al_2O_3 and the lanthanide oxides. Shyu et al. [17] reported that the reaction between CeO_2 and Al_2O_3 which transformed CeO_2 into other more stable compounds, $CeAlO_3$, under high temperature reducing conditions was expected to adversely affect the OSC by fixing one oxidation state. To avoid such effects, La^{3+} as an Al_2O_3 modifier was introduced to block the reaction between Al_2O_3 and CeO_2. Graham et al. [18] postulated that $CeO_2/La_2O_3/Al_2O_3$ showed a higher CeO_2 dispersion and a greater OSC of the CeO_2 than co-impregnated $(CeO_2 + La_2O_3)/Al_2O_3$ and $La_2O_3/CeO_2/Al_2O_3$ from the XPS results. Shelef et al. [19] showed in a model catalyst study that the presence of lanthanum oxide in the films inhibited the reduction of cerium oxide partially. In practice, the thermal stability of the TWC is very important for its commercial application. The physicochemical properties of lanthanum-modified Al_2O_3 as a function of the amount of La were investigated by XPS and CO_2 absorption [20]. As a result, a consequence of the high calcination temperature of 925 °C facilitated the diffusion of surface lanthanum into the alumina bulk to form $LaAlO_3$. Likewise, the roles of La have been focused on the enhanced thermal stability of the Al_2O_3 support or the increased OSC of the catalyst containing cerium oxide.

Co-impregnation has been known as a catalyst preparation method with a view to forming bimetallic particles [21]. Although co-impregnated Pd–Pt [21] and Pd–Rh [22] catalysts were reported for hydrocarbon oxidation and NO reduction, respectively, there is, to our knowledge, no result about the co-impregnation effect of Pd and La in the three-way catalytic reaction. Since the strong metal–support interaction is well known in Pd/La_2O_3 [23], an intimate interaction of Pd and lanthanum oxide arising from co-impregnation is expected to result in a catalyst with a novel activity. In this work, the role and the effect of La

* To whom correspondence should be addressed.

and Ce oxides on the catalytic performance and the physicochemical properties of Pd-only TWC as a function of impregnation mode were investigated by three-way catalytic reaction, X-ray photoelectron spectroscopy (XPS), X-ray diffraction (XRD), BET and hydrogen chemisorption. To elucidate the role of lanthanum oxide, the physicochemical properties of a co-impregnated Pd–La/Al_2O_3 and a successively loaded Pd/La/Al_2O_3 were compared.

2. Experimental

2.1. Catalyst preparation

All the catalysts were prepared by a wet impregnation method. The γ-Al_2O_3 support (Nishio Co., Japan) has a packed density of 0.60 g/cm^3, BET surface area of 160 m^2/g and particle size of 20–70 mesh. Nitrate forms of Pd, Ce and La were used as precursors. The metal loadings of Pd, La and Ce are 1, 3 and 5 wt%, respectively, if the number in the bracket is not described. After impregnation of La or/and Ce precursors on γ-Al_2O_3 followed by drying and calcination, Pd was consecutively impregnated for the preparation of promoted catalysts denoted as Pd/La/Al_2O_3, Pd/Ce/Al_2O_3 and Pd/Ce–La/Al_2O_3. In comparison with Pd/La/Al_2O_3, the catalyst designated as Pd–La/Al_2O_3 was prepared by co-impregnation of La and Pd precursor simultaneously. All the catalysts calcined at 873 K with air stream for 3 h were called as "fresh" catalyst. In addition, "aged" catalyst was obtained by treating the fresh catalyst at 1273 K with air stream for 10 h.

2.2. Three-way catalytic performance test

The three-way catalytic reaction was carried out at stoichiometric air/fuel ratio (14.7) and gas hourly space velocity of 72 000 h^{-1} (400 cm^3/min) in a continuous U-tube quartz reactor with simulated exhaust gas containing 6000 ppm CO, 1500 ppm NO, 500 ppm C_3H_6, 3000 ppm H_2, 6000 ppm O_2 and 13% H_2O in N_2 balance. The reactant and product gases were analyzed by a gas chromatograph (DS6200, DONAM Systems, Korea) equipped with a thermal conductivity detector for CO and a flame ionization detector for C_3H_6, and by a chemiluminescence NO_x analyzer (42H, Thermo Environmental Instruments, Inc., USA). The reaction data were measured at a desired temperature after treating the catalyst with air stream at 773 K.

2.3. Catalyst characterization

BET surface area of a catalyst was obtained from the nitrogen adsorption isotherm at 77 K in a Micromeritics ASAP 2010C analyzer. Before the measurements, all the samples were degassed to 10^{-4} Torr. For the hydrogen chemisorption, the total and reversible adsorption isotherms of hydrogen were obtained with a sample of 0.3 g at 373 K after degassing the pre-adsorbed hydrogen at 673 K and 1×10^{-5} Torr for 2 h in the same apparatus. The difference between total and reversible adsorption isotherm corresponded to the amount of hydrogen atoms chemisorbed irreversibly and reported herein. XRD experiment was performed with the target of Cu Kα (λ = 1.540598 Å) operated at 40 kV and 45 mA with a scan speed of 4°/min. XPS spectra were taken in a surface analysis chamber (LHS-10; SPECS GmbH, Germany). X-ray (Al Kα, 1486.6 eV) radiated at a power of 300 W (30 mA, 10 kV). The kinetic energy of an ejected electron was analyzed by a multiple channel detector in a hemispherical energy analyzer. The pass energy was 98 eV and the base pressure of the analysis chamber was 8×10^{-10} Torr. Energy shifts of binding energy occurred due to the electron charging effect. Each spectrum was calibrated using the peak of C 1s (284.6 eV) as a standard. The accuracy of the spectrum was ±0.2 eV. Data smoothing, subtraction of background (Shirley method), and the curve fitting (Voigt ratio 30) were taken with SPECTRA software from SPECS GmbH. The relative atomic sensitivity factor (La 3d: 9.122, Ce 3d: 8.808, Al 2p: 0.234, Pd 3d: 5.356) was obtained from [24].

3. Results

3.1. Three-way catalytic performance test

Table 1 shows the light-off temperature in which the conversion reaches 50% (T_{50}, °C) for NO, CO and C_3H_6 on various catalysts. Since the emission regulations such

Table 1
T_{50} (K) and T_{50} difference (Δ) between fresh and aged catalysts for the removal of NO, CO and C_3H_6.

		Pd/Al_2O_3	Pd/La/Al_2O_3	Pd/Ce/Al_2O_3	Pd/La–Ce/Al_2O_3	Pd–La/Al_2O_3	Pd/Ce(30)/Al_2O_3
NO	Fresh	579	583	565	510	565	529
	Aged	635	603	605	586	583	616
	Δ	56	20	40	76	18	87
CO	Fresh	580	573	485	461	546	453
	Aged	584	633	485	496	491	488
	Δ	4	60	0	35	−55	35
C_3H_6	Fresh	578	573	553	544	554	523
	Aged	606	593	584	594	577	605
	Δ	28	20	31	50	23	82

as LEV II standards in California will strictly limit NO_x other than CO or hydrocarbons, we focus on the light-off temperature for NO. Both fresh and aged Pd/Al_2O_3 reveal the highest T_{50} for all of the reactants. However, the T_{50} of fresh La- and/or Ce-promoted catalysts, whatever the loading and preparation methods, is significantly lower than that of Pd/Al_2O_3. The T_{50} differences (Δ) between fresh and aged catalysts containing La, $Pd/La/Al_2O_3$ and Pd–La/Al_2O_3, are smallest among the catalysts, indicating its excellent thermal stability under aging. Especially T_{50} of aged Pd–La/Al_2O_3 is much lower than that of $Pd/La/Al_2O_3$. This result indicates that the catalytic activity and the thermal stability are affected by the order of introducing La and Pd during the preparation of the catalysts. The promoter effect of La on the catalytic activity is significantly increased on Pd–La/Al_2O_3.

Although fresh $Pd/Ce(30)/Al_2O_3$ shows the lowest T_{50} among fresh ones, the T_{50} is drastically increased upon aging. While the fresh $Pd/Ce(30)/Al_2O_3$ shows lower T_{50} than that of fresh $Pd/Ce/Al_2O_3$, the T_{50} of aged one is much higher than that of aged $Pd/Ce/Al_2O_3$ one. It means that the catalyst containing Ce which is an activity enhancing promoter is largely deactivated on aging. In the case of Pd/La–Ce/Al_2O_3, the advantageous effect of lanthanum oxide on the enhancement of the thermal stability disappears from the large $T_{50,NO}$ difference of 76 K. In other words, the addition of La cannot maintain the high activity of fresh Pd/La–Ce/Al_2O_3.

3.2. Surface area and hydrogen chemisorption

The surface areas of all catalysts are definitely decreased on aging, as shown in table 2. $Pd/La/Al_2O_3$ shows the highest surface area among the aged catalysts. However, the surface area of the aged $Pd/Ce/Al_2O_3$ is considerably decreased, whereas that of Pd/La–Ce/Al_2O_3 is not largely decreased on aging. The surface areas of the fresh $Pd/La/Al_2O_3$ and the fresh Pd–La/Al_2O_3 are similar, but the aged $Pd/La/Al_2O_3$ has a higher surface area than the aged Pd–La/Al_2O_3, which also implies the formation of different textural structure on two catalysts after thermal aging.

The Pd dispersion of a fresh Pd/La–Ce/Al_2O_3 is the highest according to the hydrogen chemisorption data in table 3. However, its dispersion is extremely decreased after aging. Although the fresh $Pd/La/Al_2O_3$ has relatively low dispersion of 12.33%, the aged one retains the highest dispersion among the aged catalysts. Although the Pd dispersions in the fresh Pd–La/Al_2O_3 and $Pd/La/Al_2O_3$ are quite similar, the dispersion of the aged Pd–La/Al_2O_3 is drastically decreased due to the significant thermal sintering. The effect of La on the retention of high dispersion during thermal aging is not great on Pd–La/Al_2O_3 and Pd/La–Ce/Al_2O_3. The BET surface area and hydrogen chemisorption data clearly indicate that lanthanum oxides play a crucial role in maintaining the high surface area of alumina and the dispersion of Pd, especially in case of sequentially loaded $Pd/La/Al_2O_3$ catalyst under the thermal aging with O_2 at 1273 K.

3.3. XRD

Figure 1 shows the XRD patterns of the fresh catalysts. Major peaks correspond to γ-Al_2O_3 and CeO_2 phases. Only $Pd/La/Al_2O_3$ contains the broad PdO phase (figure 1(b)). Peak patterns of $Pd/Ce/Al_2O_3$ and Pd/Ce–La/Al_2O_3 are almost the same. In other words, no lanthanum related peaks are detected on a $Pd/La/Al_2O_3$ containing 1.27 μmol-La/m^2. This is in good agreement with the previous result that the

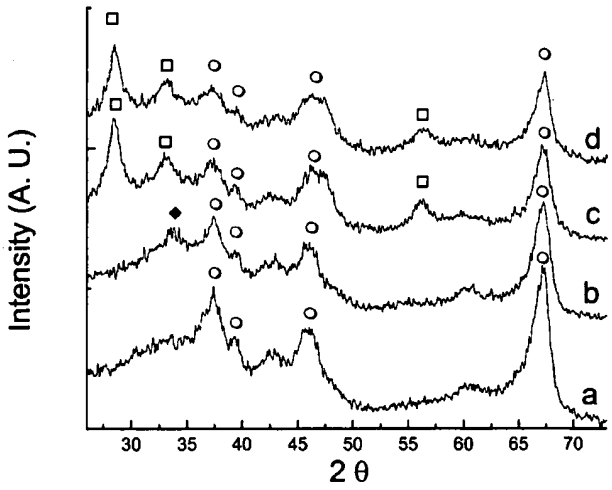

Figure 1. XRD patterns of fresh catalysts: (a) Pd/Al_2O_3, (b) $Pd/La/Al_2O_3$, (c) $Pd/Ce/Al_2O_3$ and (d) Pd/La–Ce/Al_2O_3. (o) γ-Al_2O_3, (♦) PdO and (□) CeO_2.

Table 2
BET surface areas (m^2/g) of various catalysts.

	Pd/Al_2O_3	$Pd/La/Al_2O_3$	Pd–La/Al_2O_3	$Pd/Ce/Al_2O_3$	Pd/La–Ce/Al_2O_3
Fresh	164.88	163.82	163.20	154.79	156.83
Aged	89.93	108.60	96.01	85.92	93.02

Table 3
Dispersion (%) of Pd by hydrogen chemisorption.

	Pd/Al_2O_3	$Pd/Ce/Al_2O_3$	$Pd/La/Al_2O_3$	Pd–La/Al_2O_3	Pd/La–Ce/Al_2O_3
Fresh	28.73	27.54	12.33	10.82	35.49
Aged	4.10	4.02	7.07	2.33	1.14

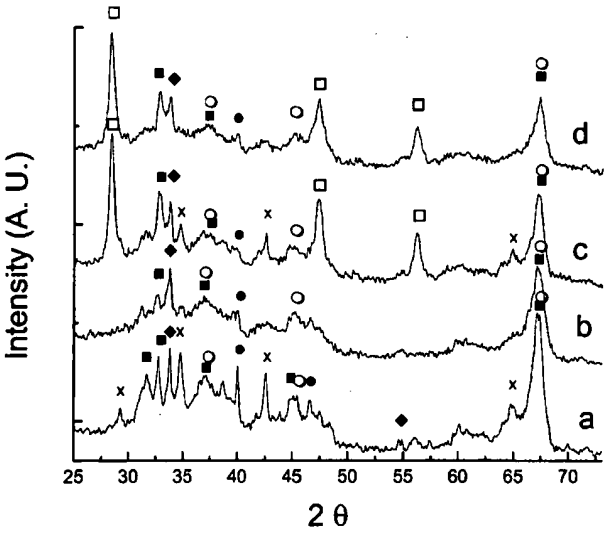

Figure 2. XRD patterns of aged catalysts: (a) Pd/Al_2O_3, (b) $Pd/La/Al_2O_3$, (c) $Pd/Ce/Al_2O_3$ and (d) $Pd/La–Ce/Al_2O_3$. (o) γ-Al_2O_3, (♦) PdO, (□) CeO_2, (■) θ-Al_2O_3, (•) Pd and (×) κ-Al_2O_3.

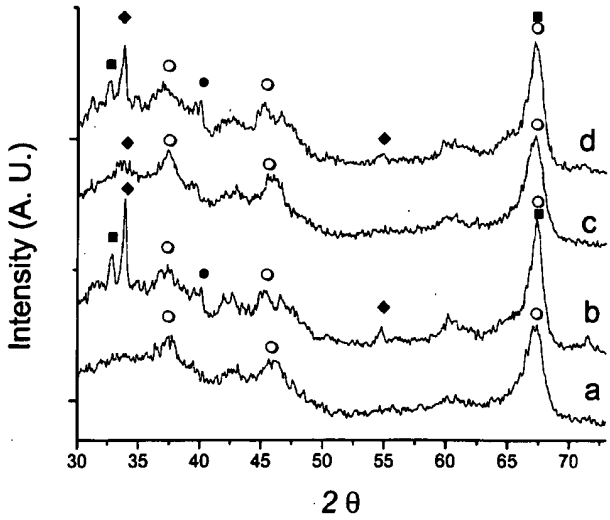

Figure 3. XRD patterns of the catalysts containing lanthanum oxide: (a) $Pd–La/Al_2O_3$ fresh, (b) $Pd–La/Al_2O_3$ aged, (c) $Pd/La/Al_2O_3$ fresh and (d) $Pd/La/Al_2O_3$ aged. (o) γ-Al_2O_3, (♦) PdO, (■) θ-Al_2O_3 and (•) Pd.

lanthana up to 8.5 μmol-La/m^2 exist in the form of a two-dimensional overlayer on the alumina support invisible by XRD [25].

After aging the catalysts, the peaks grow sharper and the new peaks such as metallic Pd, θ-Al_2O_3 and κ-Al_2O_3 come out, as shown in figure 2. Especially the growth of Pd metallic phase is noticeable in Pd/Al_2O_3. Most Al_2O_3 phases are θ-Al_2O_3 and κ-Al_2O_3 on an aged Pd/Al_2O_3. The addition of La and/or Ce oxides gives rise to the inhibition of the phase transition of γ-Al_2O_3 (figure 2 (b), (c) and (d)) to θ-Al_2O_3 and κ-Al_2O_3. Like the fresh $Pd/La/Al_2O_3$, no peaks concerning the La species such as La_2O_3 or $LaAlO_3$ are found in the other catalysts containing lanthanum oxide even after aging, because the two-dimensional La_2O_3 invisible by XRD does not act as a precursor to the formation of $LaAlO_3$ [26]. γ-Al_2O_3 phase is maintained only on aged $Pd/La/Al_2O_3$, resulting in the high surface area, as shown in table 2. Figure 3 shows the XRD patterns of La-promoted Pd/Al_2O_3. In comparison with aged $Pd/La/Al_2O_3$ (figure 3(d)), the peaks of PdO (2θ = 33.8°) and θ-Al_2O_3 (2θ = 32.8°) phases on aged $Pd–La/Al_2O_3$ (figure 3(b)) are obviously increased, which indicates that the sintering of Pd species and the phase transformation of γ-Al_2O_3 to θ-Al_2O_3 much more proceeded on a $Pd–La/Al_2O_3$ than on a $Pd/La/Al_2O_3$. These distinct textural properties after thermal aging seem to be due to the different role of La in two catalysts.

The drastic growth of the CeO_2 phase on a Ce-promoted catalyst shows a negative effect on the oxygen storage capacity which depends on CeO_2 crystalline structure [27]. The advantageous effect of La on the inhibition of phase transformation of Al_2O_3 is not so large on $Pd/La–Ce/Al_2O_3$. The change in the lattice constant of CeO_2 in the $Pd/La–Ce/Al_2O_3$ is estimated from the shifts of a peak at 2θ = 56.38°, arising from CeO_2(311) plane [28]. The 2θ of the fresh $Pd/La–Ce/Al_2O_3$ is 56.36° corresponding to that of pure CeO_2, which indicates that La–Ce solid solution is not formed. It changes to 56.20° on aging, which means that La^{3+} ions are dissolved into the CeO_2 lattice during the thermal aging, since the radius of the La^{3+} ion (1.19 Å) is larger than that of the Ce^{4+} ion (1.09 Å). The formation of La–Ce solid solution as shown in the XRD pattern by the dissolution of La^{3+} ions into CeO_2 lattice has been known as the key process in maintaining the good oxygen storage capacitor under the thermal treatment [18]. However, it is unsatisfactory to maintain the good activity and the textural property of fresh $Pd/La–Ce/Al_2O_3$ after the thermal aging according to the results of reaction performance and BET surface area.

3.4. XPS

XPS data of various Pd catalysts are summarized in table 4. When the catalysts are aged, Pd $3d_{5/2}$ peak areas become smaller, meaning that Pd surface concentration is decreased due to the thermal sintering. Such XPS results are consistent with the result of hydrogen chemisorption, as shown in table 3. Binding energy of Pd $3d_{5/2}$ in Pd/Al_2O_3 is 336.7 eV, which can be assigned to PdO by the previous XPS data [26,29]. Binding energies of Pd $3d_{5/2}$ in fresh La- and/or Ce-promoted catalysts are lower than that of Pd/Al_2O_3 by 0.5–0.7 eV, indicating the formation of less oxidized PdO_{1-x} species. After aging the Pd/Al_2O_3, the binding energy of Pd $3d_{5/2}$ shifts to 336.2 eV which is assigned to that of PdO_{1-x} species. A small shoulder appears at 338.4 eV which can be assigned as the binding energy of PdO_2 or deficiently coordinated Pd^{2+} [29]. However, the latter one seems to be more probable than the former one because PdO_2 exists only in the hydrous form [30]. As the Pd/Al_2O_3 is aged, the PdO is either reduced to the less oxidized PdO_{1-x} or diffused to the boundary site of

Table 4
Binding energy of Pd $3d_{5/2}$ and the relative surface concentration of Pd/Al.

		BE (eV)	Pd/Al (×100)
Pd/Al_2O_3	Fresh	336.7	0.50
	Aged	336.2	0.09
		338.4	0.06
$Pd/La/Al_2O_3$	Fresh	336.0	0.51
	Aged	336.2	0.19
$Pd/Ce/Al_2O_3$	Fresh	336.0	0.52
	Aged	336.8	0.18
$Pd/La–Ce/Al_2O_3$	Fresh	336.2	0.51
	Aged	336.6	0.23
$Pd–La/Al_2O_3$	Fresh	336.2	1.68
	Aged	335.5	0.42

Al_2O_3 thus to PdO interacting with Al_2O_3 having higher binding energy. Farrauto [31] suggested that the bulk-like PdO species was much more active than the PdO interacting with Al_2O_3 species in methane combustion. The addition of lanthanide oxides suppresses the formation of such PdO species on the aged catalysts (table 4) possibly by blocking the diffusion of PdO to alumina, thus resulting in the superior reactivity of the aged catalysts containing lanthanide oxide (table 1). It was described in section 3.3 that the aged $Pd–La/Al_2O_3$ showed a better activity than that of aged $Pd/La/Al_2O_3$ in spite of the lower surface area and the higher degree of crystallinity, which could be well explained by XPS data that the Pd surface concentration of the former one was more than three times larger than that of the latter one.

When $Pd–La/Al_2O_3$ is aged, the binding energy of Pd is shifted to more metal-like PdO_{1-x} species (335.5 eV). The binding energy shifts on the insulator support are influenced not only by the chemical state of the metal, but also by the final state effect arising from the size of the supported metal crystallites. However, the effects of particle size are negligible, if the supported metal particles are large enough to exhibit bulk-like valence structure. The dispersion of the samples studied here ranges between 1 and 36%, as shown in table 3. The minimum estimated average diameter of the Pd particles was 5 nm, based on the equation suggested by Bell [23]. According to the review paper by Karpinski [32], Pd particles larger than 4 nm were treated as bulk Pd. Therefore, the final state effects arising from the particle size of Pd can be excluded.

Accordingly the binding energy shift is attributed to the charge transfer from LaO_x to Pd [33], arising from the intimate interaction between Pd and La on the surface during the thermal aging. On the other hand, the thermal aging on the sequentially loaded catalyst, $Pd/La/Al_2O_3$, does not affect the electronic environment of Pd, resulting in the similar binding energy of Pd 3d to that of fresh $Pd/La/Al_2O_3$. It can be explained by relatively weak interaction between Pd and La on $Pd/La/Al_2O_3$ in comparison with that on $Pd–La/Al_2O_3$. Table 5 shows the binding energy of La $3d_{5/2}$ and the relative surface concentration of La/Al for the La-loaded catalysts. The binding energies of 833.5 and 835 eV are assigned to La $3d_{5/2}$ of pure La_2O_3 oxides and that of dispersed La_2O_3 phase, respectively [34]. Therefore, the La species on our catalysts possibly correspond to the latter one. Furthermore, the binding energy of La $3d_{5/2}$ of all La-loaded catalysts was not changed on thermal aging. In summary, the interaction between Pd and La is significant on the catalyst prepared by co-impregnating both of these, resulting in the surface-abundance of Pd and La, the improved thermal stability of Pd and the enhanced catalytic activity.

Table 5
Binding energy of La $3d_{5/2}$ and the relative surface concentration of La/Al.

		BE (eV)	La/Al (×100)
$Pd/La/Al_2O_3$	Fresh	835.8	1.82
	Aged	835.6	2.28
$Pd–La/Al_2O_3$	Fresh	835.4	3.25
	Aged	835.6	4.65
$Pd/La–Ce/Al_2O_3$	Fresh	835.7	1.40
	Aged	835.7	2.33

4. Discussion

La_2O_3 has been well known as a promoter to have a good thermal resistance. In this study, it was also confirmed that Ce and La are promoters for the catalytic activity and thermal stability, respectively. It is notable that the role of La on the Pd-only three-way catalyst is significantly affected by the impregnating order of La and Pd on γ-Al_2O_3 support. On $Pd/La/Al_2O_3$, La_2O_3 played a crucial role of inhibiting the phase transformation from γ-Al_2O_3 to θ-Al_2O_3, resulting in the maintenance of the high surface area after thermal aging. Capitan et al. [34] ascribed it to the strong interaction between La cation and the support, which resulted in a redistribution of the electronic density over Al–O–La ensembles from the spectroscopic measurements and *ab initio* calculations. On the other hand, on $Pd–La/Al_2O_3$, the intimate interaction between lanthanum oxide and Pd was a primary observation. A high surface concentration of Pd and a charge transfer from LaO_x to Pd, as shown in table 4, seemed to arise from the intimate interaction of lanthanum oxide with Pd. Therefore, the degree of interaction with Pd closely depended on the order of the addition of La during catalyst preparation. First, the major function of La on $Pd/La/Al_2O_3$ was the suppression of a thermal sintering of alumina texture through an interaction between La and Al like a La–O–Al bond which might be formed during the calcination of La/Al_2O_3 before impregnation of Pd. However, there was no significant effect of La on the electronic structure of Pd species in this case in comparison of XPS data with that of $Pd–La/Al_2O_3$. Second,

the La on Pd–La/Al_2O_3 played a main role as a promoter to enhance the thermal stability of Pd through an intimate interaction between Pd and La possibly as a form of Pd–La ensemble which seemed to be formed by the calcination of Pl–La/Al_2O_3. The higher surface concentration of Pd/Al on Pd–La/Al_2O_3 than that on Pd/La/Al_2O_3 was interesting, because Pd was finally loaded on the latter one. It could be explained by the intimate interaction between Pd and La that might be maintained on the surface during thermal aging, thus resulting in the higher surface concentration of Pd/Al and La/Al as shown in XPS. In addition, the intimate contact of Pd and La on Pd–La/Al_2O_3 might give rise to the easy charge transfer from LaO_x to Pd to form rather electron-rich PdO_{1-x} species.

Two types of PdO species were reported in the Pd catalysts supported on Al_2O_3 by Farrauto et al. [31]. One is easily reducible PdO covering Pd metal particles, which is reduced to metallic Pd in H_2 even at RT, and this PdO species have the similar binding energy to bulk PdO by XPS study [29]. The other is a stable palladium oxide strongly interacting with alumina. TPO/TPR study showed that the ratio of O to Pd was more than one, in other words, oxygen rich, and that it was reduced at higher temperature [10]. In methane combustion, the former PdO species (PdO covering metal particles) were suggested to be much more active than the latter one (PdO interacting with Al_2O_3). The binding energy of Pd $3d_{5/2}$ in aged Pd/Al_2O_3 (338.4 1eV) was higher than that of bulk PdO (336.7 eV) by 1.7 eV, as shown in table 4. It was demonstrated that the presence of lanthanide oxides suppressed the formation of PdO interacting with Al_2O_3 during thermal aging from the result of XPS. By analogy to the methane combustion, the absence of PdO interacting with Al_2O_3 on Pd/Al_2O_3 containing lanthanide oxide accounts for the higher three-way catalytic activity than Pd/Al_2O_3 after thermal aging.

In spite of the formation of the solid solution of $(Ce_xLa_{1-x})O_2$ on Pd/La–Ce/Al_2O_3, as shown figure 2, Pd/La–Ce/Al_2O_3 was rapidly deactivated upon aging. In other words, when La was co-impregnated with Ce, its thermal stabilizing effect was not observed. Therefore, an alternative method must be found to keep the excellent property of each promoter, La and Ce. To achieve the optimum performance of Pd-only three way catalyst, it was shown that ceria had to be separated from the Pd active species or promoters by physical mixing in our recent results [35].

5. Conclusions

The role of La significantly depended on the impregnating order of La and Pd on the Pd-only three-way catalyst supported on alumina. When La was co-impregnated with Pd on Pd–La/Al_2O_3, which showed a high activity, the major role of La was a promoter to enhance the thermal stability of Pd through an intimate interaction between Pd and La, resulting in the electron-rich PdO_{1-x} species. However, La predominantly interacted with alumina and played as a promoter to suppress a thermal sintering of alumina texture on Pd/La/Al_2O_3 that was prepared by loading La first and then introducing Pd serially. In the case of Pd/La–Ce/Al_2O_3, the formation of La and Ce oxides solid solution was not strong enough to maintain the high activity and the good textural property after thermal aging.

Acknowledgement

This research was funded by a national project granted from the Ministry of Commerce, Industry and Energy, and Ministry of Science and Technology (1995–1998) and partially supported by the Brain Korea 21 Project.

References

[1] J.C. Summers, W.B. Williamson and M.G. Henk, SAE paper 880 281 (1988).
[2] J.C. Summers and W.B. Williamson, in: *Environmental Catalysis*, ACS Symp. Ser., Vol. 552, ed. J.N. Armor (Am. Chem. Soc., Washington, DC, 1994) p. 94.
[3] K.C. Taylor, in: *Catalysis: Science and Technology*, Vol. 52, eds. J.R. Anderson and M. Boudart (Springer, Berlin, 1984) p. 119.
[4] H. Muraki, H. Shinjoh, H. Sobukawa, K. Yokota and Y. Fujitani, Ind. Eng. Chem. Prod. Res. Dev. 25 (1986) 202.
[5] M. Skoglundh, H. Johansson, L. Lowendahl, K. Jansson, L. Dahl and B. Hirschauer, Appl. Catal. B 7 (1996) 299.
[6] A. Lemaire, J. Massardier, H. Praliaud, G. Mabilon and M. Prigent, Stud. Surf. Sci. Catal. 96 (1995) 97.
[7] J. Noh, O-B. Yang, D.H. Kim and S.I. Woo, Catal. Today 53 (1999) 575.
[8] D.H. Kim, S.I. Woo, J. Noh and O-B. Yang, Appl. Catal. A, in press.
[9] R. Craciun and N. Dulamita, Catal. Lett. 46 (1997) 229.
[10] T.E. Hoost and K. Otto, Appl. Catal. A 92 (1992) 39.
[11] A. Trovarelli, Catal. Rev. Sci. Eng. 38 (1996) 439.
[12] B.I. Whittington, C.J. Jiang and D.L. Trimm. Catal. Today 26 (1995) 41.
[13] A.F. Diwell, R.R. Rayaram, H.A. Shaw and T.J. Truex, Stud. Surf. Sci. Catal. 71 (1991) 139.
[14] H.S. Gandhi and M. Shelef, Stud. Surf. Sci. Catal. 30 (1987) 199.
[15] B. Harrison, A.F. Diwell and C. Halett, Platinum Metals Rev. 32 (1988) 73.
[16] M. Ozawa and M. Kimura, J. Mater. Sci. Lett. 9 (1990) 291.
[17] J.Z. Shyu, W.H. Weber and H.S. Gandhi, J. Phys. Chem. 92 (1988) 4964.
[18] G.W. Graham, P.J. Schmitz, R.K. Usmen and R.W. McCabe, Catal. Lett. 17 (1993) 175.
[19] M. Shelef, L.P. Haack, R.E. Soltis, J.E. deVries and E.M. Logothetis, J. Catal. 137 (1992) 114.
[20] L.P. Haack, J.E. deVries, K. Otto and M.S. Chatta, Appl. Catal. A 82 (1992) 199.
[21] C. Micheaud, P. Marecot, M. Guerin and J. Barbier, Appl. Catal. A 171 (1998) 229.
[22] P. Araya, C. Ferrada and J. Cortes, Catal. Lett. 35 (1995) 175.
[23] T.H. Fleisch, R.H. Hicks and A.T. Bell, J. Catal. 87 (1984) 398.
[24] J.F. Moulder, U.F. Stickle, P.E. Sobol and K.D. Bomden, in: *Handbook of X-ray Photoelectron Spectroscopy* (Perkin–Elmer, Eden Prairie, MN, 1992).
[25] M. Bettman, R.E. Chase, K. Otto and W.H. Weber, J. Catal. 117 (1989) 447.
[26] B.H. Engler, D. Lindner, E.S. Lox, A. Schafer-Sindlinger and K. Ostgathe, Stud. Surf. Sci. Catal. 96 (1995) 441.

[27] C. Hardcare, R.M. Ormerod and R.M. Lambert, J. Phys. Chem. 98 (1994) 10901.
[28] T. Miki, T. Ogawa, M. Haneda, N. Karuta, A. Ueno, S. Tateishi, S. Masuura and M. Sato, J. Phys. Chem. 94 (1990) 6464.
[29] K. Otto, L.P. Haack and J.E. deVries, Appl. Catal. B 1 (1992) 1.
[30] K.S. Kim, A.F. Gossmann and N. Winograd, Anal. Chem. 46 (1974) 197.
[31] R.J. Farrauto and M.C. Hobson, Appl. Catal. A 81 (1992) 227.
[32] Z. Karpinski, Adv. Catal. 37 (1990) 45.
[33] R.H. Hicks, Q.-J. Yen and A.T. Bell, J. Catal. 89 (1984) 498.
[34] M.J. Capitan, M.A. Centeno, P. Malet, I. Carrizosa, J.A. Odriozola, A. Marquez and J. Fernandez Sanz, J. Phys. Chem. 99 (1995) 4655.
[35] H.S. So, O-B. Yang, D.H. Kim and S.I. Woo, Stud. Surf. Sci. Catal. 130 (2000) 1379.